

NATIONAL AERONAUTICS AND SPACE ADMINISTRATION

# TECHNICAL PUBLICATION

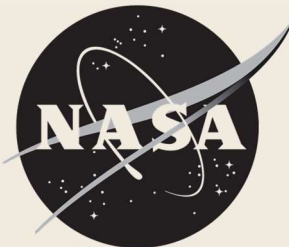
ORIGINALLY DISTRIBUTED

March 2023 as  
NASA TP-5635

PASSIVE ROCKET DIFFUSER TESTING:  
REACTING FLOW PERFORMANCE OF ADVANCED CONFIGURATIONS

By Daniel R. Jones

John C. Stennis Space Center  
Stennis Space Center, Ms.



WASHINGTON

## NASA STI Program in Profile

Since its founding, NASA has been dedicated to the advancement of aeronautics and space science. The NASA scientific and technical information (STI) program plays a key part in helping NASA maintain this important role.

The NASA STI program operates under the auspices of the Agency Chief Information Officer. It collects, organizes, provides for archiving, and disseminates NASA's STI. The NASA STI program provides access to the NTRS Registered and its public interface, the NASA Technical Reports Server, thus providing one of the largest collections of aeronautical and space science STI in the world. Results are published in both non-NASA channels and by NASA in the NASA STI Report Series, which includes the following report types:

### TECHNICAL PUBLICATION.

Reports of completed research or a major significant phase of research that present the results of NASA Programs and include extensive data or theoretical analysis. Includes compilations of significant scientific and technical data and information deemed to be of continuing reference value. NASA counter-part of peer-reviewed formal professional papers but has less stringent limitations on manuscript length and extent of graphic presentations.

### TECHNICAL MEMORANDUM.

Scientific and technical findings that are preliminary or of specialized interest, e.g., quick release reports, working papers, and bibliographies that contain minimal annotation. Does not contain extensive analysis.

**CONTRACTOR REPORT.** Scientific and technical findings by NASA-sponsored contractors and grantees.

### CONFERENCE PUBLICATION.

Collected papers from scientific and technical conferences, symposia, seminars, or other meetings sponsored or co-sponsored by NASA.

### SPECIAL PUBLICATION.

Scientific, technical, or historical information from NASA programs, projects, and missions, often concerned with subjects having substantial public interest.

### TECHNICAL TRANSLATION.

English-language translations of foreign scientific and technical material pertinent to NASA's mission.

Specialized services also include organizing and publishing research results, distributing specialized research announcements and feeds, providing information desk and personal search support, and enabling data exchange services.

For more information about the NASA STI program, see the following:

Access the NASA STI program home page at  
<http://www.sti.nasa.gov>

E-mail your question to [help@sti.nasa.gov](mailto:help@sti.nasa.gov)

Phone the NASA STI Information Desk at  
757-864-9658

Write to:  
NASA STI Information Desk  
Mail Stop 148  
NASA Langley Research Center  
Hampton, VA 23681-2199

NATIONAL AERONAUTICS AND SPACE ADMINISTRATION

# TECHNICAL PUBLICATION

ORIGINALLY DISTRIBUTED

March 2023 as  
NASA TP-5635

PASSIVE ROCKET DIFFUSER TESTING:  
REACTING FLOW PERFORMANCE OF ADVANCED CONFIGURATIONS

By Daniel R. Jones

John C. Stennis Space Center  
Stennis Space Center, Ms.



WASHINGTON

"...for the benefit of all mankind."

National Aeronautics and Space Act of 1958

## PREFACE

This report was written for a technical audience interested in the design of supersonic diffusers, but its content underpins ongoing spike ejector research expected to have broad appeal across multiple industrial sectors. It is intended to serve as a reference for interpretation of experimental data, to show the empirical limits of conventional design, and to describe some research and development work on higher-performance alternatives. The information density of graphics is far greater than that of prose. As such, the reader is encouraged to peruse the figures on pages 19-40 before reading past the background section of the text.

While its format pays homage to the government reports of the 1940s-1960s, this document was created with digital consumption in mind. Plots have been embedded in vector format to allow a high degree of magnification. Axis scales were kept constant on a per-figure basis unless otherwise noted, and repetitious labeling was omitted to keep the focus on qualitative differences between configurations. An effort was also made to keep plot markers consistent throughout the paper so that Figure 3 effectively serves as the legend for the rest.

## ACKNOWLEDGEMENTS

The author owes gratitude to the entire team of engineers and technicians at SSC who supported this test program, and to the following individuals in particular:

Project Manager	Richard Rauch	(NASA)
Project Engineer	Nicholas Nugent	(NASA)
Mechanical Design Engineer	Grady Saunders	(JTI)
Mechanical Design Engineer	Tyler McElroy	(JTI)
Mechanical Implementation Engineer	Perry Waller	(JTI)
Test Director	Stephen Rawls	(NASA)
Mechanical Ops/Test Conductor	James Hamilton	(NASA)
Mechanical Ops/Test Conductor	Angelica Baker	(NASA)
Mechanical Ops/Test Conductor	Kevin Oramous	(NASA)
Mechanical Ops/Test Conductor	Ryan McKibben	(NASA)
Controls Engineer	Marc Shoemaker	(NASA)
Controls Engineer	Alex Chew	(NASA)
Safety Engineer	Aundra Brooks-Davenport	(NASA)
DAS Engineer	Shawn Herrin	(S3)
Video Engineer	Byron Bordelon	(S3)

## ABSTRACT

Upper stage rocket engines are optimized for operation at the edge of space. Ground testing often requires simulation of high-altitude environments to prevent damage from off-design operation. Passive supersonic diffusers are an effective means of establishing the partial vacuum needed around the nozzle exit. The low cost of diffusers relative to active vacuum sources (ejectors, pumps, etc.) provides a perpetual incentive to improve their performance and expand the envelope of passively testable engines. Second-throat diffusers have been the de facto standard for rocket testing since the 1950s, and numerous studies have focused on parametric optimization of the topology. Yet, even the best second-throat designs may require more driving pressure than an upper stage engine can provide. To overcome conventional limits, engineers at NASA's Stennis Space Center (SSC) adapted an obscure cold-flow diffuser topology to the extremes of immersion in supersonic combustion products. Aerodynamic experimentation was conducted at SSC's E-3 test stand to quantify the performance of prototypical hot-fire spike diffuser hardware and enable direct comparison to prior states of the art.

A LO<sub>x</sub>/GH<sub>2</sub> thruster was contoured to approximate the regeneratively-cooled nozzle of an upper-stage engine and fired into 28 downstream diffuser configurations: 16 second-throat, 2 centerbody, and 10 spike. Temperature and pressure were recorded along the test article walls for a range of chamber pressures spanning 3.5 - 5.0 MPa. The second-throat configurations with the lowest start and unstart pressure ratios were shown to outperform equivalent systems in literature and taken as baselines for evaluation of advanced diffuser performance. Compared to these exemplars, centerbody diffusers decreased start pressure ratio by 11% but increased unstart pressure ratio by 15%. Spike diffusers reduced start and unstart pressure ratios by 24% and 9%, respectively.

## BACKGROUND

The nozzles of upper stage rocket engines are designed to expand combustion products to the low pressures found at the edge of Earth's atmosphere. Ground testing such engines in open air would overexpand the plume and risk nozzle damage from unsteady boundary layer separation. Test facilities typically incorporate some means of back pressure reduction to avoid separation during steady operation. Active, externally powered vacuum sources (encapsulating chambers, steam ejectors, etc.) may be feasible for testing low mass-flow rockets but infrastructure and operating costs can become prohibitive at larger scales. Conversely, passive rocket diffusers harness the internal power of the exhaust plume and force it to act as a jet pump for the area surrounding the nozzle.

In 1958, NASA's Langley Research Center (LaRC) drew on the data and designs of both supersonic wind tunnels and air ejectors when creating the first diffuser designed explicitly for ground testing upper stage rockets [1]. Other facilities followed suit and the cylindrical and second-throat topologies common to earlier applications quickly became the industry norm [2-9]. While both topologies are simple

and reliable, neither are particularly efficient because they permit high stagnation pressure losses to occur through Mach reflection of the core flow.

By 1960, it was realized that the addition of an aerodynamic centerbody could decrease shock losses by enabling selective expansion of the plume [9]. It was also found that annular flow forced more reflections (thus more recompression) to occur per unit length, allowing centerbody systems to operate efficiently in half the space of equivalent second-throat systems. Despite a comparatively limited number of deployments, centerbody diffusers have been evaluated in subscale experiments and implemented in full-scale tests of both developmental and flight engines [9-20].

Though it was a clear advancement over conventional diffusers, the centerbody topology also introduced two new sources of stagnation pressure loss: one set of shocks created by deflection of the core flow around the nosecone, and a second set created by returning the flow to an axial orientation through the diffuser throat. The first is inherent and easily justified; the conical shocks generated by the presence of the nosecone are weaker than the normal shocks that would occur in its absence. The second is strictly conventional; the losses from the second set of shocks would be avoided if the flow trajectory was held constant through the terminal shock. Any desired turning could be accomplished downstream in the subsonic portion of the diffuser.

In 1962, NASA's Lewis Research Center (LeRC) introduced the spike diffuser as a convenient geometry to evaluate the performance benefits of a variable-area throat in cold-flow experiments [21]. The idea was that the spike could translate forward after passing the initial shock wave at start and reduce the throat area for higher-efficiency steady operation. One byproduct of the topology was the removal of the second set of turning shocks present in centerbody configurations. The experiment was successful, and the variable-area spike diffuser was shown to provide 26% and 40% improvements in start and unstart pressure ratios, respectively. A decade later, cold-flow experimentation conducted by the U.S. Air Force on variable-area ejectors showed a similar magnitude of improvement for low-expansion jet nozzles [22-23].

Despite their aerodynamic efficiency, variable-area diffusers are suboptimal for testing rocket engines. Moving components carry higher risk of failure than their static equivalents, and modern programs are hesitant to accept any facility-induced risk to flight hardware. This is especially true if the parts need to maneuver within the volume of the nozzle, which may itself be moving due to gimbal, unsteady side loads, thermal expansion/contraction of the stage, or flex in the thrust structure. However, a static spike diffuser designed to deliver high performance in a reacting-flow environment would be tenable.

The motivation to develop a hot-fire spike diffuser came in 2018 when a preliminary subscale test series conducted at SSC found that conventional second-throat diffusers would provide insufficient start performance for passive testing of a specific upper stage. To avoid the expense of steam ejection, the program granted leeway to explore unconventional designs. The author happened upon the 1962 LeRC paper during literature review and decided to adapt the spike topology to the unique demands of rocket testing. An aerodynamic contour was designed using computational fluid dynamics (CFD) simulations, a subscale test article was fabricated to fit the existing LO<sub>x</sub>/GH<sub>2</sub> thruster, and NASA submitted a patent application to

cover the new capability [24]. A second subscale campaign was conducted during 2021 in which the rocket-tailored spike diffuser was put to the test alongside second throat and centerbody counterparts. This report describes the cumulative results of both test series and contextualizes them against an extensive backdrop of diffuser performance data aggregated from literature.

## APPARATUS

The Diagnostic Testbed Facility (DTF) thruster installed at E-3 was designed at NASA's Marshall Space Flight Center (MSFC) in the 1960s and subsequently deployed at SSC as a subscale Space Shuttle Main Engine (SSME) plume simulator [25]. The thruster features an interchangeable copper liner which allows reconfiguration of the nozzle contour as needed. Figure 1 shows the two nozzles used for this test series. Each nominally produced 3.5 kN of thrust at a chamber pressure of 4.38 MPa. One nozzle was conventionally machined with a truncated copper liner and a steel nozzle extension. The other was additively manufactured of GRCop-42 via Direct Metal Laser Sintering (DMLS) and finished with the Hot Isostatic Pressing (HIP) process. The combustion chamber of the DMLS nozzle was shortened and included integral water cooling passages. The two subscale nozzles' expansion contours were identical apart from a 0.14 cm outward step between the copper liner and steel extension which accounted for the materials' disparate coefficients of thermal expansion. As-built geometry and performance characteristics are given in Tables 1.1 and 1.2. A void was milled into the nozzle flanges to serve as a test cell volume. Propellant mixture ratios are provided on per-diffuser basis later in the paper.

Diffuser aerodynamic design was accomplished by Reynolds-Averaged Navier-Stokes simulations using the Loci/CHEM solver [26-27] with finite-rate chemistry [28],  $k-\omega$  turbulence modeling [29], compressibility correction [30], wall functions, and a calorically-imperfect ideal-gas equation of state. Diffuser contours were subject to a set of constraints expected to apply during full-scale stage testing, including maximum length and diameter, minimum turning radii for backside cooling, and minimum clearance during engine gimbal. Subscale diffuser hardware was machined from 304 stainless steel and thermal damage was mitigated by limited test duration (1-5s) rather than active cooling. Modularity simplified reconfiguration and allowed broader investigation of the trade space. Two series of instrumentation bosses were run along opposing sides of each diffuser, with one side dedicated to Stellar GT200-20A-155 pressure transducers and the other to Medtherm TCS-061-K-1.5-10F-36-11038 microsecond-response thermocouples. Calibration reports showed measurement accuracies of +/- 345 Pa and +/- 1.94 K, respectively. All sensors were sampled at 250 Hz. Heat flux densities were processed from thermocouple data using the Cook-Felderman technique [31].

## RESULTS AND DISCUSSION

### Second-Throat Configurations

Hardware components of the second-throat diffusers are depicted in Figure 2. The design philosophy of inlets A and B drew on lessons learned from a test series conducted at SSC in 2015 [32] which had a high pressure ratio budget, notable length constraints, and a primary objective of producing zero flow separation within the diffuser. The idea was that a cylindrical segment upstream of the contraction would decrease the plume's impingement angle during steady-state operation, conserve stagnation pressure, and delay boundary layer separation. While that was borne out by testing, increased volume upstream of the throat can decrease subsonic pumping efficiency and delay start. This effect has been demonstrated implicitly in contraction spacing studies which used translatable inserts inside cylindrical ducts [7,33]. Taking this into account, inlet C was fabricated with 32% less volume than inlet A. Though the referenced data suggests retaining a short cylindrical segment can be beneficial, a purely conical geometry was adopted to simplify construction.

In general, smaller second-throat areas produce better pumping performance [7,9,33,34]. However, any stagnation pressure losses incurred between the first (nozzle) and second (diffuser) throats increase the area required to pass the system's mass flow rate. During the diffuser startup process, a complex series of shock waves propagates between the two throats. The cumulative losses are commonly but conservatively approximated by assuming a normal shock sitting at the diffuser inlet. This is effectively a worst-case condition invoking losses at the highest Mach number and through the strongest type of shock. It is advantageous to have a higher-fidelity approximation of the starting flow structure when pursuing optimum performance. In this case, CFD simulation was used to estimate the losses and size the second-throat appropriately. The contraction ratio ( $A_{DT}/A_{DI}$ ) varied between 15% and 20% below the normal shock limit of 0.57, depending on the inlet.

Determining an appropriate second-throat length for optimum start/unstart performance is comparatively straightforward. For hot-fire diffusers, ensuring enough shock reflections to recompress the flow only requires a throat length-to-diameter ratio of 1-3 [1, 6, 8, 32]. Additional length buys unstart performance [8] but increases stagnation pressure lost to shocks and viscous effects. Above a ratio of 8, return on investment decreases [8]. Throat spools D and E were fabricated with length-to-diameter ratio of 7.8 and 1.7 to resolve these effects.

Constraints on spatial envelope left few design choices for the subsonic diffuser. Component F simply represents what would fit on the full-scale test stand.

These components were assembled into sixteen configurations and subjected to aerodynamic experimentation. Geometric and performance characteristics of the tested second-throat configurations are listed in Table 2. Assemblies ADF (inlet A coupled with second throat D and subsonic diffuser F), CDF, and BE were prototypes for different facility concepts. All others were byproducts of modular construction and a recognition that sensitivity studies are particularly valuable in the sparsely explored rocket diffuser trade space. AE and BE were omitted from the test matrix when CE did not start at the maximum chamber pressure deliverable at the time.

Because the test cell lies at the interface between the nozzle and diffuser, its instrumentation can provide a wealth of information on plume development in the coupled system. Plots of test cell pressure variation with chamber pressure, known as pumpdown curves, are a practical way to display that information. Pumpdown curves within literature tend to represent an idealized test in which the cell pressure is given ample time to react to incremental chamber pressure changes. Figure 3, intended to serve as a quick reference for diffuser diagnostics, takes a different approach. Its nominal pumpdown plot shows idealized curves representing multiple runs targeting different chamber pressures with changes in the driving flow occurring quicker than the test cell can respond. The timescale disparity produces fanning of the evacuation and recompression curves during start and unstart. The corresponding off-nominal plot shows idealized curves representing multiple runs, each with a different cause of undesirable behavior.

Configuration CDF received the greatest scrutiny during testing. It was the only diffuser tested with different chamber pressure ramp rates ( $dP_{cc}/dt$ ) and both the conventionally-machined and DMLS nozzles. Figure 4 depicts typical fast and slow thruster transients and shows its tendency to produce higher ramp rates when targeting higher chamber pressures. Shutdown profiles are also given. The pumpdown curves produced by CDF in response to the various nozzle and transient combinations are plotted in Figure 5. The effect of higher chamber pressure ramp rate was a distortion of the idealized curves; diffuser start and unstart pressure ratios were unchanged but evacuation of the test cell lagged plume development. The shorter chamber of the DMLS nozzle produced a 4% decrease in combustion efficiency which was enough to induce a second-throat-area non-start condition. This data is unique; it is quite unusual to have two nearly-identical nozzles with differing combustion efficiencies coupled with the same diffuser designed so close to the area limit that the combustion efficiency would be relevant. Taken collectively, the CDF data demonstrates the importance of slower chamber pressure ramp rates and complete combustion when attempting to experimentally resolve the pumpdown process. Testing of all other configurations employed the conventionally-machined nozzle.

Pumpdown curves of all starting second-throat diffusers are compared in Figure 6. Data was plotted without smoothing or down sampling. Density of points provides qualitative insight on how quickly the system moved through a given portion of the curve and how much variation occurred test-to-test. Nominal plume development followed the pattern described in Figure 3 with the individual curves stretched or compressed along the dimension of driving pressure ratio according to the diffuser's performance. Off-nominal plots include oscillatory pseudo-starts resulting from insufficient throat length (AF, B, BF, C, CF) and non-starts resulting from insufficient pressure ratio (all others).

Relative performance of the three inlet geometries can be parsed from the data shown. Configurations without a throat spool were too short to achieve absolute start without first pushing through the oscillatory pseudo-start mode. For this subset, diffuser performance was most sensitive to length and inlet A produced the best results. The addition of either throat spool stabilized start behavior and the lower volume of inlet C reliably provided the best performance.

Variation of performance with assembly type is shown in Figure 7. Trends matched expectations. Standalone inlets gave the worst performance. Improvements in both start and unstart pressure ratios were observed with the attachment of a subsonic diffuser. Further improvement was obtained on both fronts by adding the short throat spool. Switching to the long throat spool improved unstart pressure ratio at the expense of slightly degraded start performance. Removal of the subsonic diffuser universally decreased performance. Figure 8 recasts performance variation in terms of diffuser length. Unstart pressure ratio improved with increased length regardless of assembly type. Start pressure ratio improved through a total-length-to-throat-diameter ratio of 8, then decreased at different rates depending on whether the additional length was dedicated to a subsonic diffuser or a longer throat. Longer diffusers were also noted to be more sensitive to inlet design.

Once a diffuser reaches steady state, pressure measurements along its wall can shed light on the shock structure contained within. This is especially true if the data is used to ground CFD. Meaningful predictive simulations are difficult to achieve because solutions to the Navier-Stokes equations are not unique. In practice, this means that a solver may produce a started, unstarted, or oscillatory solution for a given pressure ratio, and that solution may also be highly path-dependent. An analyst may not be able to tell *a priori* which would best approximate reality. However, postdictive simulation can enable accurate reconstruction of pressure data and visualization of hot-fire flow fields that would be impossible to produce experimentally. This approach is incredibly useful for understanding diffuser behavior even though it requires some cherry-picking of the CFD results.

Figure 9 shows experimental and simulated steady-state wall pressures for each second-throat diffuser during nominal and off-nominal operation. The plots are accompanied by visualizations of CFD-produced Mach number gradients to show the internal shock structure. Non-started flow fields were effectively identical for all diffusers. A large cap shock was positioned near the exit of the nozzle with RSS reflections [35] extended from the nozzle lip and attached to the diffuser inlet. The started shock structures of the standalone inlet configurations were very similar, the difference being that the shock pushed out into the diffuser inlet just enough to isolate the test cell.

Adding the subsonic diffuser created a different shock structure in each inlet. A cap shock was observed in configuration AF which gave rise to a large subsonic core flow that only managed supersonic reacceleration at the end of its throat. BF produced a regular reflection of the impingement shock, flow separation in the contraction, and a large barrel shock terminating with a Mach disk in the subsonic diffuser. CF produced a Mach reflection of the impingement shock. Downstream flow reaccelerated quickly but separated in its contraction.

With the addition of either throat spool, inlet A reliably produced regular reflections of the impingement shock and inlet C produced Mach reflections. The longer throat spool provided sufficient space for multiple reflections to occur. Configuration BEF behaved similarly to BF, with a regular reflection of the impingement shock, separation in the contraction, and a barrel shock sitting in the throat. The longer throat spool adversely impacted the flow. In BD, separation bubbles formed immediately downstream of impingement and at the transition into

the throat. Mach reflection of the terminal shock occurred ~3/4 through the throat. In BDF, impingement caused strong separation in the inlet and the flow did not recover until its transition into the throat. The flow separated ~3/4 through the throat but reattached at its end before separating again in the subsonic diffuser. The unusual shock structure was very repeatable and did not change with increased pressure ratio. In light of the CDF data captured with the DMLS nozzle, it was hypothesized that the higher losses created by inlet B's steeper contraction angle combined with the minor losses induced by the successive additions of throat length were causing the configurations to incrementally approach the minimum second-throat area. Observations were consistent with throat restriction; pressure built upstream of the throat and caused separation in the contraction. CFD simulations failed to capture the nuanced separation behavior exhibited by BD and BDF in their started states.

Temperature measurements can be equally useful in determining the behavior inside a diffuser. It may be impossible to distinguish between centerline Mach and regular reflections from wall pressure data, but the higher radiant heat flux of a Mach disk will show up in temperature data. This effect is visible in several of the peak pressure-normalized heat flux density plots shown at the right of each visualization in Figure 9. The magnitude of peak 0.1-s thermal loads often varied widely along the length of a given diffuser depending on the flow structure. Values typically spanned 5-60 W/m<sup>2</sup>-Pa<sup>0.8</sup> but fluxes as high as 90 W/m<sup>2</sup>-Pa<sup>0.8</sup> were noted in some configurations. The sensors did not necessarily experience peak rates synchronously but the tight agreement between starting and non-starting runs reveals that they primarily occurred immediately prior to start. This makes sense; the non-started shock structure creates a hot subsonic core flow surrounded by annular shock reflections propagating along the diffuser walls. As soon as supersonic flow is established, both temperature and pressure drop, resulting in reduced heat flux to the walls. There are some exceptions to this. For example, if a strong shock forms in the diffuser during steady operation, the started value may be higher than the non-started. The downstream separation shock in configuration CDF is an example.

A few caveats apply to the heat transfer data. Pressure measurements took priority in this test series, and thermocouple installation was performed less rigorously. Upon inspection, some were found to protrude into the flow and were not filed back to flush in the interest of time. As their primary purpose was to prevent test article damage by enabling redlines on temperature, conservative values were not considered problematic. Accordingly, there is some unquantified amount of conservatism in the reported heat flux values.

Photographs of test article hardware are provided in Figure 10.

## Centerbody Configurations

A modular approach was also taken in the design of the centerbody diffuser hardware. The centerbody and shell, depicted in Figure 11, were both constructed in removable segments. Each shell segment had two instrumentation ports centered axially and clocked 180° circumferentially. The hollow centerbody was attached to a dedicated shell spool via 45° struts of obround cross-section. Two interchangeable nosecones and the first cylindrical segment featured internal instrumentation bosses. The tip of each nosecone was fitted with a thermocouple. Cables were routed into the centerbody through the struts.

Aerodynamic contours of the two tested configurations are given in Figure 12, with geometric and performance characteristics provided in Table 3. The difference between the nosecones is slight, just enough to provide insight on the sensitivity of the system to the penetration depth into the nozzle. CB-1 started and unstarted occurred at the same pressure ratio. CB-2's 1° increase in nosecone half-angle and resultant decrease in penetration depth increased start pressure ratio and decreased unstart pressure ratio. A general difference in pumpdown efficacy can also be seen in Figure 13; the RSS progression was faster and occurred at lower driving and cell pressures in CB-1.

While the plume development in both configurations broadly followed the same trends described in Figure 3, a few additional features are discernible in the pumpdown curves. Differences arose as the plume began to impinge on the nosecone tip. A bow shock formed around the leading edge and a  $\lambda$ -shock pattern was established on the centerbody in addition to the RSS reflections along the nozzle wall. As the plume continued to push downstream, the RSS tendrils impinged upon the shell wall and evacuated the test cell. Each of these phenomena produced a downward inflection point on the pumpdown curve. Further increase of driving pressure resulted first in full flow of the nozzle and plume attachment on the shell wall, then separation of the boundary layer from the shell and attachment to the centerbody. The shock cells subsequently expanded outward until the plume attached to both walls simultaneously and started the diffuser. This sequence showed up as a 'double-knee' shape in the pumpdown curves. The progression is annotated with illustrations in Figure 13.

In Figure 14, the steady-state pressures of CB-2 represent the two final stages of the sequence. In the non-started case, the plume structure is comparable to a free jet core flow which happens to be wrapped around a centerbody, and the smooth pressure rise along the shell wall suggests that it behaves similarly. No pressure data was captured along the centerbody but CFD indicated a high degree of variation through numerous shock reflections. In the started case, reflection of the impingement shock gave rise to a separation bubble on the centerbody. The flow recovered quickly and terminal separation occurred  $\sim 2/3$  through the throat with the shock train remaining attached to the centerbody wall. CB-1 was not tested at steady non-started conditions. In the started case, the small change in nosecone geometry produced significant differences in the shock structure, with boundary layer separation occurring further upstream and higher wall temperatures observed throughout the throat (not shown).

Normalized rates of heat transfer were comparable in magnitude to second-throat configurations, with peaks of  $20\text{-}60 \text{ W/m}^2\text{-Pa}^{0.8}$  primarily occurring immediately prior to start. Nosecone tips were an exception; fluxes of  $50\text{-}80 \text{ W/m}^2\text{-Pa}^{0.8}$  occurred shortly after ignition as plume impingement began. Nevertheless, these higher thermal loads were similar to those in second-throat configurations induced by shock reflections along the wall or Mach disks along the centerline. Cooling would have been readily achievable in a full-scale system. That said, the subscale hardware was uncooled and slight erosion was observed on both nosecones after several tests. Photos of the damage are shown in Figure 15. The damage to nosecone 2 could be described as a slight ripple around the edges of a shallow, previously-molten pool of steel surrounding the thermocouple. Nosecone 1 did not fare as well. Liquid metal began to streak downstream and score small channels into the profile. The damage to both nosecones mostly affected surface texture and did not significantly change their bulk geometries. Testing continued with the objective of assessing any aerodynamic impacts. Though the damage undoubtedly altered the flowfield in its immediate vicinity, no measurable difference in pumpdown efficacy or steady-state flow structure were discernible in the data.

### Spike Configurations

Aerodynamic design of the spike diffuser began with modification of the 1962 LeRC topology [21] to make it practical for testing full-scale rockets. The nosecone was blunted to allow backside cooling, the diffuser-inlet-to-nozzle exit ratio was increased to accommodate gimbal, the inlet was flared outward to accommodate high nozzle exit angles, and the subsonic diffuser was routed axially to prevent damage to supporting infrastructure. The spike tip was also positioned upstream of the nozzle exit in order to force the conical shock formation at lower Mach number. Numerous variants of the modified topology were evaluated using Loci/CHEM simulations over the course of an intense two-week design window. Crude manual optimization produced a baseline contour depicted in the drawings of Figure 16.

Each tested configuration was defined by an assembly of six components: one nosecone, one set of spike and shell segments which defined the inlet and throat profiles, another set of spike and shell segments which formed a subsonic diffuser, and one aft support claw which fixed the spike to the shell. Small stacks of washers were inserted between the claw and other components as needed to change spike position. As with the other diffusers, two series of instrumentation bosses were installed on opposing sides, one dedicated to pressure transducers and the other to thermocouples. Three thermocouples were installed in the original steel nosecone of the spike, with one placed at the tip and two along the inlet section. Tip erosion was monitored between tests and the nosecone was refinished with a slightly larger radius once the accumulated damage progressed from pooling around the thermocouple to streaking downstream. The spike was later modified to accept uninstrumented but interchangeable Inconel 718 nosecones of varying tip radii. A set of smaller tailcone segments was also fabricated. Aerodynamic contours of all spike diffuser components are detailed in Figure 17. The baseline configuration was defined by the core spike

and shell components coupled with nosecone 3 and tailcone X, designated SPK-3X in this report.

Table 4 provides a list of all tested assemblies alongside corresponding geometric and performance characteristics. Sensitivities to nosecone blunting and spike position are determinable from the given data. Increases in nosecone radius led to worse start performance but the effect was small. As shown in Figure 18, the degradation between nosecones 1 and 4 was only 2%. Impact on unstart pressure ratio was more significant, with a 5.5% degradation observed. Axial position of the spike was a stronger determinant of performance, as shown in Figure 19. Downstream translation of 0.72 cm from its minimum-starting position produced 7% and 6% degradations in start and unstart pressure ratio, respectively. Moving the spike upstream of the minimum precluded start and tripled the steady-state cell pressure. Switching subsonic diffusers from X to Y gave mixed but mostly undesirable results. With nosecone 3, 2.8% and 4.8% increases were observed in start and unstart pressure ratio. With nosecone 4, a 0.8% decrease was noted in start pressure ratio but a 2.6% increase in unstart pressure ratio.

Taken as a group, the spike diffuser variants represented only minor changes to the overall geometry. Differences in performance were also small, with a 9% difference observed between the best- and worst- starting configurations. This consistency is seen in the pumpdown curves of Figure 20. All nominal cases produced the same structural progression observed in the centerbody diffusers, though initial impingement on the flared inlet was less severe and did not produce the 'double-knee'. The spike diffusers were also much more efficient at pre-start pumping; the entire plume development sequence occurred at lower chamber and cell pressure ratios. Another point of note came from the position sensitivity data. As the spike was incrementally moved toward the shell test-to-test, pumping efficacy increased until the throat area reached its minimum limit and starting was no longer possible. This bracketed the spike diffuser's minimum contraction ratio between 0.38 and 0.39.

Consistency was also observed in the steady-state flow fields depicted in Figure 21. All started configurations produced similar shock structures characterized by conical shock propagation from the nosecone to the inlet and 2-3 impingement shock reflections through the annular throat prior to boundary layer separation. The highest degree of variation was observed downstream of separation. Depending on the driving pressure ratio and strength of the incident shock, the plume would detach either solely from the shell or from both walls before reattaching to the spike. Any residual supersonic cells invariably shocked down quickly after reaching the subsonic diffuser. All pressure ratio non-starts exhibited similar behavior as well. The boundary layer separated from both nozzle and spike walls and a large recirculation bubble formed on the spike upstream of the nozzle exit. Reattachment occurred in the diffuser inlet. For all tailcone X configurations but one, the plume detached from the spike and attached to the shell at the transition to the diffuser throat before shocking to subsonic. The plume remained attached to the spike in tailcone Y configurations.

The only standout shock structure was that of the non-start produced by insufficient throat area ( $SPK-4X$ ,  $dx/R_{NE} = -0.029$ ). Like the second-throat restriction suspected in BDF, pressure buildup in the inlet was needed to pass the mass flow

through the throat. A large separation bubble consumed most of the inlet while an annulus of reflected shocks lined the contraction. Flow regained supersonic conditions in the throat.

Peak normalized rates of heat transfer were asynchronous but invariably prior to start. The nosecone experienced its maximum shortly after ignition as plume impingement began. By contrast, the most intense thermal loads observed downstream in the diffuser occurred immediately prior to start. No strong Mach reflections were present in the steady flow fields to drive heating beyond the pre-start maxima. Rates of  $50\text{-}70 \text{ W/m}^2\text{-Pa}^{0.8}$  were observed in the instrumented nosecone. With the spike in its baseline position or aft, the thermal environments through the inlet and throat were comparatively benign and the walls experienced  $20\text{-}50 \text{ W/m}^2\text{-Pa}^{0.8}$ . In the aerodynamically-optimum forward position, maximum energy flow into the nosecone was unchanged, but inlet and throat values jumped to  $75\text{-}125 \text{ W/m}^2\text{-Pa}^{0.8}$ . No data was captured in the tailcone segments.

Several photographs taken of the spike diffuser hardware during testing show thermal effects on the hardware and are provided in Figure 22. Featured phenomena include boundary layer separation along the shell wall made visible by external condensation of atmospheric humidity, steel nosecone erosion prior to its refinishing, and bands of discoloration on the polished stainless identifying shock reflections along the spike. Photos of installation and test are also shown.

### Performance Comparison

The advanced diffusers described above produce clear aerodynamic benefits over their conventional second-throat counterparts. The large disparities in pumping performance become apparent when the pumpdown curves of each topology's best-starting diffuser are juxtaposed, as in Figure 23. At every point along the curve, the spike diffuser produced better pumping performance than the centerbody, which in turn outperformed the second-throat. As a result, the plume was able to move through its characteristic structural progression at lower driving pressures. SPK-1X demonstrated start/unstart pressure ratio improvements of 24%/23% compared to the best-starting second-throat diffuser (CEF) and 25%/9% compared to the best-unstarting second throat diffuser (CDF). These improvements were accomplished in a compact spatial envelope; SPK-1X was 46% shorter than CEF, 57% shorter than CB-1, and 68% shorter than CDF. By contrast, CB-1 gave modest and mixed results with respective start/unstart improvements of 11%/3% vs. CEF and 12%/-15% vs. CDF.

The pressure-normalized heat fluxes discussed in prior sections are useful for parsing flow structures within a set of similar diffusers. However, raw values are more appropriate for assessing differences between topologies because the advanced diffusers produce the pre-start maxima at lower driving pressures. The most severe absolute rates of heat transfer observed in CEF and CB-1 were comparable. CEF experienced  $11.5 \text{ MW/m}^2$  along its inlet while the spike and shell of CB-1 experienced  $11.3 \text{ MW/m}^2$  and  $11.4 \text{ MW/m}^2$ , respectively. SPK-1X, tested without nosecone instrumentation and only in the forward spike position, sustained a much higher maximum of  $19.2 \text{ MW/m}^2$  on its shell. This likely could have been reduced to  $\sim 9 \text{ MW/m}^2$  by moving the spike downstream to its baseline position and incurring

start/unstart performance penalties of ~2-3%. SPK-3X was the closest tested configuration. Its nosecone experienced a maximum of  $11.9 \text{ MW/m}^2$ , which is only 3.5% higher than CEF's peak heat flux, yet the configuration still provided start/unstart pressure ratio improvements of 22%/21% vs. CEF and 23%/5% vs. CDF. As discussed in prior sections, these heat flux values are quantitatively conservative but, taken qualitatively, can be considered clear evidence that a spike diffuser's thermal loads may be kept on par with those of second-throat topologies without sacrificing augmented aerodynamic performance.

### Start Performance: A 30 km Perspective

An extensive literature review was conducted to ensure that the performance gains cited above accurately captured the potential of advanced diffuser topologies. Experimental data was compiled from a variety of additional sources [36-65] to reveal the empirical limits of conventional diffuser design. Key geometric and performance parameters of 1058 distinct configurations were assembled into a database for ease of meta-analysis. While great effort was dedicated to finding and cataloging every relevant data point available to the author, the compendium was not intended to provide an exhaustive review of all diffuser applications. Several criteria were established to keep the database focused on the application of single-engine testing:

<u>Qualifiers</u>	<u>Disqualifiers</u>
- Determinable geometry.	- Clustered, gimballed, annular, or asymmetric driving nozzles.
- Negligible secondary mass flow.	- Diffusers with centerline turns.
- Starting pressure ratio data.	- Substantial axial gap between the nozzle exit and diffuser inlet.
- Reported inlet Mach number or inlet-to-nozzle-throat area ratio.	- Steam as the motive fluid.

The decision to exclude systems driven by steam may seem counterintuitive given that most rockets generate copious amounts in their exhaust, but its expansion is dominated by multiphase effects even when superheated in the chamber. In practical terms, maintaining single-phase steam through a rocket-like expansion process requires a rocket-like combustion process upstream.

Diffuser inlet conditions were used in the performance database to contextualize start and unstart pressure ratios of all configurations. If either the inlet Mach number or area ratio were unreported in the original source, a quasi-one-dimensional calculation was performed to fill in the missing value. For non-reacting flows, this was done with the isentropic relations [66] using a fixed isentropic exponent. For reacting flows, NASA's Chemical Equilibrium with Applications (CEA) code [67] was used. Data was sorted by motive fluid into four groups: solid propellants, common liquid propellants and ethane, air/nitrogen, and everything else. Ethane's conspicuous inclusion among the common liquid propellants is explained by the author in previous memoranda [44, 68]. Frontiers of empirically-demonstrated performance were found for cylindrical and second-throat topologies on a per-group basis, as applicable. Configuration CEF defines the frontier of second-throat start

performance at its Mach number and area ratio. This is easily seen in Figure 24, where the full database of start pressure ratios is plotted against diffuser inlet conditions to give a sense of how performance varies with motive fluid, as viewed from fluidic and geometric perspectives. Given this broader context, the author is confident that CEF is an exemplary representative of conventional diffuser design and is an appropriate standard to which advanced diffusers may be compared. Figure 25 plots all known advanced diffuser data against the same cylindrical and second-throat frontiers. The centerbody and spike diffusers presented in this study sit comfortably below the conventional curves. All other hot-fire/ethane advanced diffuser data points are tied to unpublished relatives of the present study, with the exception of one centerbody configuration used by the German Aerospace Center (DLR) to test the Vulcain engine [13-16]. All plotted data is available in Tables 5-7.

## LOOKING FORWARD

Design time for the advanced diffusers featured in this report was notably constrained, and the contours were products of rudimentary manual optimization. More rigorous techniques may further enhance aerodynamic performance. It is also noted that the stagnation pressure saved by forcing a conical shock at the diffuser inlet would increase with higher Mach number and lower isentropic exponent. This has significant implications for applications beyond rocket testing. On the high-Mach side, one could easily imagine implementation in hypersonic wind tunnels (many still use constant-area diffusers), or in industrial multistage ejector systems. On the low-isentropic-exponent side, ejector-based refrigeration cycles could see particular benefit. SSC is currently developing spike-based air and steam ejectors intended to reduce the operating costs of NASA's current and future facilities.

## CONCLUDING REMARKS

Performance characteristics of second-throat, centerbody, and spike diffusers have been experimentally assessed in pursuit of economical means of upper-stage rocket engine testing. Extensive literature review has been conducted to ensure exemplary second-throat diffuser performance and enable fair, direct comparison between topologies. Starting pressure ratio reductions of 11% and 24% were achieved with centerbody and spike configurations, respectively. Peak heat fluxes observed within the spike diffuser were particularly high in the aerodynamically-optimum configuration operating just above the minimum throat area. This was alleviated by shifting the spike slightly downstream. The shifted configuration started at a pressure ratio 22% lower and experienced a maximum heat flux 3.5% higher than the best conventional design.

## NOMENCLATURE

A	Area	R	Radius
$c^*$	Characteristic Velocity	RSS	Restricted Shock Separation
CON	Conical Geometry	T	Temperature
D	Diameter	t	Time
FAIR	Nozzle with fairing attached to produce axial exit flow	TIC	Truncated Ideal Contour
FSS	Free Shock Separation	TOC	Thrust Optimized Contour
L	Length	TOP	Thrust Optimized Parabolic
M	Mach Number	WT	Wind Tunnel
NR	Not Reported	x	Axial Position
O:F	Oxidizer-to-Fuel Mass Ratio	$\gamma$	Isentropic Exponent
P	Pressure	$\Delta$	Nosecone Penetration Depth
		$\theta$	Angle

### Subscripts

0	Stagnation Condition	DT	Diffuser Throat
BACK	External Condition at Diffuser Exit	MIN	Minimum
BODY	Throat Portion of Centerbody	NC	Nosecone
CB	Centerbody	NE	Nozzle Exit
CC	Combustion Chamber	NT	Nozzle Throat
CELL	Test Cell	SPK	Spike
CYL	Cylindrical	ST	Second Throat
D	Diffuser	SUB	Subsonic
DI	Diffuser Inlet	TIP	Tip of Nosecone
		TAIL	Tapered Aft Section of Centerbody

## REFERENCES

1. Hagginbothom Jr, W. : "Straight-Pipe Diffuser Thruststand for Measuring High Altitude Rocket Performance," JANAF RKT2395, 1958.
2. Jones, W. Aukerman, C. and Gibb, J. : "Experimental Performance of a Hydrogen-Fluorine Rocket Engine at Several Chamber Pressures and Exhaust-Nozzle Expansion Area Ratios," NASA TM X-387, 1960.
3. Aukerman, C. and Church, B. : "Experimental Hydrogen-Fluorine Rocket Performance at Low Pressures and High Area Ratios," NASA TM X-724, 1963.
4. Sivo, J. and Peters, D. : "Comparison of Rocket Performance Using Exhaust Diffuser and Conventional Techniques for Altitude Simulation," NASA TM X-100, 1959.
5. Mickola, R. : "Performance Summary of the Supersonic Diffuser and its Application to Altitude Testing of Captive Rocket Engines," AFFTC-TR-60-1, Addendum 1, 1961.
6. Roschke, E., Massier, P. and Gier, H. : "Experimental Investigation of Exhaust Diffusers for Rocket Engines," JPL-TR-32-210, 1962.
7. Sivo, J., Meyer, C., and Peters, D. : "Experimental Evaluation of Rocket Exhaust Diffusers for Altitude Simulation," NASA TN D-298, 1960.
8. Rao, G. V. R. : "Short Diffuser for Testing Rocket Nozzles," in Liquid Rockets and Propellants, 1960, pp. 89-93.
9. Chamberlain, J. and Olson, R. : "Development of an Exhaust Diffuser for Ground Testing Rocket Engines," in Liquid Rockets and Propellants, 1960, pp. 99-116.
10. Hale, J., and Gobbel, W. : "Diffuser Auxiliary Ejector Development for the Design of the J-3 LEM Descent Exhaust System," AEDC-TR-65-255, 1965.
11. "Centerbody Diffuser Study," Aerojet-General RN-S-0243, 1965.
12. German, R. C. and Paneschi, J. H. : "Improved Methods for Determining Second-Throat Diffuser Performance of Zero-Secondary-Flow Ejector Systems," AEDC-TR-65-124, 1965.
13. Schäfer, K. : "Simulation of Environmental Flight Conditions by Advanced Altitude Simulation." DLR Institute of Space Propulsion, 2004.
14. Schäfer, K., Böhm, C., Kronmuller, H. and Zimmermann, H. : "Development of P4.1 Altitude Simulation for VINCI Engine," DGLR, 2005.
15. Schäfer, K., Zimmermann, H., Schmidt, V., Suslov, D. and Stark, R. : "Advanced Nozzle Testing in Flight Conditions," 42nd AIAA Joint Propulsion Conference, 2006.
16. "Safety and Environment Masterplan 2020 of DLR's Rocket Test Center Lampoldshausen," 6th IAASS Conference, 2013.
17. Edwards, D., Weaver, H., and Kastner, C. : "Cold-Flow Testing of a Proposed Integrated Center-Body Diffuser/Steam Blocker Concept for Plum Brook Station's B-2 Test Facility," NASA TP 2009-215293, 2009.
18. Klem, M., Smith, T., Wadel, M., Meyer, M., Free, J., and Cikanek, H. : "Liquid Oxygen/Liquid Methane Propulsion and Cryogenic Advanced Development," IAC-11-C4.1.5, 2011.
19. Melcher, J., and Allred, J. : "Liquid Oxygen / Liquid Methane Test Results of the RS-18 Lunar Ascent Engine at Simulated Altitude Conditions at NASA White Sands Test Facility," AIAA 2009-4949, 2009.

20. Yeon, H. I., You, I., Kim, W. C., Im, J. N., and Ko, Y. S. : "An Experimental Study on Startup Characteristics of a Center Body Diffuser for High Altitude Simulation," Transcripts of the Korean Society of Mechanical Engineers, vol. 40, no. 2, 2016.
21. Church, B., Jones, W. and Quentmeyer, R. : "Performance Evaluation of Fixed- and Variable-Area Rocket Exhaust Diffusers Using Single and Clustered Nozzles With And Without Gimbaling," NASA TN D-1306, 1962.
22. Taylor, D., Duesterhaus, D. and Simmons, M. : "Diffuser Studies," AEDC-TR-73-198, 1973.
23. Taylor, D., Duesterhaus, D., Lee, F. and Simmons, M. : "Variable-Area Ejector Development," AEDC-TR-76-97, 1976.
24. Jones, D. : "Hot-Fire Spike Diffuser," US Patent Application No. 16/890,117, 2020.
25. Raines, N., Bircher, F., and Chenevert, D. : "A Subscale Test Facility for Liquid Rocket Propulsion Diagnostics at Stennis Space Center," AIAA-91-3363-CP, AIAA Joint Propulsion Conference, Sacramento, CA, 1991.
26. Luke, E., and George, T., "Loci: A Rule-Based Framework for Parallel Multidisciplinary Simulation Synthesis," Journal of Functional Programming, Volume 15, Issue 03, 2005.
27. Luke, E., Tong, X-L., Wu, J., Tang, L., and Cinnella, P., "CHEM: A Chemically Reacting Flow Solver for Generalized Grids", AIAA 2003.
28. Shang, H.M., Chen, Y.S., Liaw, P., Chen, C.P. and Wang, T.S., "Investigation of Chemical Kinetics Integration Algorithms for Reacting Flows," AIAA Paper 95-0806, 33rd Aerospace Sciences Meeting and Exhibit, 1995.
29. Wilcox, D. C., "Formulation of the k- $\omega$  Turbulence Model Revisited", AIAA Journal, vol. 46, no. 11, 2008.
30. Menter, F. R., "Two-Equation Eddy-Viscosity Turbulence Models for Engineering Applications," AIAA Journal, vol. 32, no. 8, 1994.
31. Cook, W., and Felderman, E. : "Reduction of Data from Thin-Film Heat-Transfer Gages: A Concise Numerical Technique," AIAA Journal, 1966.
32. Jones, D., Allgood, D. and Saunders, G. : "Passive Rocket Diffuser Testing: Reacting Flow Performance of Four Second-Throat Geometries," NASA TM 2016-219221, 2016.
33. German, R. and Bauer, R. : "Effects of Diffuser Length on the Performance of Ejectors Without Induced Flow," AEDC-TN-61-89, 1961.
34. Diggins, J., and Lange, A. : "A Systematic Study of a Variable Area Diffuser for Supersonic Wind Tunnels," NAVORD Report 2421, 1952.
35. Frey, M., and Hagemann, G., "Restricted Shock Separation in Rocket Nozzles," Journal of Propulsion and Power, vol. 16, no. 3, 2000.
36. Unpublished internal data from Space Shuttle Main Engine test program at NASA Stennis Space Center, 1991-1997.
37. Annamalai, K., Visvanathan, K., Sriramulu, V. and Bhaskaran, K. A. : "Evaluation of the Performance of Supersonic Exhaust Diffuser Using Scaled Down Models," Exp. Therm. Fluid Sci., vol. 17, no. 3, pp. 217-229, 1998.
38. Unpublished internal data from J-2X test program at NASA Stennis Space Center, 2011-2013.
39. Unpublished internal data from subscale Orion Orbital Maneuvering Engine / White Sands Diffuser test program at NASA Stennis Space Center, 2015.

40. Ashokkumar, R., Sankaran, S., Srinivasan, K. and Sundararajan, T. : "Effects of Vacuum Chamber and Reverse Flow on Supersonic Exhaust Diffuser Starting," Journal of Propulsion and Power, vol. 31, no. 2, 2015.
41. Yilmaz, C., McCormick, J., Benhidjeb-Carayon, A., Whitehead, B., Gabl, J., and Pourpoint, T. : "Design and Performance Evaluation of an Exhaust Diffuser for Altitude Testing of Chemical Rocket Engines," AIAA Propulsion and Energy Forum, Virtual, 2020.
42. Unpublished internal data from subscale Space Launch System Exploration Upper Stage diffuser test program conducted at Purdue University for NASA Stennis Space Center, 2020-2021.
43. Back, L., Cuffel, R. and Massier, P. : "Flow and Heat Transfer Measurements Along a Cooled Supersonic Diffuser," AIAA Journal, vol. 22, no. 6, 1984.
44. Jones, D. : "Physical Simulation of Rocket Exhaust Aerodynamics Using Heated Ethane: Prototypical Experiments," NASA TM 2020-5009122, 2020.
45. Kantrowitz, A. and Donaldson, C. : "Preliminary Investigation of Supersonic Diffusers," NACA ACR No. L5D20, 1945.
46. Wegener, P. and Lobb, R. K.. : "NOL Hypersonic Tunnel No. 4 Results II: Diffuser Investigation," NAVORD REPORT 2376, 1952.
47. Barton, D. and Taylor, D. : "An Investigation of Ejectors Without Induced Flow, Phase I," AEDC-TN-59-145, 1959.
48. Taylor, D., Barton, D. and Simmons, M. : "An Investigation of Cylindrical Ejectors Equipped with Truncated Conical Inlets - Phase II," AEDC-TN-60-224, 1960.
49. Fortini, A. : "Performance Investigation of a Nonpumping Rocket-Ejector System for Altitude Simulation," NASA TN D-257, 1959.
50. Bauer, R. and German, R. : "Some Reynolds Number Effects of The Performance of Ejectors Without Induced Flow," AEDC-TN-61-87, 1961.
51. Bauer, R. and German, R. : "The Effect of Second Throat Geometry on the Performance of Ejectors Without Induced Flow," AEDC-TN-61-133, 1961.
52. Holzman, A., Tick, S. and Hinck, E. : "Summary of Experience in the Use of Exhaust Diffusers for Rocket Testing," in Liquid Rockets and Propellants, 1960, pp. 77-88.
53. Jones, W., Price Jr, H. and Lorenzo, C. : "Experimental Study of Zero-Flow Ejectors Using Gaseous Nitrogen," NASA TN D-203, 1960.
54. Panesci, J. H. and German, R. C. : "An Analysis of Second-Throat Diffuser Performance for Zero-Secondary-Flow Ejector Systems," AEDC-TDR-63-249, 1963.
55. Hale, J. W. : "Comparison of Diffuser-Ejector Performance With Five Different Driving Fluids," AEDC-TDR-63-207, 1963.
56. Hale, J. W. : "Influence of Pertinent Parameters on Ejector-Diffuser Performance With and Without Ejected Mass," AEDC-TDR-64-134, 1964.
57. Herron, R. D. : "An Investigation of Ejector Systems Using Very Large Diffusers," AEDC-TR-68-216, 1968.
58. Annamalai, K., Satyanarayana, T., Sriramulu, V. and Bhaskaran, K. : "Development of Design Methods for Short Cylindrical Supersonic Exhaust Diffuser," Experiments in Fluids, vol. 29, no. 4, 2000.
59. Park, B. H., Lim, J. H., and Yoon, W. : "Fluid Dynamics in Starting And Terminating Transients of Zero-Secondary Flow Ejector," International Journal of Heat and Fluid Flow, vol. 29, no. 1, pp. 327–339, 2008.

60. Sung, H.-G., Yeom, H.-W., Yoon, S., Kim, S.-J. and Kim, J. : "Investigation of Rocket Exhaust Diffusers for Altitude Simulation," Journal of Propulsion and Power, vol. 26, no. 2, 2010.
61. Park, B. H., Lim, J., Park, S., Lee, J. H. and Yoon, W. : "Design and Analysis of A Second-Throat Exhaust Diffuser for Altitude Simulation," Journal of Propulsion and Power, vol. 28, no. 5, 2012.
62. Kim, W. C., Yu, I. S., Kim, T. W., Park, J. S., Ko, Y. S. and Kim, M. S. : "A Study on Performance Characteristics of Second Throat Exhaust Diffuser with Back Pressure," Transcripts of the Korean Society of Mechanical Engineers, vol. 41, no. 9, 2017.
63. Jeon, J. S., Kim, W. C., Yeoun, H. I., Kim, M. S., Ko, Y. S. and Han, Y. M. : "An Experimental Study on Performance of Second Throat Exhaust Diffusers of Different Configuration," Transcripts of the Korean Society of Mechanical Engineers, vol. 38, no. 4, 2014.
64. Fouladi, N., Farahani, M. and Mirbabaei, A. R. : "Performance Evaluation of a Second Throat Exhaust Diffuser with a Thrust Optimized Parabolic Nozzle," Aerospace Science and Technology, vol. 94, 2019.
65. Yilmaz, C., Whitehead, B., and Pourpoint, T. : "Numerical & Experimental Investigation of a Diffuser-Ejector System Performance using Cold Gas Thrusters with Conical & Thrust Optimized Bell Nozzles," AIAA Propulsion and Energy Forum, Virtual, 2021.
66. Ames Research Staff : "Equations, Tables, and Charts for Compressible Flow, "NACA TR-1135, 1953.
67. Gordon, S., and McBride, B. : "Computer Program for Calculation of Complex Chemical Equilibrium Compositions and Applications", NASA RP-1511, 1994.
68. Jones, D. : "Physical Simulation of Rocket Exhaust Aerodynamics Using Heated Ethane: Conceptual Foundations," NASA TM 2019-220446, 2019.

TR. This Report

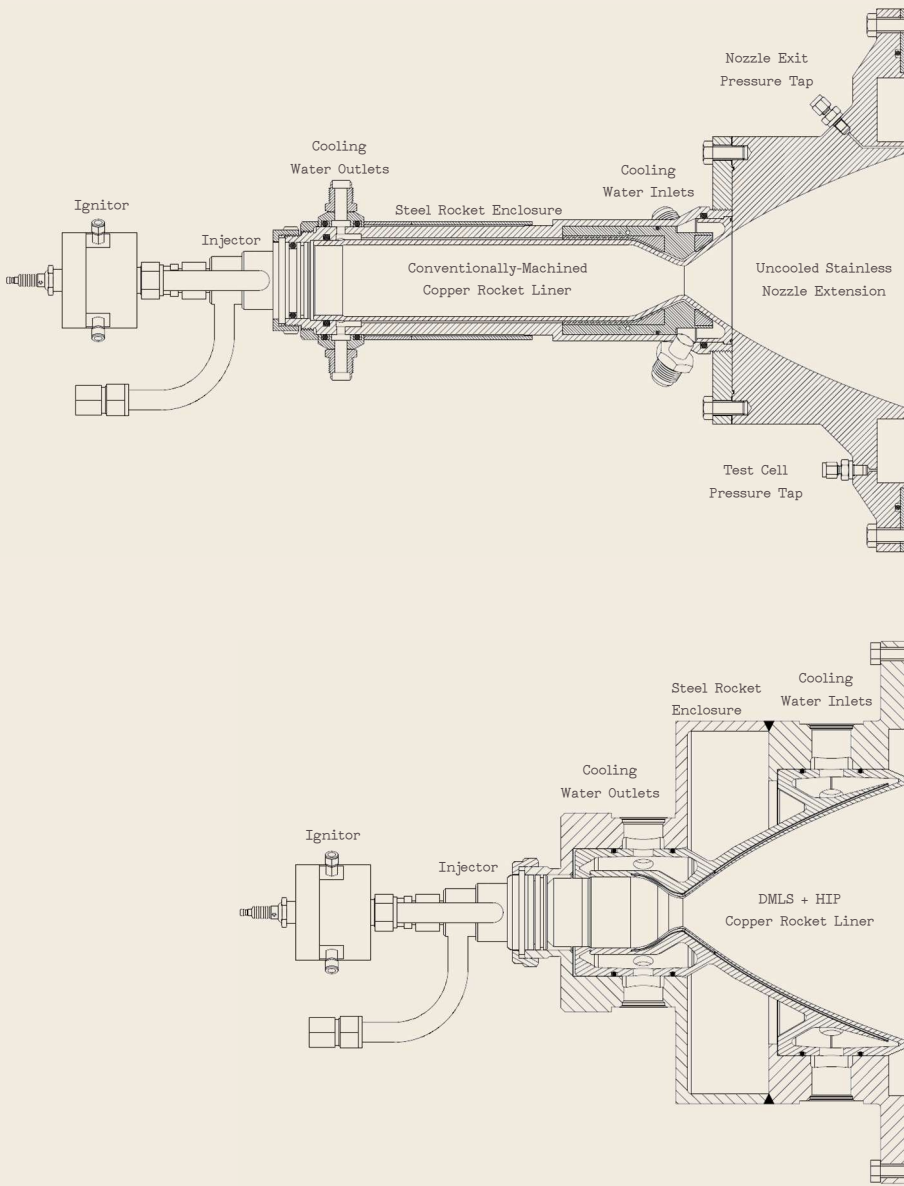


Figure 1. Cross-sections of DTF Thruster nozzle assemblies.

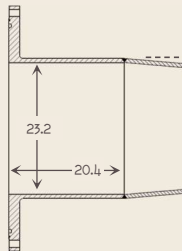
Nozzle	Contour	$L_{CC}$	$D_{NT}$	$\frac{A_{CC}}{A_{NT}}$	$\frac{A_{NE}}{A_{NT}}$	$\theta_{NE}$	No. of Tests	Mean $c^*/c^*_{CEA}$
Conv.	TOP	27.2	2.31	6.1	76.7	19	205	0.98
DMLS	TOP	7.29	2.34	6.0	76.4	19	5	0.94

Table 1.1 Nozzle geometry and performance characteristics.

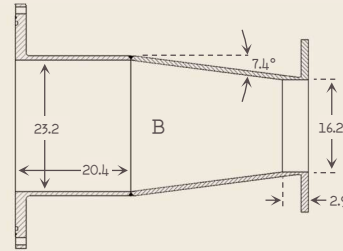
Copper Liner				Steel Extension			
x	r	x	r	x	r	x	r
0.000	1.156	0.826	1.683	3.750	3.788	10.75	7.474
0.012	1.156	0.935	1.763	3.969	3.927	10.97	7.570
0.025	1.157	1.045	1.844	4.188	4.064	11.19	7.665
0.038	1.159	1.154	1.925	4.407	4.199	11.41	7.760
0.051	1.162	1.263	2.005	4.626	4.332	11.63	7.854
0.063	1.165	1.373	2.086	4.845	4.164	11.85	7.947
0.076	1.169	1.482	2.166	5.063	4.593	12.07	8.039
0.088	1.173	1.592	2.246	5.282	4.721	12.28	8.130
0.100	1.179	1.701	2.326	5.501	4.847	12.50	8.221
0.111	1.185	1.811	2.405	5.720	4.971	12.72	8.311
0.123	1.191	1.920	2.484	5.939	5.094	12.94	8.400
0.133	1.198	2.029	2.562	6.157	5.215	13.16	8.488
0.143	1.204	2.139	2.640	6.376	5.335	13.38	8.576
0.154	1.211	2.248	2.718	6.595	5.453	13.60	8.662
0.162	1.217	2.358	2.795	6.814	5.570	13.82	8.749
0.173	1.224	2.467	2.872	7.033	5.686	14.03	8.834
0.186	1.232	2.576	2.948	7.252	5.800	14.25	8.919
0.202	1.242	2.686	3.024	7.470	5.913	14.47	9.003
0.220	1.255	2.795	3.099	7.689	6.025	14.69	9.086
0.243	1.270	2.905	3.173	7.908	6.135	14.91	9.169
0.271	1.289	3.014	3.248	8.127	6.245	15.13	9.251
0.304	1.312	3.123	3.321	8.346	6.353	15.35	9.333
0.345	1.340	3.233	3.395	8.564	6.460	15.57	9.414
0.394	1.373	3.342	3.467	8.783	6.566	15.78	9.495
0.453	1.415	3.452	3.559	9.002	6.671	16.00	9.574
0.525	1.466	3.561	3.611	9.221	6.774	16.22	9.654
0.612	1.528	3.670	3.682	9.440	6.877	16.44	9.733
0.716	1.603	3.750	3.734	9.658	6.979	16.66	9.811
				9.877	7.080	16.88	9.888
				10.10	7.180	17.10	9.965
				10.31	7.279	17.32	10.04
				10.55	7.377	17.54	10.12

Table 1.2 Conventionally-machined nozzle profile, dimensions given in cm.

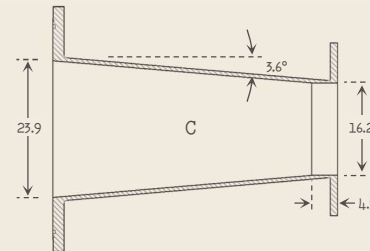
Inlets



A  
23.2  
20.4  
4.9°  
16.2  
4.5

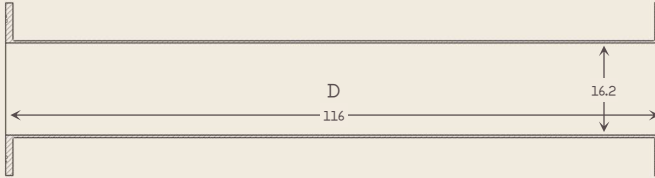


B  
23.2  
20.4  
7.4°  
16.2  
2.9

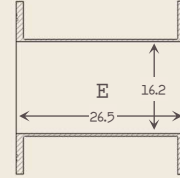


C  
25.9  
20.4  
3.6°  
16.2  
4.5

Throats

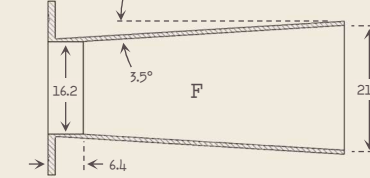


D  
116  
16.2



E  
26.5  
16.2

Subsonic Diffuser



F  
21.8  
6.4  
3.5°

Figure 2. Cross-sections of second-throat diffuser components. Linear dimensions given in cm.

Diffuser Assembly	$\frac{A_{DI}}{A_{NT}}$	$\theta_{DI}$	$\frac{A_{DT}}{A_{DI}}$	$\frac{A_{DT}}{A_{NE}}$	$\frac{A_{DE}}{A_{DT}}$	$\frac{L_D}{D_{DT}}$	$\frac{L_D}{D_{DI}}$	No. of Tests	Avg. 0:F	$M_{DI}$	$\frac{P_{CC}}{P_{BACK}}$	$\left(\frac{P_{CELL}}{P_{CC}}\right) \times 10^5$
[deg]												
A	100.7	4.9	0.49	0.64	-	4.1	2.0	4	5.9	4.78	625	59.4
AF	100.7	4.9	0.49	0.64	1.82	7.3	3.6	4	6.0	4.76	55.4	52.4
AEF	100.7	4.9	0.49	0.64	1.82	8.9	4.4	4	6.1	4.73	50.7	46.9
AD	100.7	4.9	0.49	0.64	-	11.2	5.5	4	6.0	4.76	60.7	39.3
ADF	100.7	4.9	0.49	0.64	1.82	14.5	7.1	19	6.1	4.73	51.7	36.3
B	100.7	7.4	0.49	0.64	-	3.1	1.5	3	5.7	4.84	63.7	63.3
BF	100.7	7.4	0.49	0.64	1.82	6.3	3.1	6	6.1	4.73	60.0	56.3
BEF	100.7	7.4	0.49	0.64	1.82	8.0	3.9	5	6.0	4.76	48.6	45.6
BD	100.7	7.4	0.49	0.64	-	10.3	5.0	6	6.1	4.73	55.4	42.7
BDF	100.7	7.4	0.49	0.64	1.82	13.5	6.6	14	6.0	4.76	48.6	37.6
C	106.9	3.6	0.46	0.64	-	3.1	1.4	4	6.0	4.80	629	62.9
CE	106.9	3.6	0.46	0.64	-	4.8	2.2	5	5.9	4.83	-	-
CF	106.9	3.6	0.46	0.64	1.82	6.3	2.9	10	6.0	4.80	56.1	51.0
CEF	106.9	3.6	0.46	0.64	1.82	8.0	3.7	9	6.0	4.80	45.6	42.2
CD	106.9	3.6	0.46	0.64	-	10.3	4.7	5	6.1	4.77	53	38.9
CDF	106.9	3.6	0.46	0.64	1.82	13.5	6.2	26	6.0	4.80	46.3	109

Table 2. Summary of second-throat diffuser assembly geometric and performance characteristics.

□ Absolute start: Occurs at the minimum  $P_{CC}/P_{BACK}$  which stably isolates the test cell from downstream conditions if the inflow conditions are held constant.

○ Approximate start: Occurs at the  $P_{CC}/P_{BACK}$  obtained by extrapolation of the initial evacuation slope to the steady-state  $P_{CELL}/P_{CC}$  line. Often conservative, but useful when absolute start is indeterminate due to insufficient data resolution or a physical lag in test cell evacuation relative to supersonic plume development.

Approximations will converge to the absolute start curve if any of the following are achieved:

- 1)  $dP_{CC}/dt$  is low enough to keep  $dP_{CELL}/dt$  near zero prior to start.
- 2)  $P_{CC}/P_{BACK}$  does not overshoot the required starting point.
- 3) Test cell volume is small and evacuation is nearly instantaneous.

△ Unstart: Occurs at the  $P_{CC}/P_{BACK}$  below which the test cell is affected by downstream conditions. Onset is independent of  $dP_{CC}/dt$ , though the slope of the subsequent recompression will vary with  $dP_{CC}/dt$  and test cell volume.

✗ Non-start: occurs when the diffuser fails to start, either due to insufficient pressure ratio or insufficient second-throat area.

Operation with insufficient pressure ratio will produce a pumpdown curve nearly identical to that of a starting diffuser, except that it reverses prior to test cell evacuation. A distinct curve may be produced as the driving pressure is reduced, caused by a hysteresis effect in the boundary layer separation within the nozzle.

Operation with insufficient second-throat area will also produce a pumpdown curve initially similar to that of a starting diffuser. However, once the plume begins to expand beyond the nozzle, the diffuser cannot "swallow the shocks" and the flow will lock into a structure characterized by annular shock reflections extending from the nozzle exit to the diffuser inlet.  $P_{CELL}$  remains elevated near impingement levels as  $P_{CC}$  increases.

◊ Pseudo-start: oscillatory start/unstart behavior that occurs when a diffuser is operating with sufficient  $P_{CC}/P_{BACK}$  to force the plume boundary to the diffuser inlet, but insufficient recompression in the throat to keep attachment stable. Absolute start can still be achieved by increasing  $P_{CC}/P_{BACK}$ .

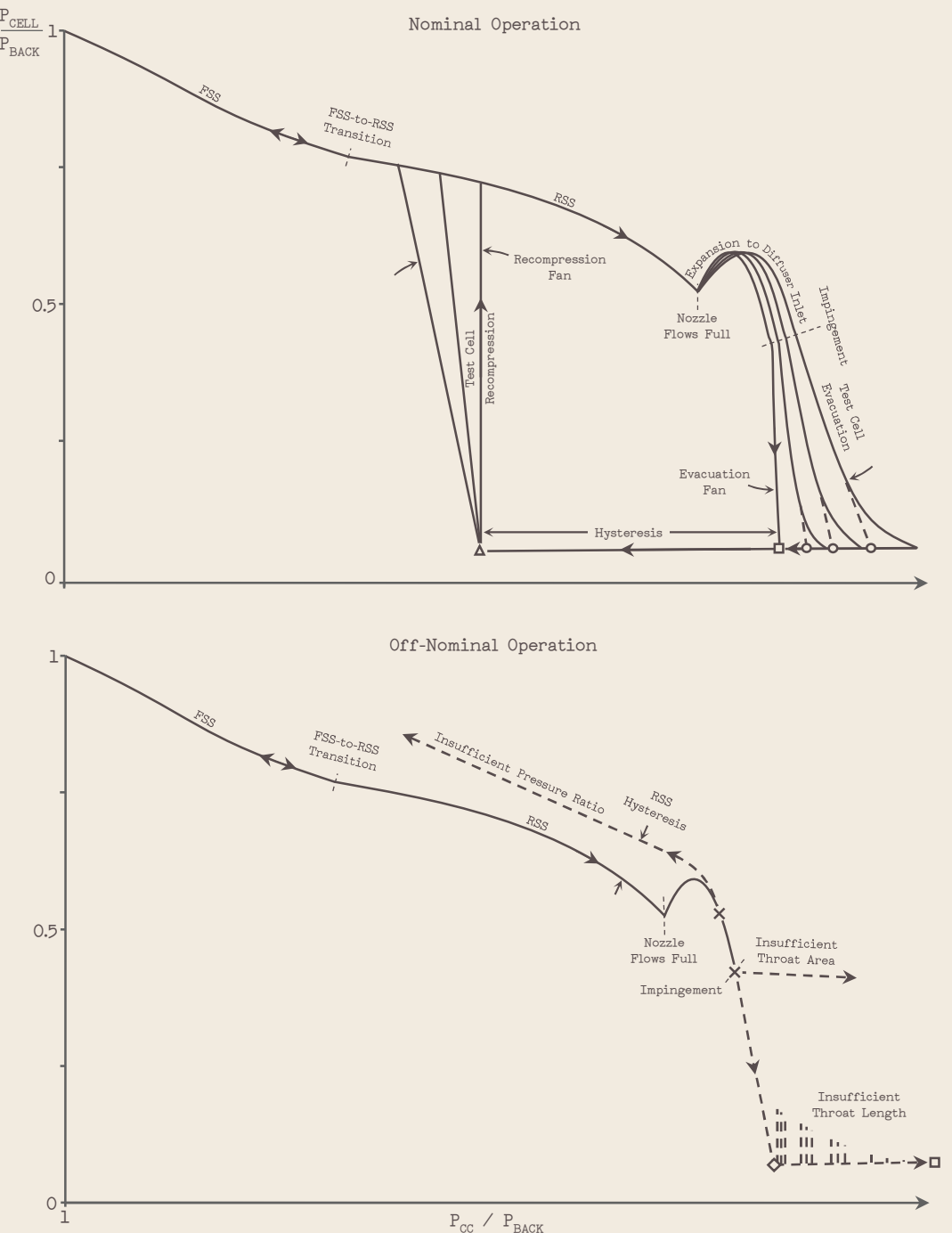


Figure 3. Idealized nominal and off-nominal diffuser pumpdown curves showing plume behavior at varying  $P_{CC}$  ramp rates.

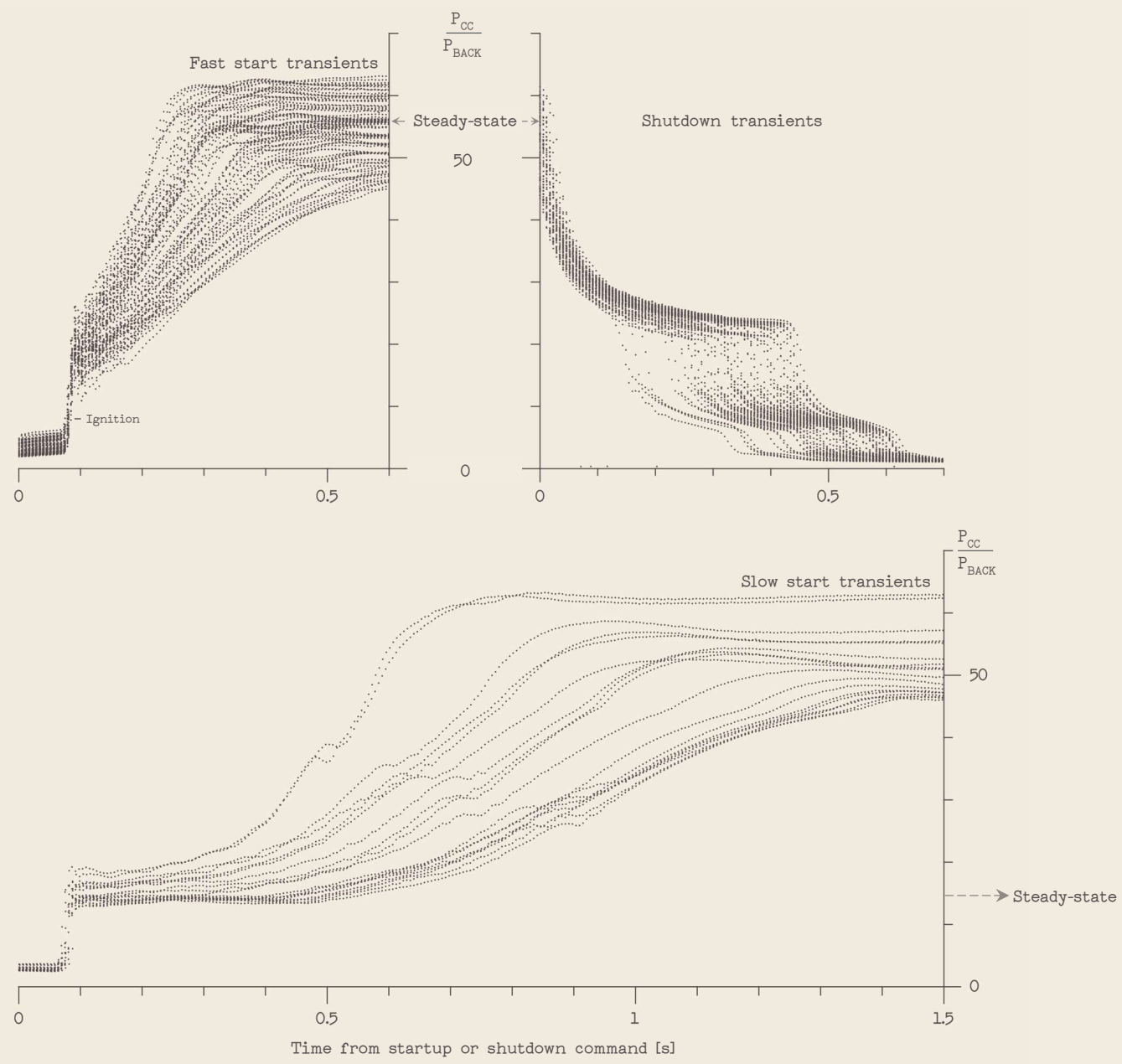


Figure 4. Typical thruster transients.

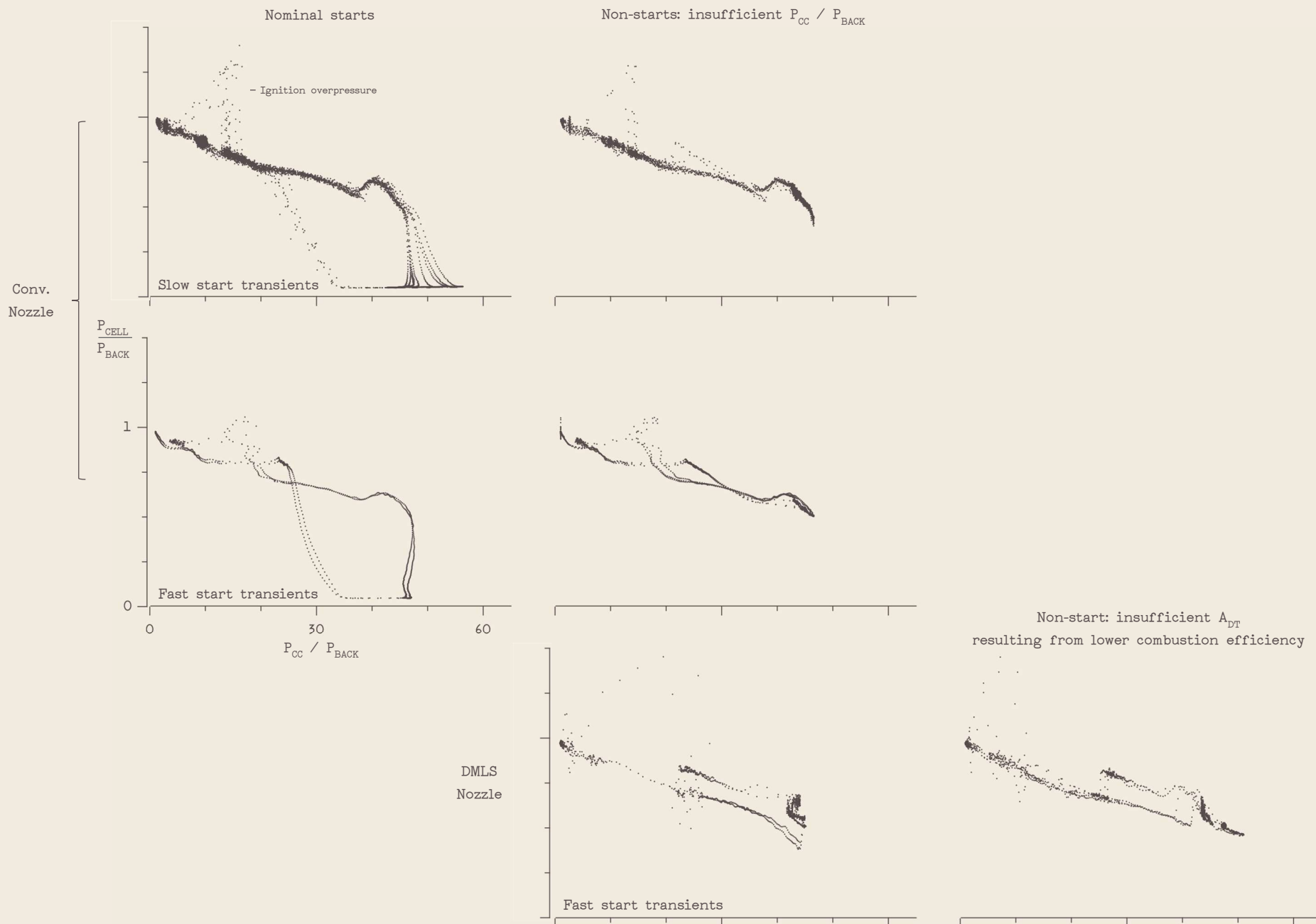


Figure 5. Pumpdown curves, CDF configuration operating with both nozzles and differing  $P_{CC}$  transients.

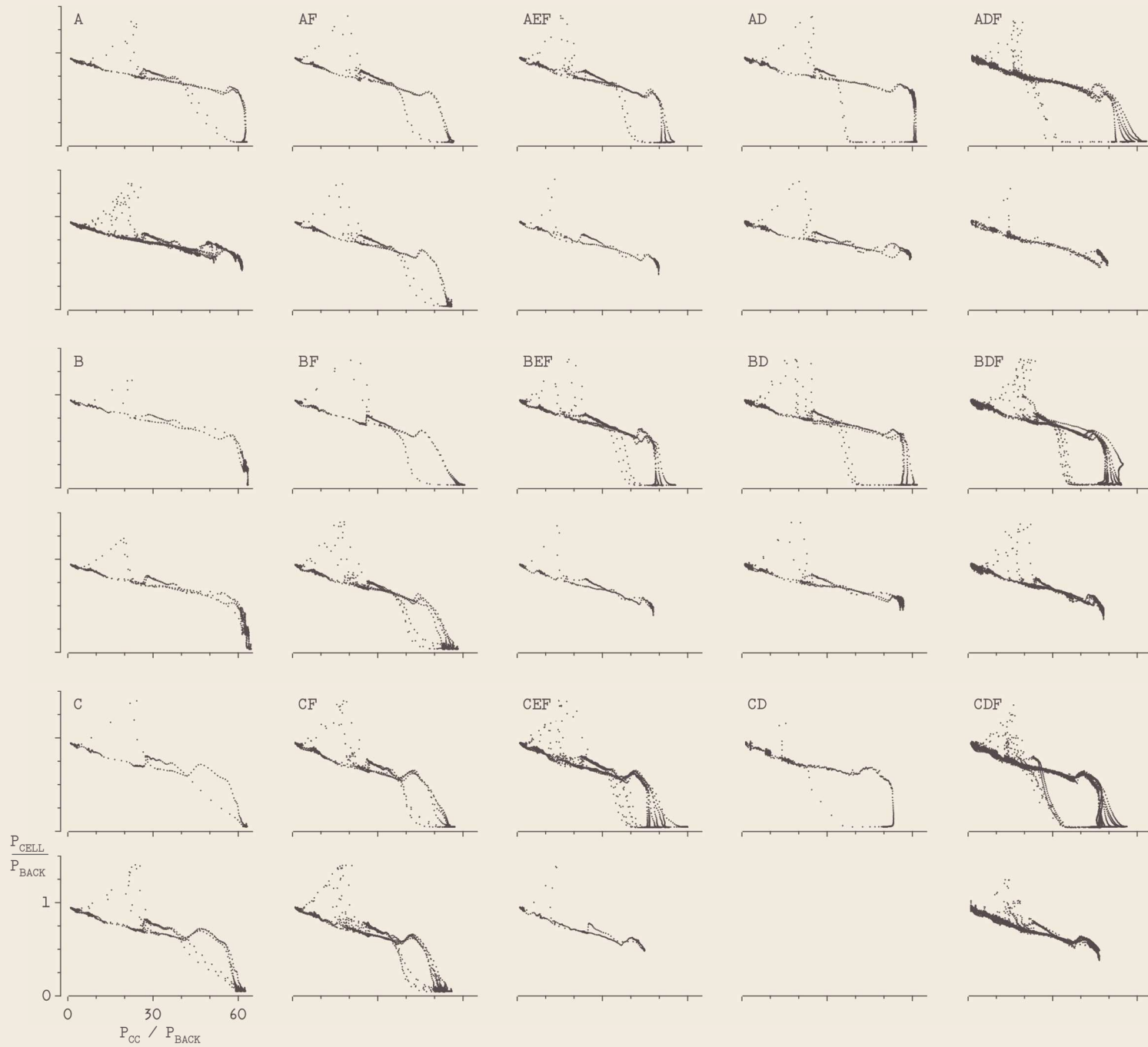


Figure 6. Pumpdown curves, nominal (top) and off-nominal (bottom) behavior of second-throat configurations which achieved absolute start.

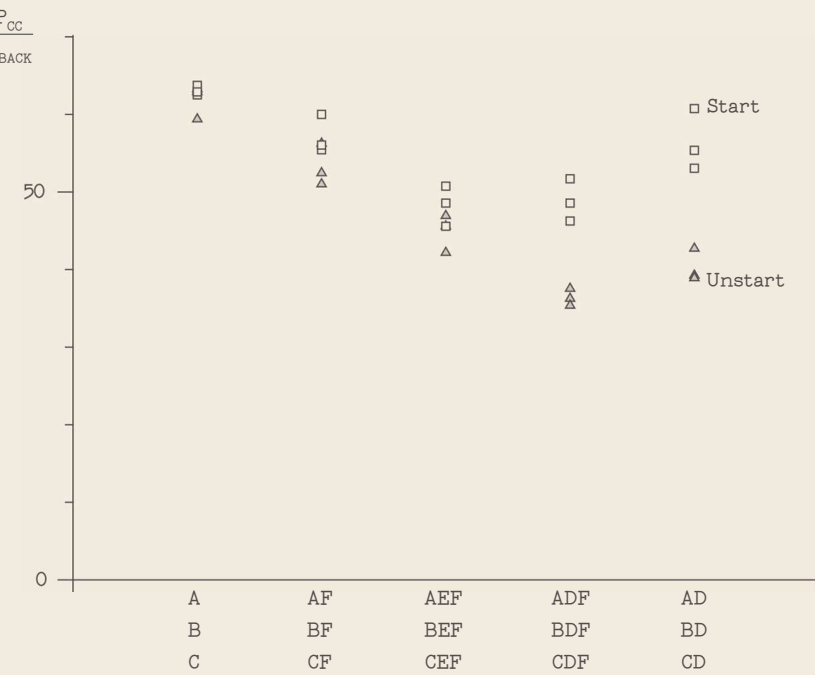


Figure 7. Second-throat start and unstart pressure ratios grouped by assembly type.

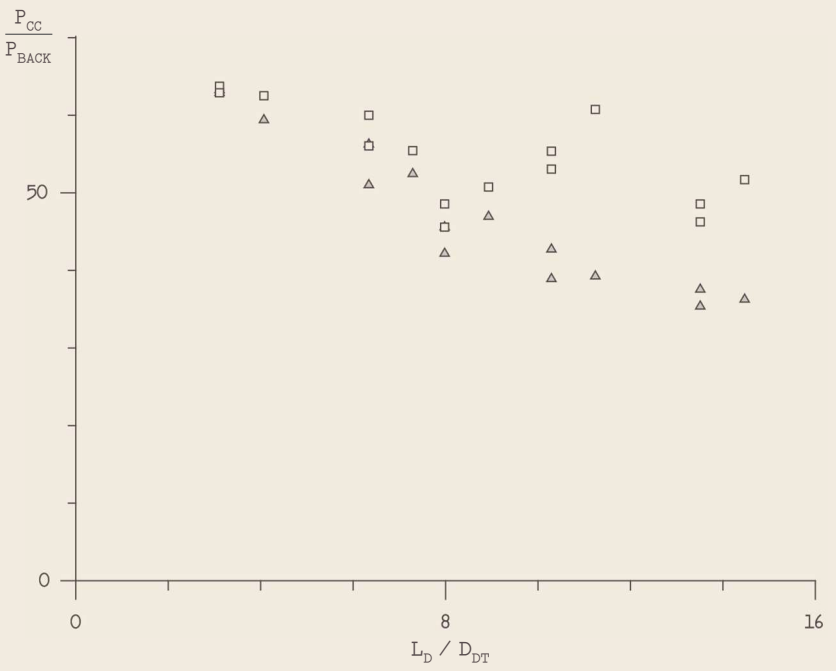


Figure 8. Sensitivity of start and unstart performance to diffuser length.

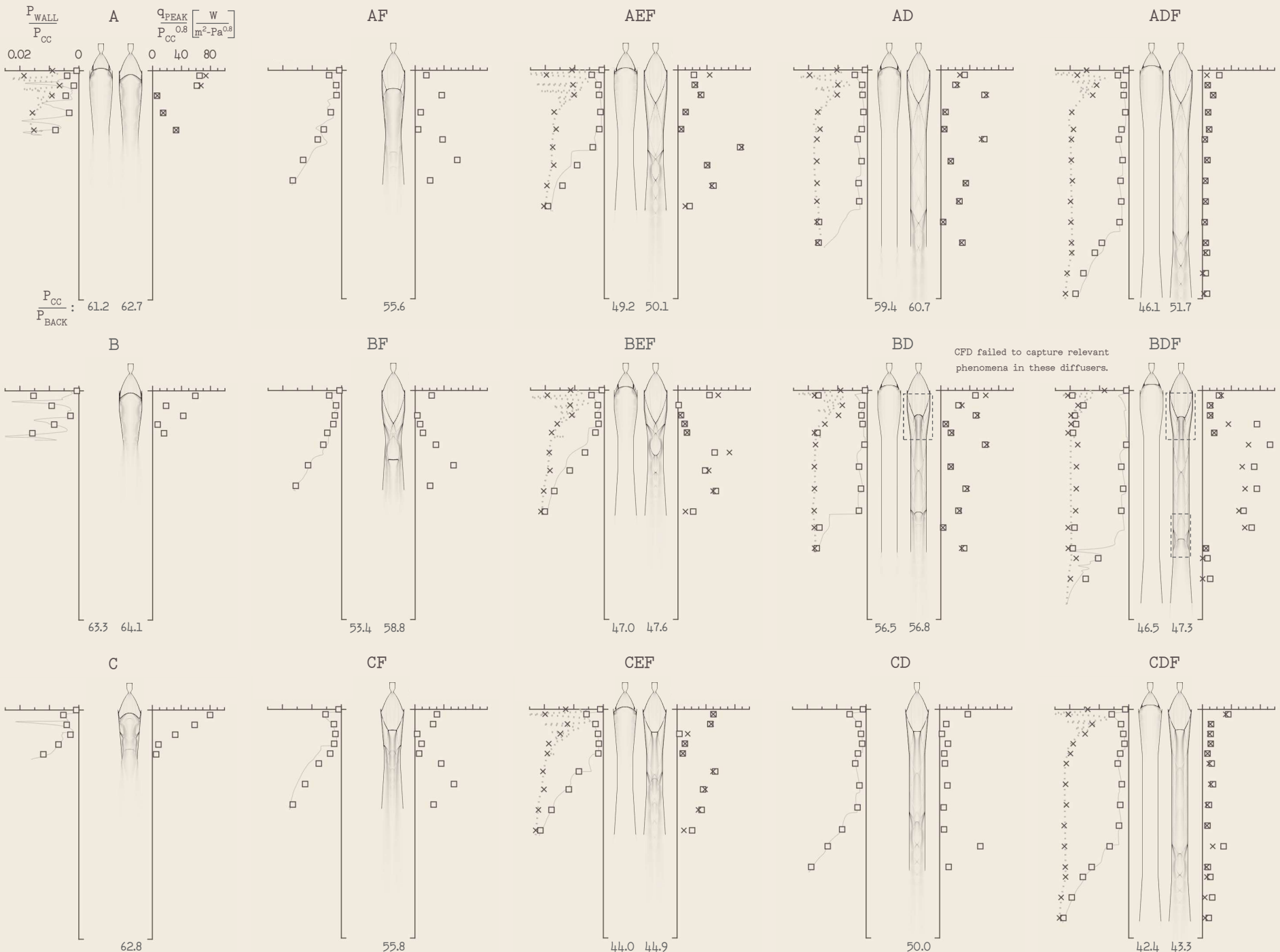


Figure 9. Spatial representations of flow characteristics for second-throat diffusers during nominal and off-nominal runs. Left: Experimental (markers) and CFD (lines) steady-state wall pressures. Center: Corresponding CFD-produced shock structures. Right: Experimental  $P_{CC}$ -normalized peak 0.1-second heat flux densities.



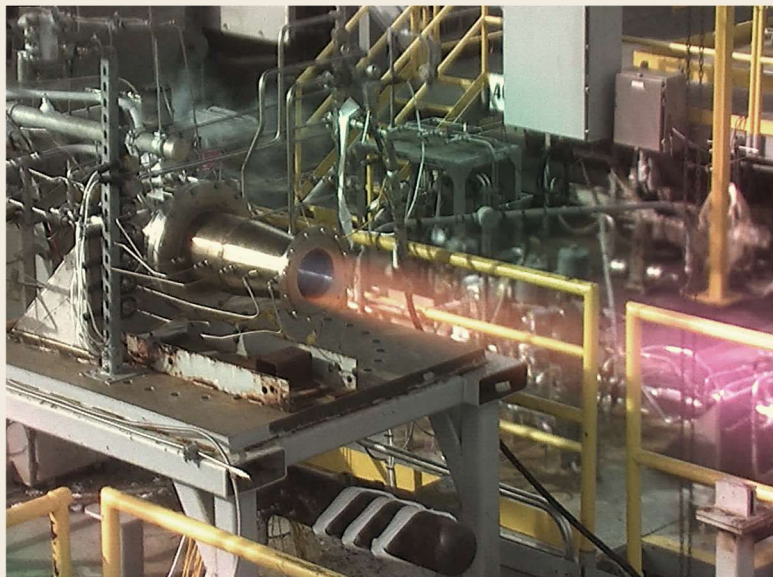
DMLS and conventionally-machined rocket liners.



Diffuser segments.



Configuration ADF on the stand.



Configuration B during steady-state operation.

Figure 10. Photos of rocket and second-throat diffuser hardware.

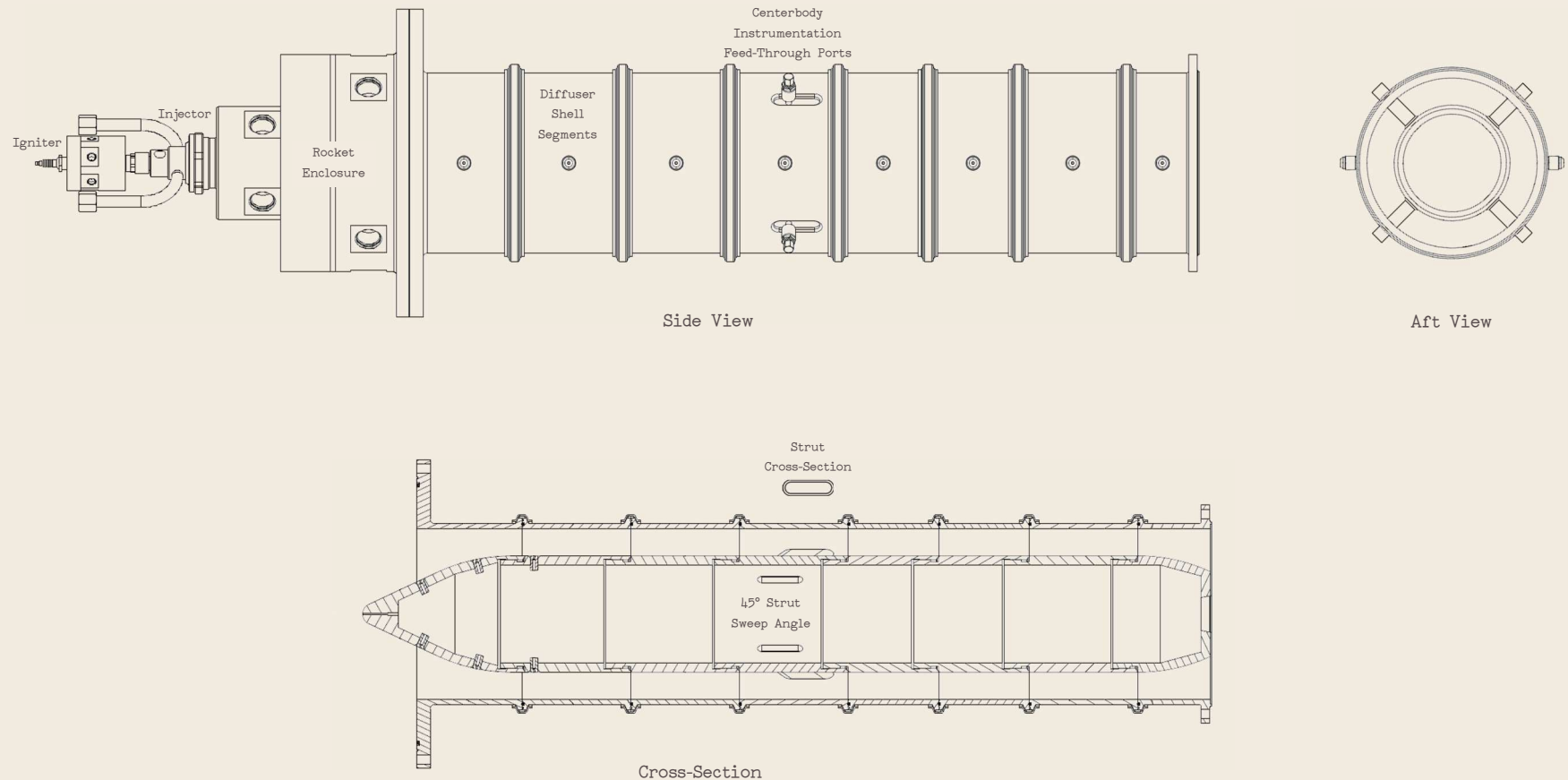


Figure 11. CB-1 hardware configuration.

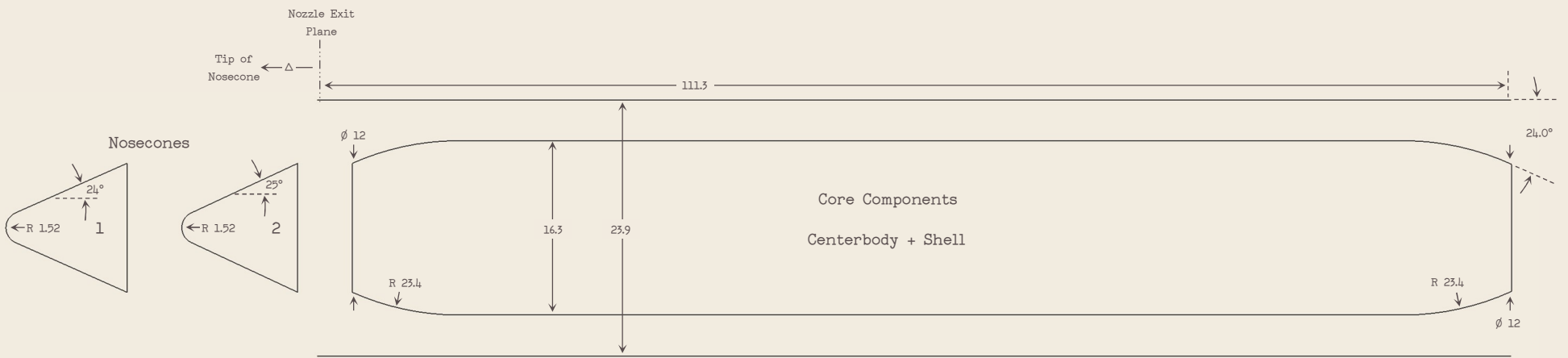


Figure 12. Aerodynamic contours of centerbody diffuser components. Linear dimensions given in cm.

Contour	$\frac{\Delta}{R_{NE}}$	$\frac{R_{TIP}}{R_{NE}}$	$\theta_{TIP}$	$\frac{A_{DI}}{A_{NT}}$	$\frac{A_{DT}}{A_{DI}}$	$\frac{A_{DT}}{A_{NE}}$	$\frac{L_{SHL}}{D_{DI}}$	No. of Tests	Avg. 0:F	$M_{DI}$	$\frac{P_{CC}}{P_{BACK}}$	$\left(\frac{P_{CELL}}{P_{CC}}\right) \times 10^5$
[deg]												
CB-1	0.79	0.15	24	106.9	0.54	0.74	4.66	8	6.0	4.81	40.8	40.8
CB-2	0.75	0.15	25	106.9	0.54	0.74	4.66	12	6.2	4.75	41.2	40.5

Table 3. Summary of centerbody diffuser geometric and performance characteristics.

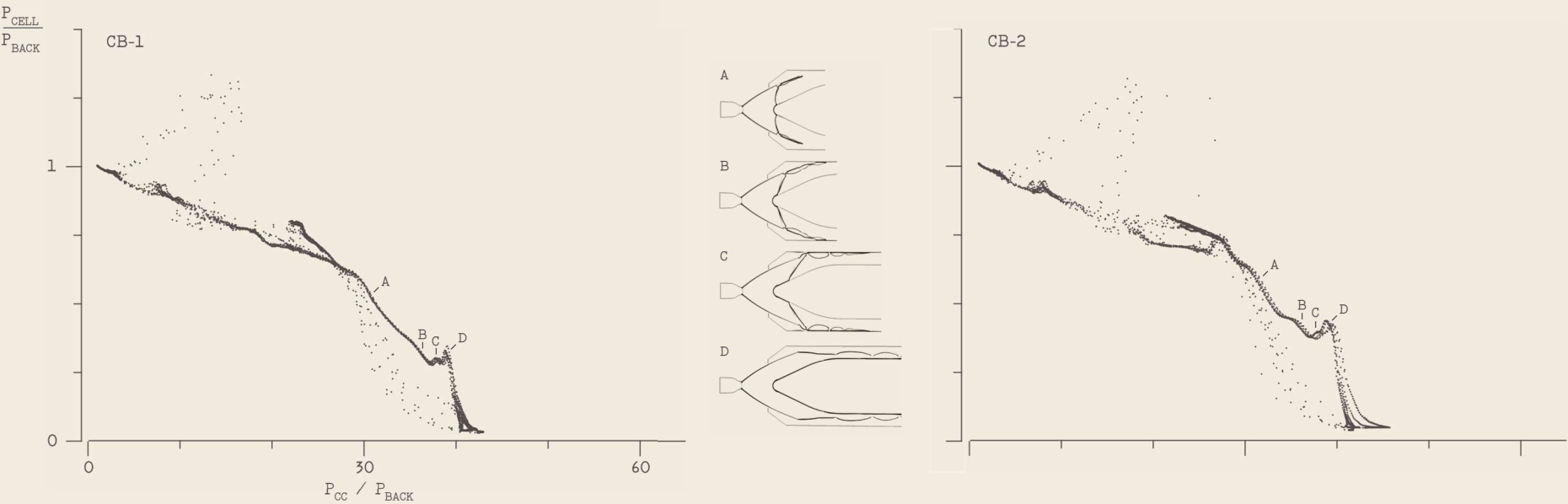


Figure 13. Centerbody diffuser pumpdown curves with annotated details of plume development around the nosecone. CFD illustrations used CB-2 geometry.

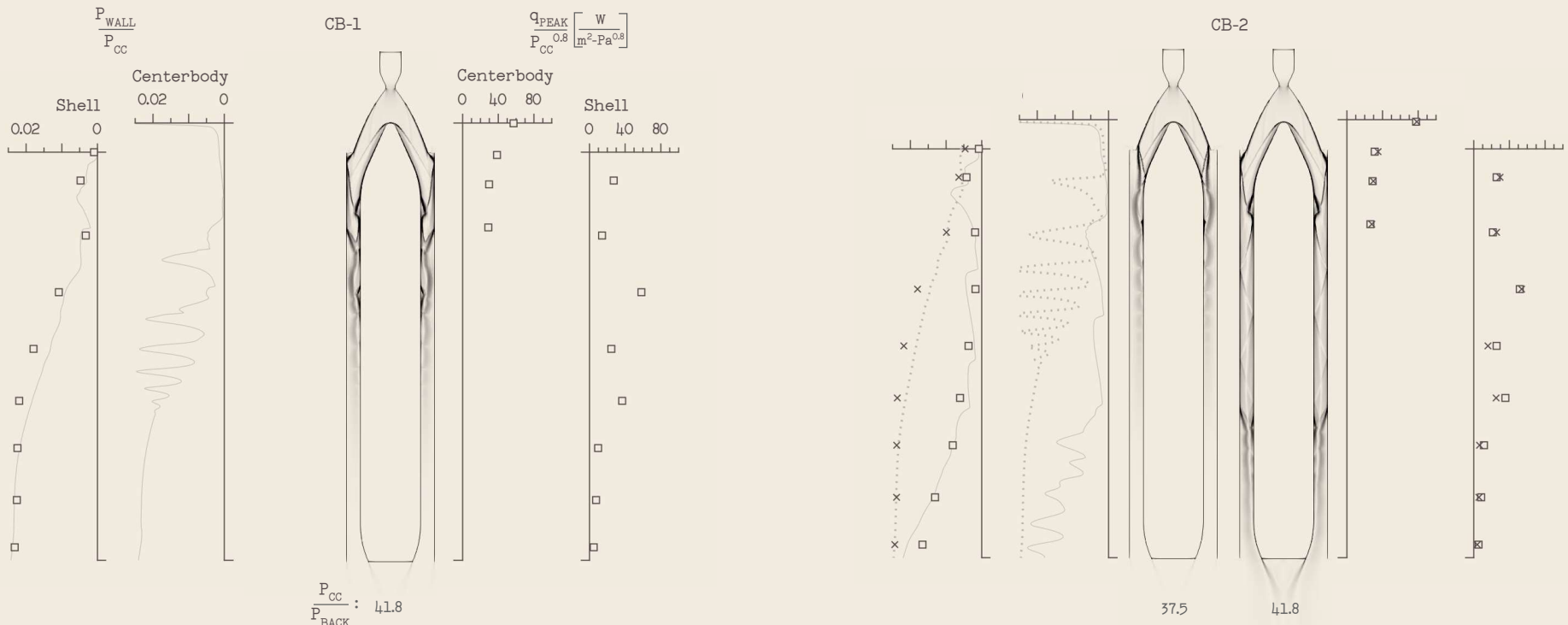
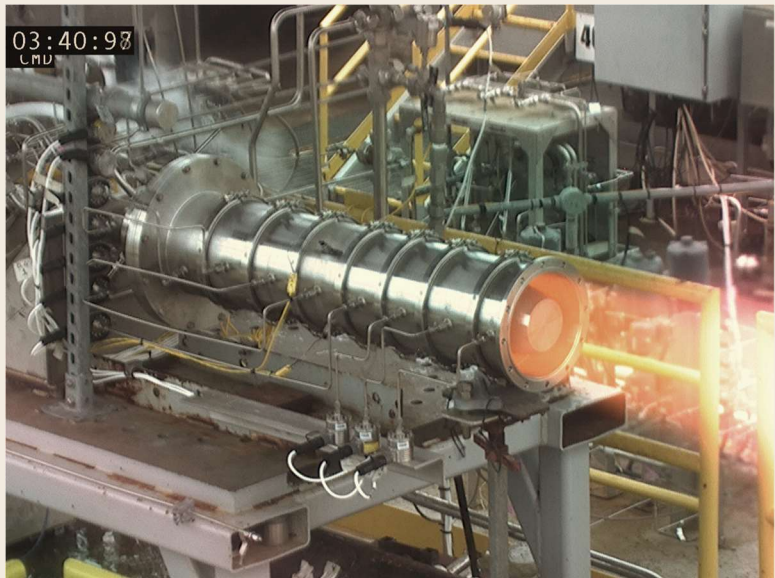


Figure 14. Spatial representations of flow characteristics for centerbody diffusers during nominal and off-nominal runs. Left: Experimental (markers) and CFD (lines) steady-state wall pressures. Center: Corresponding CFD-produced shock structures. Right: Experimental  $P_{CC}$ -normalized peak 0.1-second heat flux densities.



Steady-state operation.



Front view of nosecone 1 erosion after 11.4 seconds of firing..

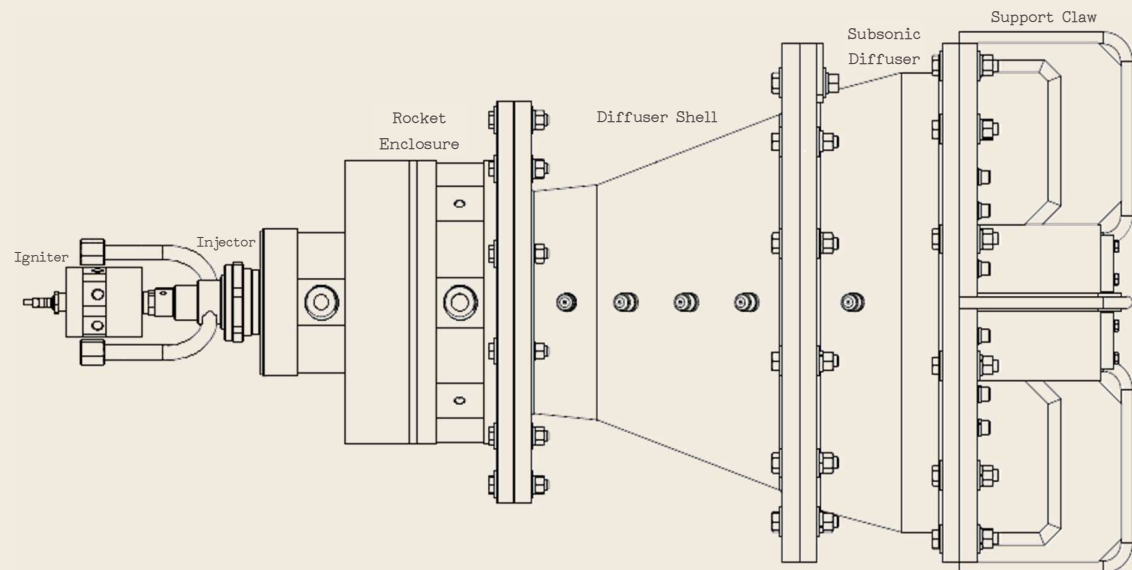


Inspection of nosecone 2 erosion after 14 seconds of firing.

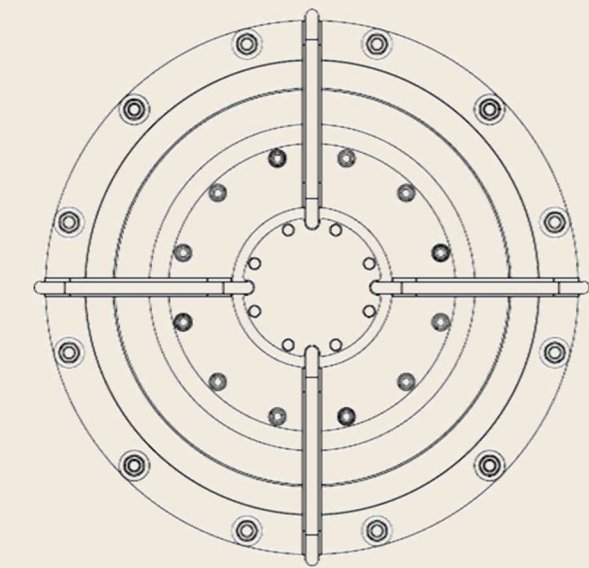


Side view of nosecone 1 erosion after 11.4 seconds of firing.

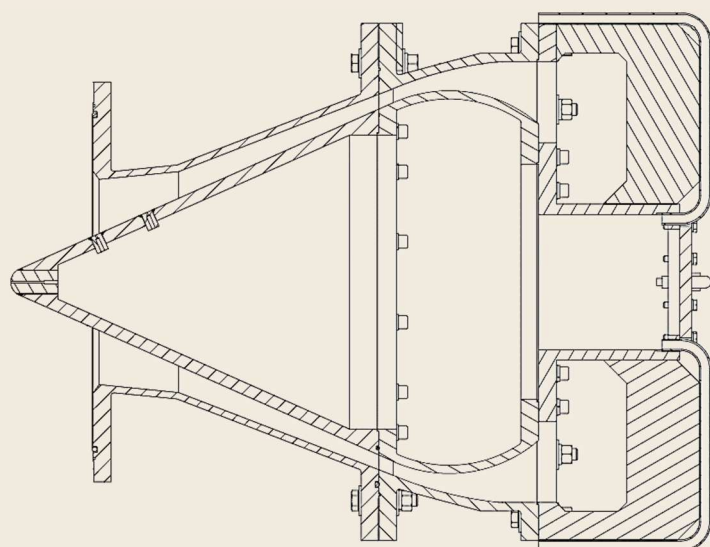
Figure 15. Photos of centerbody diffuser hardware.



Side View



Aft View



Diffuser Cross-Section

Figure 16. SPK-3X hardware configuration.

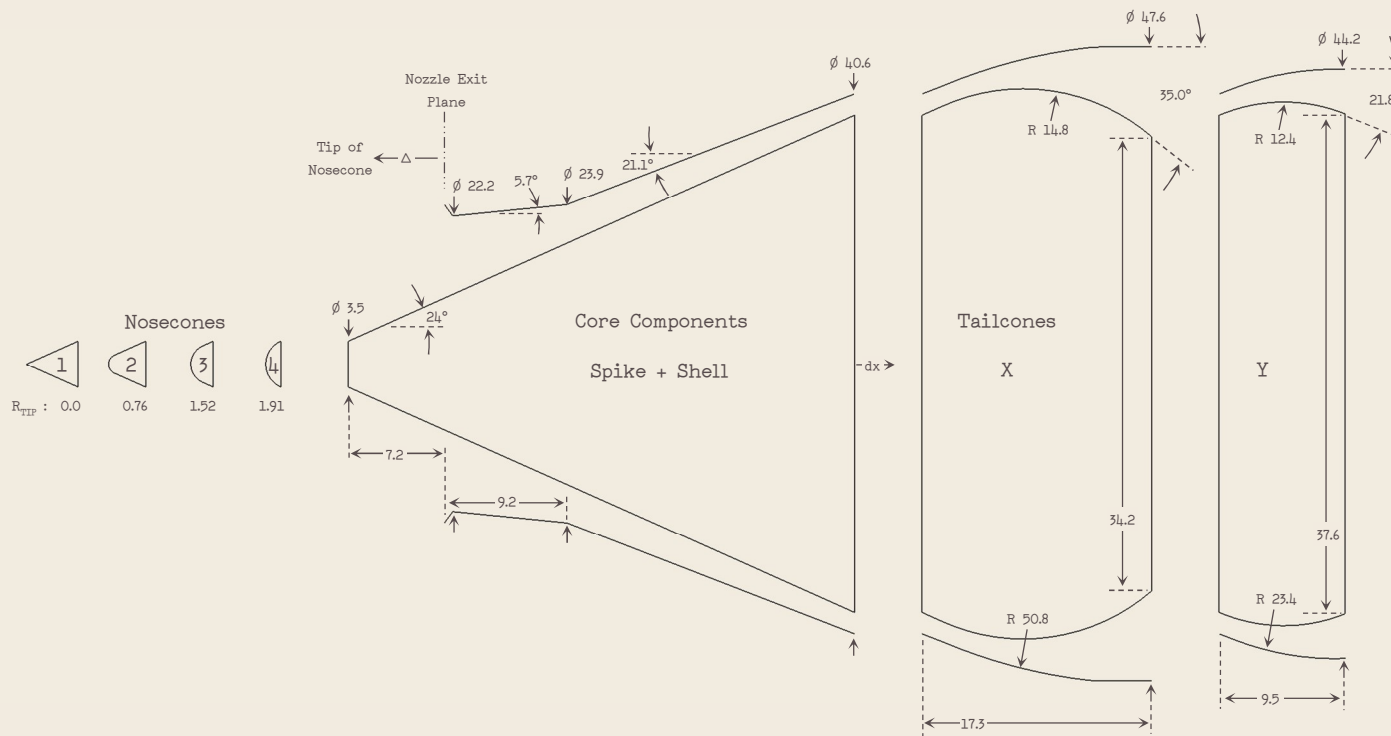


Figure 17. Aerodynamic contours of spike diffuser components. Linear dimensions given in cm.

Contour	$\frac{dx}{R_{NE}}$	$\frac{\Delta}{R_{NE}}$	$\frac{R_{TIP}}{R_{NE}}$	$\theta_{TIP}$ [deg]	$A_{DI}$				$L_{SHL}$	No. of Tests	Avg. O:F	$M_{DI}$	$\frac{P_{CC}}{P_{BACK}}$	$\left(\frac{P_{CELL}}{P_{CC}}\right) \times 10^5$
					$A_{NT}$	$A_{DI}$	$A_{DT}$	$A_{NE}$						
SPK-1X	-0.014	1.11	0.00	24	106.9	0.39	0.54	2.0	7	6.1	4.74	34.6	323	104.1
SPK-2X	-0.014	1.00	0.08	24	106.9	0.39	0.54	2.0	5	6.1	4.76	34.9	32.7	101.1
SPK-3X	-0.014	0.89	0.15	24	106.9	0.39	0.54	2.0	5	6.1	4.76	35.2	33.1	101.9
	0	0.88	0.15	24	106.9	0.40	0.55	2.0	9	6.1	4.76	35.7	33.7	110.5
SPK-4X	-0.029	0.85	0.19	24	106.9	0.38	0.53	2.0	2	5.8	4.85	-	-	-
	-0.014	0.84	0.19	24	106.9	0.39	0.54	2.0	9	6.0	4.79	35.3	34.0	113.2
	0	0.82	0.19	24	106.9	0.40	0.55	2.0	8	6.1	4.76	36.3	34.7	106.8
	0.057	0.82	0.19	24	106.9	0.43	0.59	2.0	6	5.6	4.91	37.8	35.9	116.0
SPK-3Y	-0.014	0.89	0.15	24	106.9	0.39	0.54	1.7	5	6.0	4.79	36.2	34.7	98.2
SPK-4Y	-0.014	0.84	0.19	24	106.9	0.39	0.54	1.7	10	6.1	4.76	35.0	34.9	89.9

Table 4. Summary of spike diffuser geometric and performance characteristics.

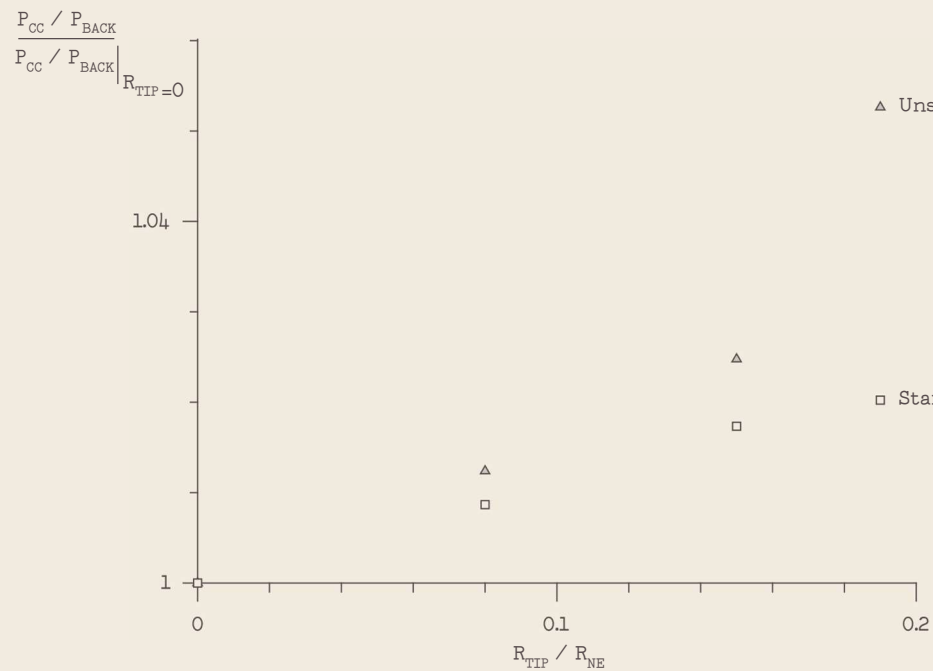


Figure 18. Sensitivity of spike performance to tip radius. Tailcone X installed.

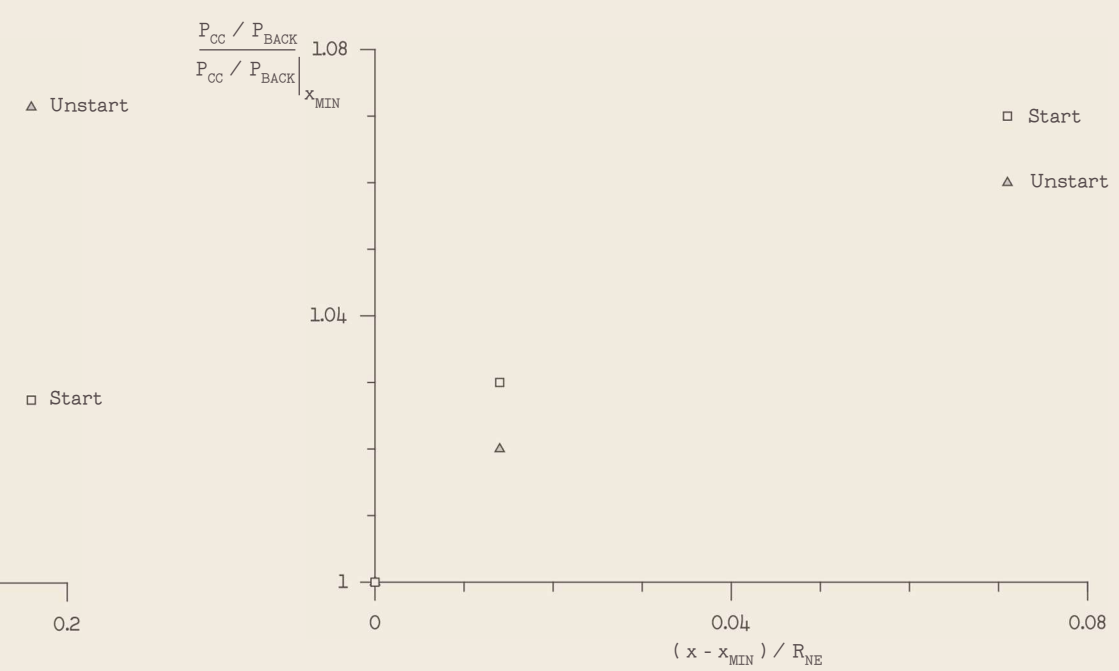


Figure 19. Sensitivity of SPK-4X to spike position.

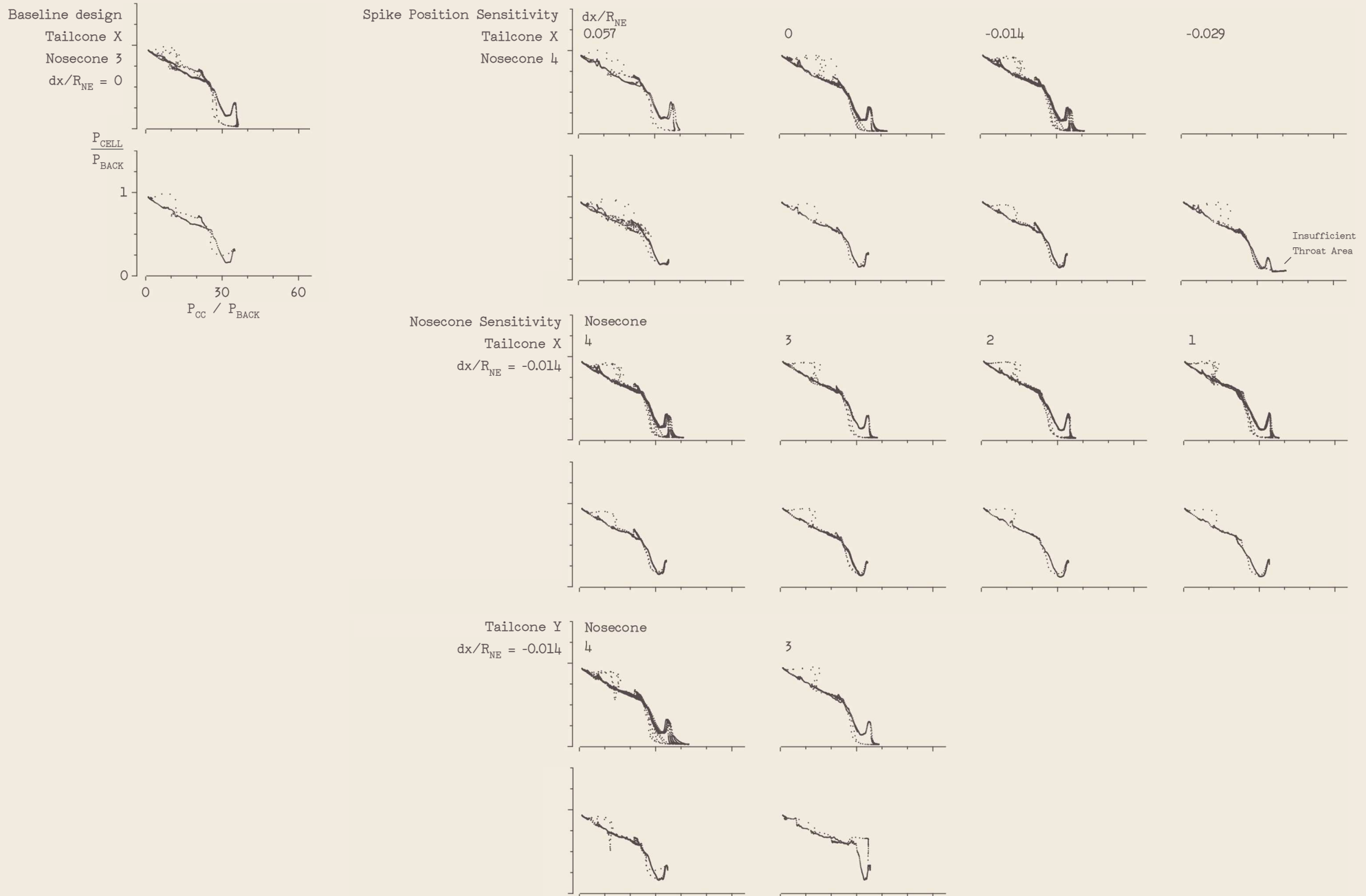


Figure 20. Nominal (top) and off-nominal (bottom) pumpdown curves for all spike configurations.

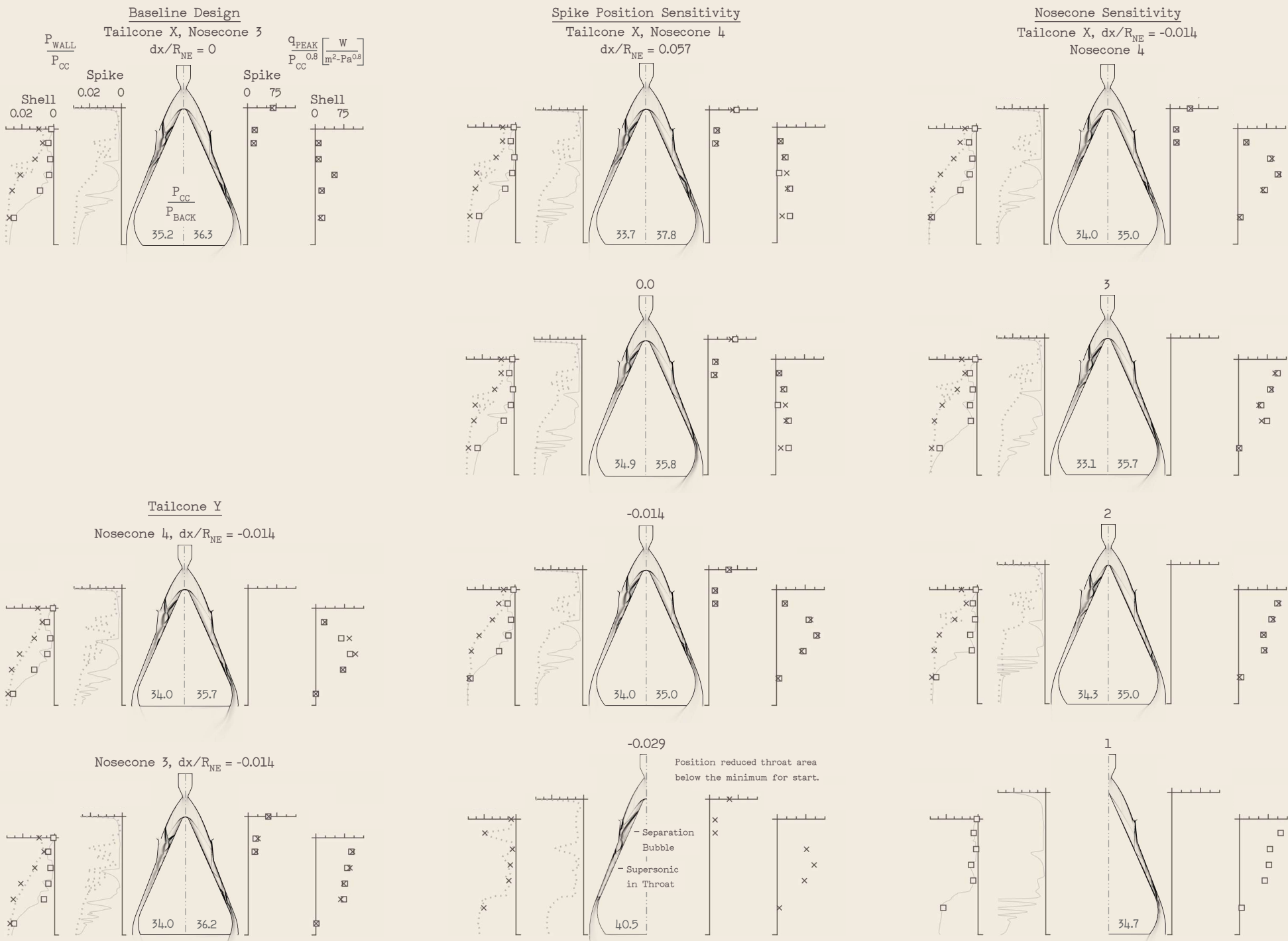
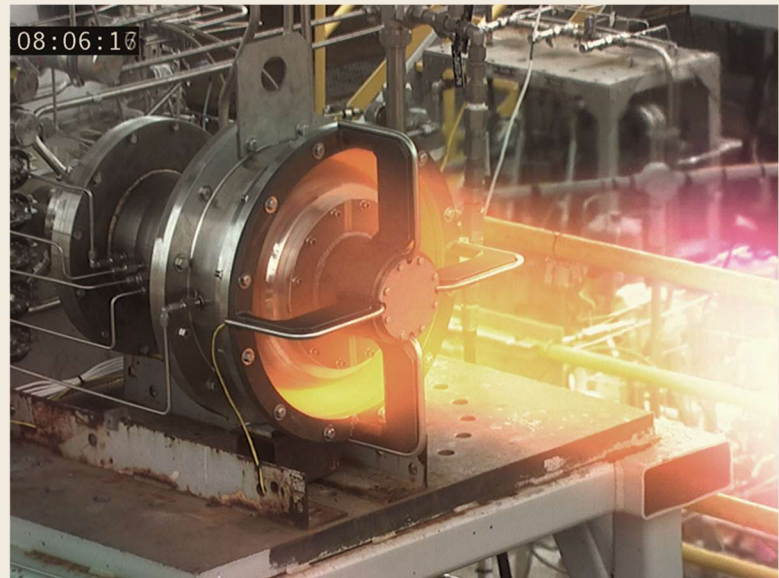


Figure 21. Spatial representations of flow characteristics for spike diffusers during nominal and off-nominal runs. Left: Experimental (markers) and CFD (lines) steady-state wall pressures. Center: Corresponding CFD-produced shock structures. Right: Experimental  $P_{CC}$ -normalized peak 0.1-second heat flux densities.



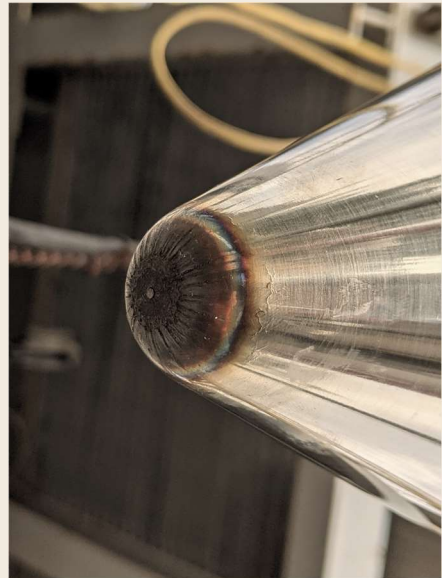
Side view during installation.



Steady-state operation.



Shell-wall boundary layer separation line revealed by external condensation.



Erosion of nosecone 3 after 13.7 seconds of firing.



Discolored bands indicate separation and reattachment points on spike wall.

Figure 22. Photos of spike diffuser hardware.

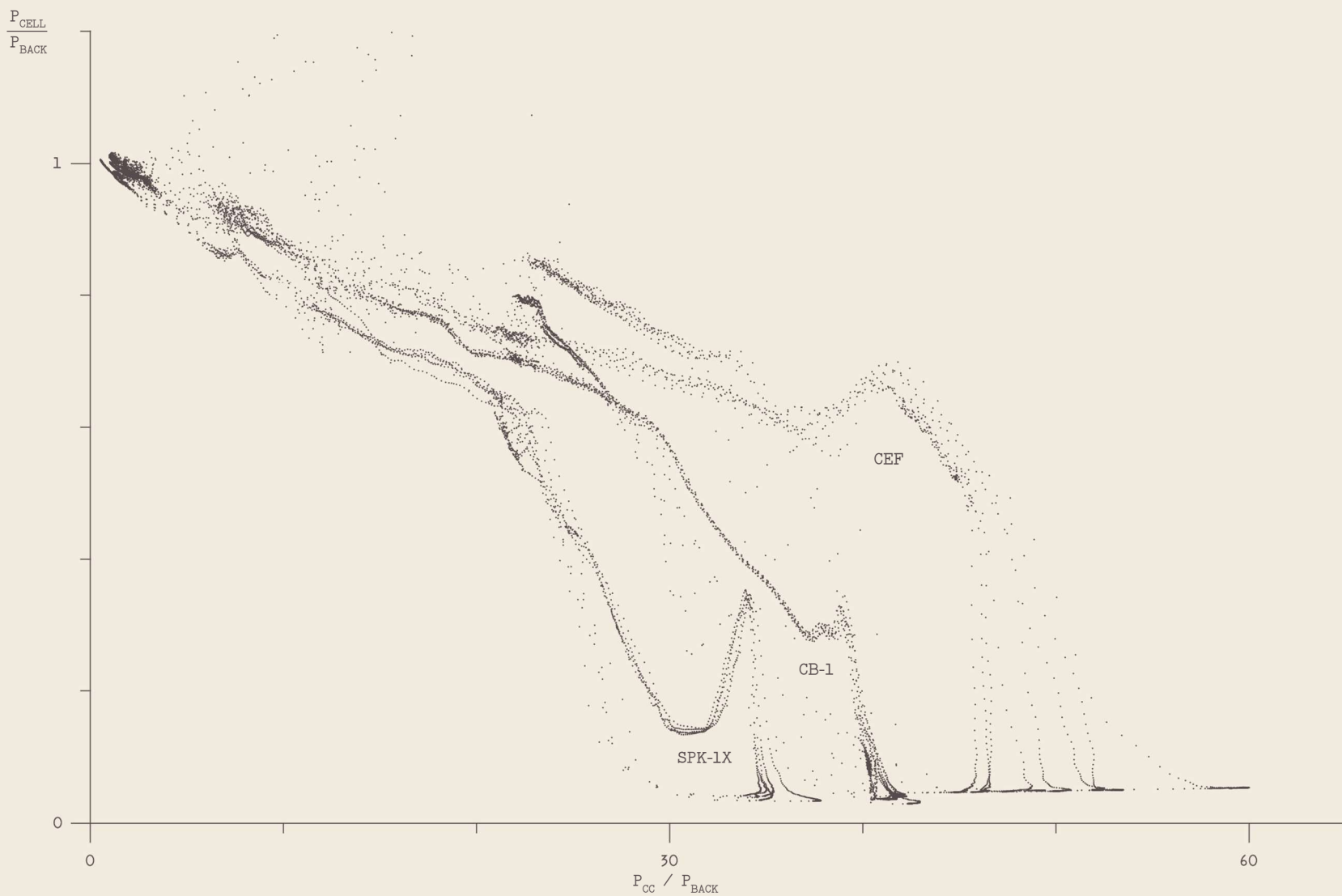


Figure 23. Pumpdown performance comparison: best-starting diffusers of each topology.

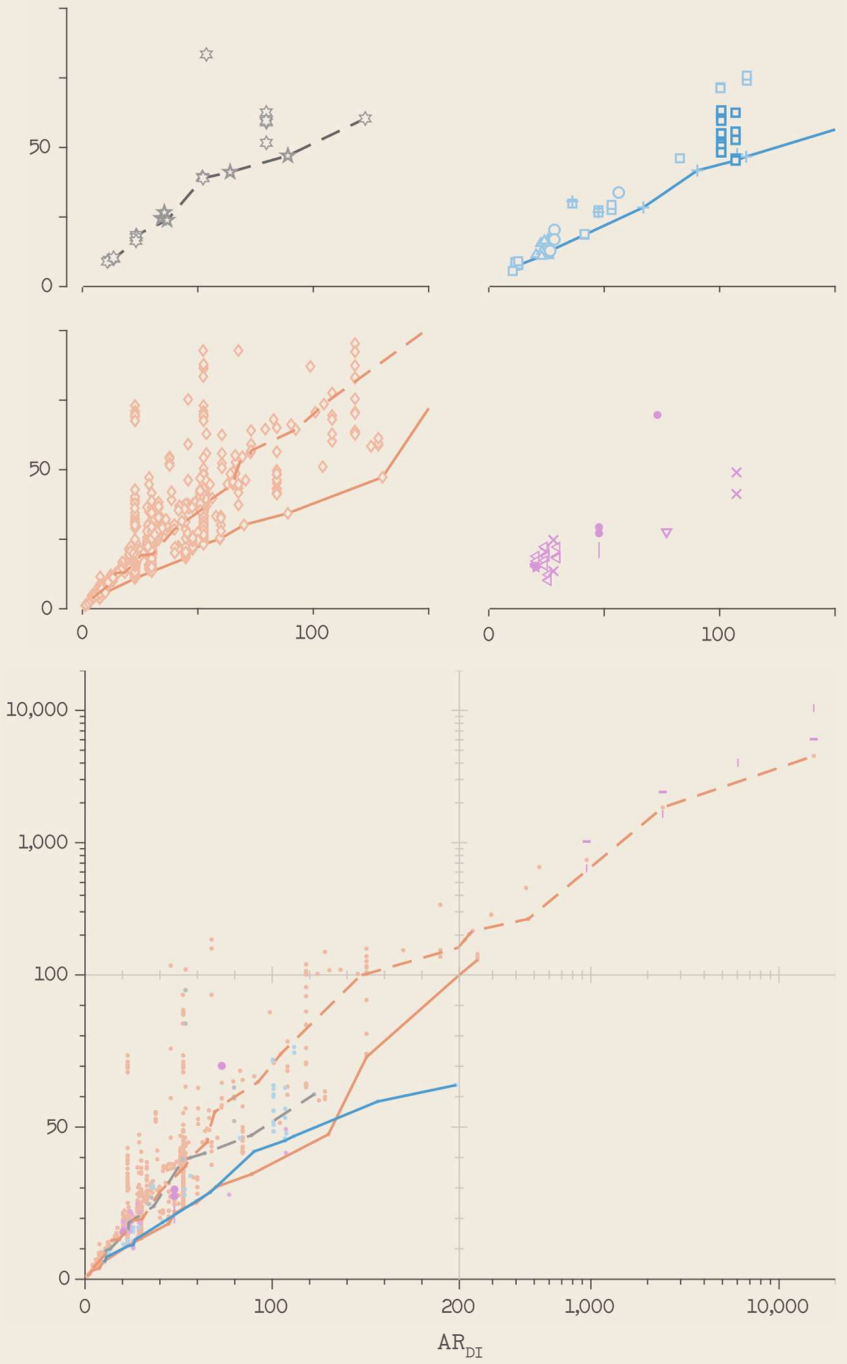
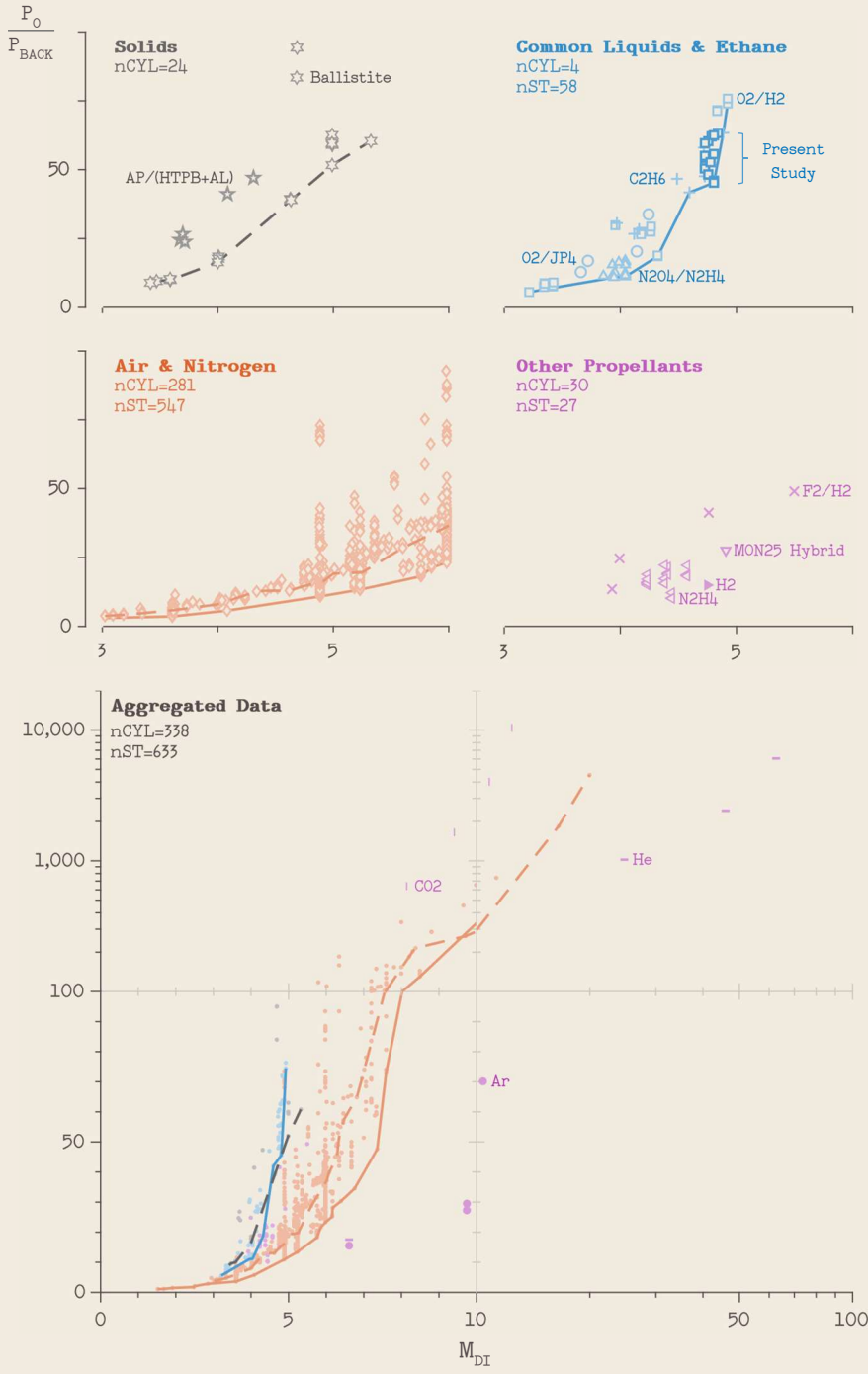


Figure 24. Empirical frontiers of cylindrical (dashed) and second-throat (solid) diffuser starting performance.

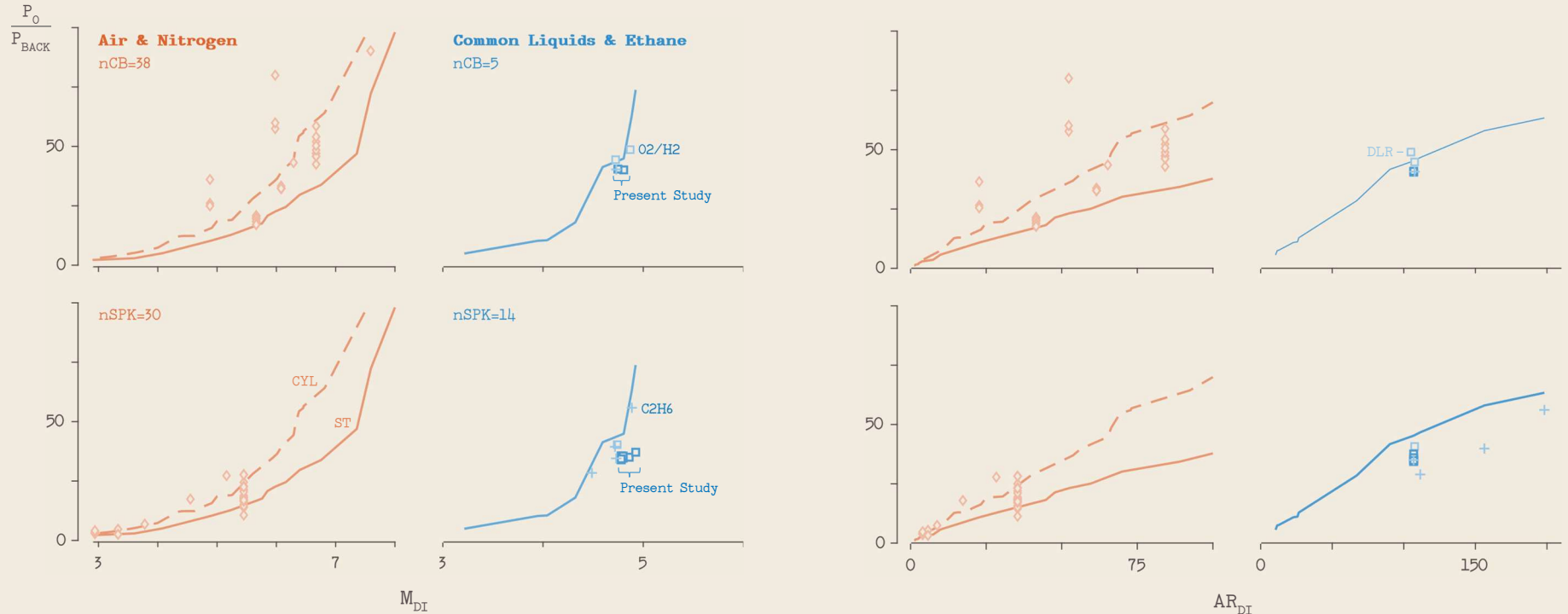


Figure 25. Centerbody and spike diffuser starting performance plotted alongside cylindrical and second-throat empirical frontiers.

Table 5.1 - Hot-Fire Cylindrical and Second-Throat Diffuser Data

No. Ref. Entity Year										Nozzle Configuration										Diffuser Configuration										Performance		
No.	Ref.	Entity	Year	Propellants	O:F	Type	D <sub>NT</sub>	Ref. P <sub>o</sub>	A <sub>NE</sub> A <sub>NT</sub>	θ <sub>NE</sub>	Name	A <sub>DL</sub> A <sub>NT</sub>	M <sub>DL</sub>	A <sub>DT</sub> A <sub>DL</sub>	A <sub>DT</sub> A <sub>NE</sub>	A <sub>DE</sub> A <sub>DT</sub>	θ <sub>DL</sub>	θ <sub>DT</sub>	θ <sub>SUB</sub>	L <sub>DL</sub> D <sub>DL</sub>	L <sub>DT</sub> D <sub>DT</sub>	L <sub>D</sub> D <sub>DT</sub>	P <sub>o</sub> P <sub>BACK</sub>	(P <sub>CEL</sub> P <sub>o</sub> ) × 10 <sup>5</sup>								
									[cm]	[MPa]										← [deg]	→											
1	[1]	NASA LaRC	1958	Ballistite	NR	CON	3.45	11.7	44.0	15.0	-	53.7	4.69	100	1.22	-	-	0	-	-	1.8	1.8	95.0	84.0	132							
2	[1]	NASA LaRC	1958	Ballistite	NR	CON	3.45	11.7	44.0	15.0	-	53.7	4.68	100	1.22	-	-	0	-	-	9.0	9.0	84.0	NR	150							
3	[1]	NASA LaRC	1958	Ballistite	NR	CON	3.45	11.7	44.0	15.0	-	53.7	4.69	100	1.22	-	-	0	-	-	13.8	13.8	95.0	30.0	172							
4	[1]	NASA LaRC	1958	Ballistite	NR	CON	2.18	11.7	88.2	15.0	-	108	5.22	100	1.22	-	-	0	-	-	13.8	13.8	105.0	80.0	64.1							
5	[2]	NASA LeRC	1959	LF2/LH2	3.9	TOP	9.95	5.0	25.0	NR	-	28.0	3.99	100	1.12	NR	-	0	5	NR	NR	9.8	24.8	24.8	177							
6	[2]	NASA LeRC	1959	LF2/LH2	3.9	TOP	9.95	5.0	25.0	NR	-	28.0	3.95	0.53	0.59	NR	6	0	5	NR	NR	7.1	13.6	NR	254							
7	[2]	NASA LeRC	1959	LF2/LH2	3.9	TOP	9.95	5.0	100	9.0	-	107	5.50	0.46	0.49	NR	6	0	5	NR	5.3	6.3	49.3	NR	49.7							
8	[3]	NASA LeRC	1959	LF2/LH2	3.9	CON	9.95	0.4	100	15.0	-	107	4.76	0.46	0.49	NR	6	0	5	NR	5.3	6.3	41.5	NR	NR							
9	[4]	NASA LeRC	1959	LOX/JP-4	2.5	CON	3.05	4.1	25.0	15.0	-	28.4	4.11	100	1.14	-	-	0	-	-	6.6	6.6	20.5	20.5	695							
10	[5]	EAFB	1960	JPN Ballistite	NR	CON	2.13	8.4	5.8	15.0	-	11.6	3.47	100	2.00	-	-	0	-	-	10.0	10.0	9.6	9.6	271							
11	[5]	EAFB	1960	JPN Ballistite	NR	CON	2.13	8.4	5.8	15.0	-	13.5	3.59	100	2.34	-	-	0	-	-	9.7	9.7	10.0	10.0	240							
12	[5]	EAFB	1960	JPN Ballistite	NR	CON	2.13	8.4	5.8	15.0	-	23.4	4.01	100	4.04	-	-	0	-	-	8.1	8.1	18.6	18.6	113							
13	[5]	EAFB	1960	JPN Ballistite	NR	CON	2.13	8.4	5.8	15.0	-	10.8	3.42	100	1.87	1.7	-	0	3.5	-	10.5	15.6	9.0	9.0	311							
14	[5]	EAFB	1960	JPN Ballistite	NR	CON	2.13	8.4	5.8	15.0	-	52.0	4.63	100	8.99	1.7	-	0	3.5	-	11.7	16.8	39.6	39.6	15.5							
15	[5]	EAFB	1960	JPN Ballistite	NR	CON	2.13	8.4	5.8	15.0	-	79.6	4.99	100	13.8	1.7	-	0	3.5	-	16.0	21.1	63.0	63.0	25.4							
16	[5]	EAFB	1960	JPN Ballistite	NR	CON	2.13	8.4	9.6	15.0	-	13.5	3.59	100	1.41	-	-	0	-	-	9.7	9.7	10.4	10.4	260							
17	[5]	EAFB	1960	JPN Ballistite	NR	CON	2.13	8.4	9.6	15.0	-	23.3	4.00	100	2.43	-	-	0	-	-	8.1	8.1	17.8	17.8	95.5							
18	[5]	EAFB	1960	JPN Ballistite	NR	CON	2.13	8.4	9.6	15.0	-	52.0	4.63	100	5.43	-	-	0	-	-	11.7	11.7	39.6	39.6	27.8							
19	[5]	EAFB	1960	JPN Ballistite	NR	CON	2.13	8.4	9.6	15.0	-	79.7	4.99	100	8.32	1.6	-	0	3.5	-	16.0	20.3	59.4	59.4	16.8							
20	[5]	EAFB	1960	JPN Ballistite	NR	CON	2.13	8.4	19.5	15.0	-	23.2	4.00	100	1.19	-	-	0	-	-	8.1	8.1	16.5	16.5	158							
21	[5]	EAFB	1960	JPN Ballistite	NR	CON	2.13	8.4	19.5	15.0	-	52.3	4.63	100	2.68	1.7	-	0	3.5	-	11.7	16.8	39.2	39.2	23.0							
22	[5]	EAFB	1960	JPN Ballistite	NR	CON	2.13	8.4	19.5	15.0	-	79.6	4.99	100	4.08	1.7	-	0	3.5	-	16.0	21.1	60.0	60.0	11.7							
23	[5]	EAFB	1960	JPN Ballistite	NR	CON	2.13	8.4	19.5	15.0	-	123	5.33	100	6.28	1.7	-	0	3.5	-	10.0	15.1	60.8	60.8	9.9							
24	[5]	EAFB	1960	JPN Ballistite	NR	CON	2.13	8.4	63.2	15.0	-	79.7	4.99	100	1.26	1.7	-	0	3.5	-	16.0	21.1	52.0	52.0	18.3							
25	[6]	NASA JPL	1960	N2H4/N2O4	1.0	TOC	1.40	1.0	20.3	12.8	-	25.7	4.04	0.80	1.01	-	5	0	-	0.06	4.5	6.0	17.1	17.1	NR							
26	[6]	NASA JPL	1960	N2H4/N2O4	1.0	TOC	1.40	1.0	20.3	12.8	1A	25.7	4.04	0.80	1.01	-	5	0	-	0.06	8.5	10.0	16.6	16.6	NR							
27	[6]	NASA JPL	1960	N2H4/N2O4	1.0	TOC	1.40	1.0	20.3	12.8	-	25.7	4.01	0.51	0.65	4	0	0	10	0.06	10.0	12.9	11.2	11.2	NR							
28	[6]	NASA JPL	1960	N2H4/N2O4	1.0	TOC	1.40	1.0	20.3	12.8	3	22.5	3.95	0.58	0.65	4	5	0	6.5	0.07	10.0	13.6	11.5	10.5	NR							
29	[6]	NASA JPL	1960	N2H4/N2O4	1.0	TOC	1.40	1.0	20.3	12.8	-	25.7	4.04	0.51	0.65	4	5	0	6.5	0.06	6.0	9.9	12.2	11.9	NR							
30	[6]	NASA JPL	1960	N2H4/N2O4	1.0	TOC	1.40	1.0	20.3	12.8	-	25.7	4.04	0.51	0.65	4	5	10	6.5	0.06	9.5	12.3	12.6	12.6	NR							
31	[6]	NASA JPL	1960	N2H4/N2O4	1.0	TOC	1.40	1.0	20.3	12.8	-	25.7	4.04	0.51	0.65	4	5	0	10	0.06	10.0	13.1	11.5	11.5	NR							
32	[6]	NASA JPL	1960	N2H4/N2O4	1.0	TOC	1.40	1.0	20.3	12.8	-	22.5	3.95	0.58	0.65	4	5	0	6.5	0.07	10.0	14.2	15.6	10.9	NR							
33	[6]	NASA JPL	1960	N2H4/N2O4	1.0	TOC	1.40	1.0	20.3	12.8	2A	25.7	4.04	0.51	0.65	4	5	0	10	0.06	10.0	13.9	15.6	12.0	NR							
34	[6]	NASA JPL	1960	N2H4/N2O4	1.0	CON	1.40	1.0	20.3	17.8	3	25.7	4.01	0.51	0.65	4	5	0	10	0.06	10.0	13.1	11.7	11.7	NR							
35	[6]	NASA JPL	1960	N2H4/N2O4	1.0	CON	1.40	1.0	20.3	17.8	2A	24.1	3.99	0.54	0.65	2	5	0	6.5	0.07	10.0	13.1	16.5	12.3	NR							
36	[6]	NASA JPL	1960	N2H4/N2O4	1.0	TOC	1.40	1.0	20.3	12.8	-	20.5	3.85	0.53	0.54	4	-7	0	6.5	-	10.0	13.8	11.5	10.6	NR							
37	[6]	NASA JPL	1960	N2H4/N2O4	1.0	TOC	13.77	1.0	20.0	12.8	I	23.0	3.95	0.58	0.66	17	5	0	6.2	0.06	10.1	19.9	12.7	10.3	54.2							
38	[6]	NASA JPL	1960	N2H4/N2O4	1.0	TOC	13.79	1.0	20.4	12.8	II	22.9	3.95	0.58	0.65	17	5	0	6.2	0.09	10.1	17.5	11.0	11.0	450							
39	[7]	NASA LeRC	1960	LOX/JP-4	2.5	CON	3.05	4.1	25.0	15.0	-	28.4	3.72	100	1.14	-	-	0	-	-	6.6	6.6	17.0	17.0	NR							
40	[7]	NASA LeRC	1960	LOX/JP-4	2.5	CON	3.05	4.1	50.2	15.0	-	56.3	4.21	100	1.12	-	-	0	-	-	10.4	10.4	34.0	34.0	NR							
41	[8]	Rocketdyne	1960	LOX/JP-4	2.5	TOP	5.84	1.8	20.0	9.0	Ψ=1.68	26.6	3.66	0.56	0.74	1.7	15	0	15	-	1.0	2.3	12.9	NR	1079							
42	[9]	P&W	1960	LOX/LH2	5.0	TOP	2.54	NR	10.0	9.0	S7	10.4	3.22	0.56	0.58	2.5	5.6	0.5	5.0	-	6.6	11.6	5.6	NR	NR							
43	[9]	P&W	1960	LOX/LH2	5.0	TOP	1.27	NR	40.0	9.0	S7	4.15	4.32	0.56	0.58	2.5	5.6	0.5	5.0	-	6.6	11.6	18.7	NR	NR							
44	[9]	P&W	1960	LOX/LH2	5.0	TOP	12.70	2.1	40.0	9.0	S8	4.15	4.32	0.56	0.58	2.5	5.6	0.5	5.0	-	6.6	11.6	19.0	NR	NR							
45	[36]	NASA SSC	1991	LOX/LH2	6.0	TOP	26.18	20.7	77.5	5.4	B-1	112	4.92	0.74	1.07	-	4.7	0	-	-	5.3	6.3	74.5	64.6	160							
46	[36]	NASA SSC	1995	LOX/LH2	6.0	TOP	26.18	20.7	77.5	5.4	A-2	112	4.92	0.74	1.07	-	4.7	0	-	-	5.3	6.3	76.3	69.7	177							
47	[36]	NASA SSC	1996	LOX/LH2	6.0	TOP	27.61	18.9	69.4	5.4	B-1	100	4.85	0.74	1.08	-	4.7	0	-	-	5.3	6.3	72.1	66.3	160							
48	[36]	NASA SSC	1997	LOX/LH2	6.0	TOP	27.64	18.9	69.4	5.4	A-2	100	4.83	0.74	1.08	-	4.7	0	-	-	5.3	6.3	71.8	59.5	162							
49	[37]	ISRO	1998	AP/(HTPB+AL)	2.1																											

Table 5.2 - Intermediate Cylindrical and Second-Throat Diffuser Data

No.	Ref.	Entity	Year	Nozzle Configuration					Diffuser Configuration										Performance						
				Propellants	Type	D <sub>NT</sub>	Ref. P <sub>o</sub>	A <sub>NE</sub> A <sub>NT</sub>	θ <sub>NE</sub>	Name	A <sub>DI</sub> A <sub>NT</sub>	M <sub>DI</sub>	A <sub>DT</sub> A <sub>DI</sub>	A <sub>DT</sub> A <sub>NE</sub>	A <sub>DE</sub> A <sub>DT</sub>	θ <sub>DI</sub>	θ <sub>DT</sub>	θ <sub>SUB</sub>	L <sub>DI</sub> D <sub>DI</sub>	L <sub>DT</sub> D <sub>DT</sub>	L <sub>D</sub> D <sub>DT</sub>	P <sub>o</sub>	P <sub>BACK</sub>	(P <sub>CELL</sub> ) × 10 <sup>5</sup>	
84	[6]	NASA JPL	1960	Decomposed N2H4	TOC	1.402	1.03	20.3	12.8	-	20.5	4.23	1.00	1.01	-	-	-	-	11.6	11.6	16.3	NR	NR		
85	[6]	NASA JPL	1960	Decomposed N2H4	TOC	1.402	1.03	20.3	12.8	1B	20.5	4.23	1.00	1.01	-	-	-	-	13.6	13.6	16.1	NR	NR		
86	[6]	NASA JPL	1960	Decomposed N2H4	TOC	1.402	1.03	20.3	12.8	-	20.5	4.23	1.00	1.01	-	-	-	-	15.6	15.6	15.9	NR	NR		
87	[6]	NASA JPL	1960	Decomposed N2H4	TOC	1.402	1.03	20.3	12.8	-	20.5	4.23	1.00	1.01	-	-	-	-	19.6	19.6	15.6	NR	NR		
88	[6]	NASA JPL	1960	Decomposed N2H4	TOC	1.402	1.03	20.3	12.8	-	20.5	4.23	1.00	1.01	-	-	-	-	24.0	24.0	15.4	NR	NR		
89	[6]	NASA JPL	1960	Decomposed N2H4	TOC	1.402	1.03	20.3	12.8	-	24.8	4.41	1.00	1.22	-	-	-	-	5.1	5.1	21.7	NR	NR		
90	[6]	NASA JPL	1960	Decomposed N2H4	TOC	1.402	1.03	20.3	12.8	-	24.8	4.41	1.00	1.22	-	-	-	-	8.8	8.8	19.4	NR	NR		
91	[6]	NASA JPL	1960	Decomposed N2H4	TOC	1.402	1.03	20.3	12.8	-	24.8	4.41	1.00	1.22	-	-	-	-	12.4	12.4	19.1	NR	NR		
92	[6]	NASA JPL	1960	Decomposed N2H4	TOC	1.402	1.03	20.3	12.8	-	24.8	4.41	1.00	1.22	-	-	-	-	17.8	17.8	19.0	NR	NR		
93	[6]	NASA JPL	1960	Decomposed N2H4	TOC	1.402	1.03	20.3	12.8	-	24.8	4.41	1.00	1.22	-	-	-	-	21.8	21.8	18.9	NR	NR		
94	[6]	NASA JPL	1960	Decomposed N2H4	TOC	1.402	1.03	20.3	12.8	-	29.5	4.57	1.00	1.46	-	-	-	-	3.0	3.0	22.3	NR	NR		
95	[6]	NASA JPL	1960	Decomposed N2H4	TOC	1.402	1.03	20.3	12.8	-	29.5	4.57	1.00	1.46	-	-	-	-	4.7	4.7	18.9	NR	NR		
96	[6]	NASA JPL	1960	Decomposed N2H4	TOC	1.402	1.03	20.3	12.8	-	29.5	4.57	1.00	1.46	-	-	-	-	6.3	6.3	18.7	NR	NR		
97	[6]	NASA JPL	1960	Decomposed N2H4	TOC	1.402	1.03	20.3	12.8	-	29.5	4.57	1.00	1.46	-	-	-	-	8.0	8.0	18.7	NR	NR		
98	[6]	NASA JPL	1960	Decomposed N2H4	TOC	1.402	1.03	20.3	12.8	-	29.5	4.57	1.00	1.46	-	-	-	-	9.7	9.7	18.7	NR	NR		
99	[6]	NASA JPL	1960	Decomposed N2H4	TOC	1.402	1.03	20.3	12.8	-	29.5	4.57	1.00	1.46	-	-	-	-	13.0	13.0	18.7	NR	NR		
100	[6]	NASA JPL	1960	Decomposed N2H4	TOC	1.402	1.03	20.3	12.8	-	29.5	4.57	1.00	1.46	-	-	-	-	16.3	16.3	18.5	NR	NR		
101	[6]	NASA JPL	1960	Decomposed N2H4	TOC	1.402	1.03	20.3	12.8	-	29.5	4.57	1.00	1.46	-	-	-	-	20.0	20.0	18.3	NR	NR		
102	[6]	NASA JPL	1960	Decomposed N2H4	TOC	1.402	1.03	20.3	12.8	-	20.5	4.23	0.72	0.72	1.8	3.0	0.0	6.5	-	0.5	3.2	19.0	NR	NR	
103	[6]	NASA JPL	1960	Decomposed N2H4	TOC	1.402	1.03	20.3	12.8	-	20.5	4.23	0.65	0.66	2.0	3.0	0.0	6.5	0.94	0.5	3.8	15.9	14.1	NR	
104	[6]	NASA JPL	1960	Decomposed N2H4	TOC	1.402	1.03	20.3	12.8	-	20.5	4.23	0.65	0.66	-	3.0	0.0	-	-	12.0	11.5	15.1	11.5	NR	
105	[6]	NASA JPL	1960	Decomposed N2H4	TOC	1.402	1.03	20.3	12.8	-	20.5	4.23	0.65	0.66	2.0	3.0	0.0	6.5	-	12.0	13.0	15.8	10.5	NR	
106	[6]	NASA JPL	1960	Decomposed N2H4	TOC	1.402	1.03	20.3	12.8	-	20.5	4.23	0.65	0.66	2.0	3.0	0.0	6.5	-	12.0	14.9	15.9	10.6	NR	
107	[6]	NASA JPL	1960	Decomposed N2H4	TOC	1.402	1.03	20.3	12.8	-	20.5	4.23	0.65	0.66	2.0	3.0	0.0	6.5	0.94	12.0	15.0	17.2	10.6	NR	
108	[6]	NASA JPL	1960	Decomposed N2H4	TOC	1.402	1.03	20.3	12.8	-	24.1	4.38	0.54	0.65	2.0	3.0	0.0	6.5	1.65	12.0	16.0	17.4	10.6	NR	
109	[6]	NASA JPL	1960	Decomposed N2H4	TOC	1.402	1.03	20.3	12.8	-	24.1	4.38	0.63	0.75	2.0	3.0	0.0	6.5	1.65	12.0	16.1	22.4	NR	NR	
110	[6]	NASA JPL	1960	Decomposed N2H4	TOC	1.402	1.03	20.3	12.8	-	24.1	4.38	0.54	0.65	2.0	5.0	0.0	6.5	0.07	3.0	7.8	15.7	14.7	NR	
111	[6]	NASA JPL	1960	Decomposed N2H4	TOC	1.402	1.03	20.3	12.8	-	24.1	4.38	0.54	0.65	2.0	5.0	0.0	6.5	0.07	4.0	8.7	15.7	13.2	NR	
112	[6]	NASA JPL	1960	Decomposed N2H4	TOC	1.402	1.03	20.3	12.8	-	24.1	4.38	0.54	0.65	2.0	5.0	0.0	6.5	0.07	5.0	9.5	15.7	11.4	NR	
113	[6]	NASA JPL	1960	Decomposed N2H4	TOC	1.402	1.03	20.3	12.8	-	24.1	4.38	0.54	0.65	2.0	5.0	0.0	6.5	0.07	6.0	10.3	15.7	11.2	NR	
114	[6]	NASA JPL	1960	Decomposed N2H4	TOC	1.402	1.03	20.3	12.8	2B	24.1	4.38	0.54	0.65	2.0	5.0	0.0	6.5	0.07	8.0	11.9	15.7	10.7	NR	
115	[6]	NASA JPL	1960	Decomposed N2H4	TOC	1.402	1.03	20.3	12.8	-	24.1	4.38	0.54	0.65	2.0	5.0	0.0	6.5	0.07	10.0	13.4	15.7	10.7	NR	
116	[6]	NASA JPL	1960	Decomposed N2H4	TOC	1.402	1.03	20.3	12.8	-	24.1	4.38	0.54	0.65	2.0	5.0	0.0	6.5	0.07	12.0	15.1	15.7	10.4	NR	
117	[6]	NASA JPL	1960	Decomposed N2H4	TOC	1.402	1.03	20.3	12.8	-	25.7	4.44	0.51	0.65	4.0	5.0	0.0	10	0.06	10.0	15.6	12.3	10.2	NR	
118	[6]	NASA JPL	1960	Decomposed N2H4	TOC	1.402	1.03	20.3	12.8	3	25.7	4.44	0.51	0.65	4.0	5.0	0.0	10	0.06	10.0	13.1	10.4	9.8	NR	
119	[6]	NASA JPL	1960	Decomposed N2H4	TOC	1.402	1.03	20.3	12.8	-	25.7	4.44	0.51	0.65	4.0	5.0	0.0	6.5	0.06	10.0	13.5	10.2	9.8	NR	
120	[6]	NASA JPL	1960	Decomposed N2H4	TOC	1.402	1.03	20.3	12.8	-	25.7	4.44	0.51	0.65	4.0	0.0	0	6.5	0.06	10.0	13.7	10.2	9.7	NR	
121	[45]	NASA JPL	1983	CH3OH:Air = 32.26	CON	4.059	0.69	9.9	10.0	NR	9.9	4.08	0.72	0.72	NR	0.0	0	8.0	NR	11.0	5.7	5.7	4768		
122	[44]	NASA SSC	2020	C2H6, TO=535 K	TOP	0.318	5.00	76.9	19.1	CDF-E	107.6	4.73	0.46	0.64	2	3.6	0.0	3.5	-	7.3	14.0	48.0	32.4	125	
123	[42]	NASA SSC	2020	C2H6, TO=535 K	TOP	0.313	18.94	69.4	5.4	ND4-E	90.4	4.60	0.57	0.74	-	6.0	0.0	-	0.44	2.8	4.9	57.8	47.3	83	
124	[42]	NASA SSC	2020	C2H6, TO=535 K	TOP	0.475	9.89	36.5	6.0	ND4-E	47.5	4.12	0.57	0.74	-	6.0	0.0	-	0.44	2.8	4.9	26.9	25.5	151	
125	[42]	NASA SSC	2020	C2H6, TO=635 K	TOP	0.485	10.34	60.0	20	SRP-2	67.0	4.16	0.50	0.45	2.0	6.0	0.0	3.5	-	8.0	13.4	28.6	23.1	309	
126	[42]	NASA SSC	2020	C2H6, TO=635 K	TOP	0.376	10.34	100	15	SRP-2	111.5	4.49	0.50	0.45	2.0	6.0	0.0	3.5	-	8.0	13.4	47.0	43.9	128	
127	[42]	NASA SSC	2020	C2H6, TO=635 K	TOP	0.318	10.34	140	11	SRP-2	156.3	4.72	0.50	0.45	2.0	6.0	0.0	3.5	-	8.0	14	58.4	48.4	66	
128	[42]	NASA SSC	2020	C2H6, TO=635 K	TOP	0.282	10.34	177	7.5	SRP-2	198.2	4.89	0.50	0.45	2.0	6.0	0.0	3.5	-	8.0	13.4	63.8	59.2	55	
129	[42]	NASA SSC	2021	C2H6, TO=515 K	FAIR	0.318	4.39	15.0	0.0	CYL-E	36.2	3.97	1.00	2.41	-	-	-	-	11.6	11.6	30.8	28.2	516		

Table 5.3 - Cold-Flow Cylindrical and Second-Throat Diffuser Data

No.	Ref.	Entity	Year	Nozzle Configuration					Diffuser Configuration										Performance		
Gas	T<sub>0</sub>	Type	D<sub>NT</sub>	Ref. P<sub>o</sub>	A<sub>NE</sub> A<sub>NT</sub>	θ<sub>NE</sub>	Name	A<sub>DI</sub> A<sub>NT</sub>	M<sub>DI</sub>	A<sub>DT</sub> A<sub>DI</sub>	A<sub>DT</sub> A<sub>NE</sub>	A<sub>DE</sub> A<sub>DT</sub>	θ<sub>DI</sub>	θ<sub>DT</sub>	θ<sub>SUB</sub>	L<sub>DI</sub> D<sub>DI</sub>	L<sub>DT</sub> D<sub>DT</sub>	L<sub>D</sub> D<sub>DT</sub>	P<sub>o</sub>	P<sub>BACK</sub>	(P<sub>CELL</sub>) × 10<sup>5</sup>



<tbl\_r cells="23" ix="3" maxc

Table 5.3 (Continued) - Cold-Flow Cylindrical and Second-Throat Diffuser Data

No.	Ref.	Entity	Year	Nozzle Configuration					Diffuser Configuration									Performance																						
				Gas	T <sub>0</sub>	Type	D <sub>NT</sub>	Ref. P <sub>0</sub>	A <sub>NE</sub> /A <sub>NT</sub>	θ <sub>NE</sub>	Name	A <sub>DI</sub> /A <sub>NT</sub>	M <sub>DI</sub>	A <sub>DT</sub> /A <sub>DI</sub>	A <sub>DT</sub> /A <sub>NE</sub>	A <sub>DE</sub> /A <sub>DT</sub>	θ <sub>DI</sub>	θ <sub>DT</sub>	θ <sub>SUB</sub>	L <sub>DI</sub> /D <sub>DI</sub>	L <sub>DT</sub> /D <sub>DT</sub>	L <sub>D</sub> /D <sub>DT</sub>	P <sub>0</sub> /P <sub>BACK</sub>	(P <sub>CELL</sub> /P <sub>0</sub> ) × 10 <sup>5</sup>																
				[K]		[cm]	[MPa]		[deg]									< [deg] >																				Start	Unst.	NR
158	[46]	NAVORD	1952	Air	289	2D Wedge	0.03	3.04	465	5.6	-	465	9.70	NR	NR	NR	NR	-	NR	-	0.0	NR	265.0	NR	NR	5.8	5.8	1030												
159	[47]	AEDC	1959	Air	478	CON	5.59	0.31	3.6	18	a	7.50	3.61	1.00	2.11	11.1	-	0	4.0	-	3.0	19.6	5.8	5.8	NR	54.3	54.3	277												
160	[47]	AEDC	1959	Air	478	CON	5.59	0.31	3.6	18	b	15.2	4.24	1.00	3.70	6.3	-	0	4.0	-	3.0	13.7	9.9	9.9	NR	15.9	15.9	277												
161	[47]	AEDC	1959	Air	478	CON	5.59	0.31	3.6	18	c	20.8	4.77	1.00	5.83	4.0	-	0	4.0	-	3.0	10.1	15.9	15.9	NR	8.0	8.0	585												
162	[47]	AEDC	1959	Air	478	CON	4.72	0.31	5.0	18	a	10.6	3.99	1.00	2.12	11.1	-	0	4.0	-	3.0	19.6	8.0	8.0	NR	13.7	13.8	387												
163	[47]	AEDC	1959	Air	478	CON	4.72	0.31	5.0	18	b	18.5	4.63	1.00	3.70	6.3	-	0	4.0	-	3.0	13.7	13.8	13.8	NR	10.1	10.1	160												
164	[47]	AEDC	1959	Air	478	CON	4.72	0.31	5.0	18	c	29.2	5.20	1.00	5.83	4.0	-	0	4.0	-	3.0	10.1	22.1	22.1	NR	10.1	22.1	160												
165	[47]	AEDC	1959	Air	478	CON	3.21	0.31	10.8	18	a	23.0	4.90	1.00	2.13	11.1	-	0	4.0	-	3.0	19.6	16.7	16.7	NR	18.1	18.1	181												
166	[47]	AEDC	1959	Air	478	CON	3.21	0.31	10.8	18	b	39.8	5.60	1.00	3.69	6.3	-	0	4.0	-	3.0	13.7	28.9	28.9	NR	10.8	10.8	108												
167	[47]	AEDC	1959	Air	478	CON	3.21	0.31	10.8	18	c	62.8	6.24	1.00	5.81	4.0	-	0	4.0	-	3.0	10.1	45.0	45.0	NR	56.0	56.0	56.0												
168	[47]	AEDC	1959	Air	478	CON	2.49	0.31	18	18	a	38.6	5.56	1.00	2.14	11.1	-	0	4.0	-	3.0	19.6	29.3	29.3	NR	121	121	121												
169	[47]	AEDC	1959	Air	478	CON	2.49	0.31	18	18	b	66.4	6.32	1.00	3.69	6.3	-	0	4.0	-	3.0	13.7	4.90	4.90	NR	66.0	66.0	66.0												
170	[47]	AEDC	1959	Air	478	CON	2.49	0.31	18	18	c	105	7.01	1.00	5.81	4.0	-	0	4.0	-	3.0	10.1	74.1	74.1	NR	34.8	34.8	34.8												
171	[47]	AEDC	1959	Air	478	CON	2.11	0.31	25	18	a	53.3	6.00	1.00	2.13	11.1	-	0	4.0	-	3.0	19.6	39.1	39.1	NR	98.0	98.0	98.0												
172	[47]	AEDC	1959	Air	478	CON	2.11	0.31	25	18	b	92.4	6.81	1.00	3.70	6.3	-	0	4.0	-	3.0	13.7	64.8	64.8	NR	52.5	52.5	52.5												
173	[47]	AEDC	1959	Air	478	CON	2.11	0.31	25	18	c	114	7.55	1.00	5.83	4.0	-	0	4.0	-	3.0	10.1	101.7	101.7	NR	26.8	26.8	26.8												
174	[48]	AEDC	1959	Air	478	CON	5.59	0.31	3.56	18	a	7.50	3.61	1.00	2.11	11.1	-12	0	4.0	-	3.0	19.6	6.1	6.1	NR	402	402	402												
175	[48]	AEDC	1959	Air	478	CON	5.59	0.31	3.56	18	a	7.50	3.61	1.00	2.11	11.1	-24	0	4.0	-	3.0	19.6	6.4	6.4	NR	295	295	295												
176	[48]	AEDC	1959	Air	478	CON	5.59	0.31	3.56	18	a	7.50	3.61	1.00	2.11	11.1	-18	0	4.0	-	3.0	19.6	6.7	6.7	NR	252	252	252												
177	[48]	AEDC	1959	Air	478	CON	5.59	0.31	3.56	18	b	13.2	4.24	1.00	3.70	6.3	-18	0	4.0	-	3.0	13.7	10.2	10.2	NR	179	179	179												
178	[48]	AEDC	1959	Air	478	CON	5.59	0.31	3.56	18	c	13.2	4.24	1.00	3.70	6.3	-24	0	4.0	-	3.0	13.7	10.8	10.8	NR	137	137	137												
179	[48]	AEDC	1959	Air	478	CON	5.59	0.31	3.56	18	c	20.8	4.77	1.00	5.83	4.0	-24	0	4.0	-	3.0	10.1	17.2	17.2	NR	68.0	68.0	68.0												
180	[48]	AEDC	1959	Air	478	CON	5.59	0.31	3.56	18	c	20.8	4.77	1.00	5.83	4.0	-30	0	4.0	-	3.0	10.1	18.9	18.9	NR	52.9	52.9	52.9												
181	[48]	AEDC	1959	Air	478	CON	5.59	0.31	3.56	18	c	20.8	4.77	1.00	5.83	4.0	-35	0	4.0	-	3.0	10.1	16.1	16.1	NR	48.5	48.5	48.5												
182	[48]	AEDC	1959	Air	478	CON	3.21	0.31	10.8	18	a	23.0	4.90	1.00	2.13	11.1	-12	0	4.0	-	3.0	19.6	17.0	17.0	NR	99.4	99.4	99.4												
183	[48]	AEDC	1959	Air	478	CON	3.21	0.31	10.8	18	a	23.0	4.90	1.00	2.13	11.1	-24	0	4.0	-	3.0	19.6	17.5	17.5	NR	64.6	64.6	64.6												
184	[48]	AEDC	1959	Air	478	CON	3.21	0.31	10.8	18	b	39.8	5.60	1.00	3.69	6.3	-18	0	4.0	-	3.0	13.7	30.4	30.4	NR	60.7	60.7	60.7												
185	[48]	AEDC	1959	Air	478	CON	3.21	0.31	10.8	18	b	39.8	5.60	1.00	3.69	6.3	-30	0	4.0	-	3.0	13.7	28.7	28.7	NR	98.1	98.1	98.1												
186	[48]	AEDC	1959	Air	478	CON	2.49	0.31	18	18	a	38.6	5.56	1.00	2.14	11.1	-12	0	4.0	-	3.0	19.6	39.4	39.4	NR	53.1	53.1	53.1												
187	[48]	AEDC	1959	Air	478	CON	2.49	0.31	18	18	a	38.6	5.56	1.00	2.14	11.1	-24	0	4.0	-	3.0	19.6	4.23	4.23	NR	36.0	36.0	36.0												
188	[49]	NASA LeRC	1959	N2	AMB	CON	0.64	4.46	9.0	15	100"	16.0	4.46	1.00	1.78	-	-	0	-	-	12.0	12.0	14.2	14.2	282	282	282													
189	[49]	NASA LeRC	1959	N2	AMB	CON	0.64	4.46	9.0	15	125"	25.0	5.00	1.00	2.78	-	-	0	-	-	9.6	9.6	19.3	19.3	130	130	130													
190	[49]	NASA LeRC	1959	N2	AMB	CON	0.64	4.46	9.0	15	150"	36.0	5.47	1.00	4.00	-	-	0	-	-	6.7	6.7	30.8	30.8	107	107	107													
191	[49]	NASA LeRC	1959	N2	AMB	CON	0.64	4.46	9.0	15	150"	36.0	5.47	1.00	4.00	-	-	0	-	-	5.3	5.3	28.5	28.5	87.7	87.7	87.7													
192	[49]	NASA LeRC	1959	N2	AMB	CON	0.64	4.46	9.0	15	150"	36.0	5.47	1.00	4.00	-	-	0	-	-	8.0	8.0	28.5	28.5	70.2	70.2	70.2													
193	[49]	NASA LeRC	1959	N2	AMB	CON	0.64	4.46	9.0	15	175"	49.0	5.89	1.00	5.44	-	-	0	-	-	6.9	6.9	38.7	38.7	64.6	64.6	64.6													
194	[33,501]	AEDC	1960	Air	297	CON	5.59	2.68	3.6	18	a	7.66	3.63	1.00	2.11	-	-	0	-	-	1.6	NR	11.5	7.2	1060	1060	1060													
195	[33,501]	AEDC	1960	Air	297	CON	5.59	2.68	3.6	18	a	7.66	3.63	1.00	2.11	-	-	0	-	-	3.0	NR	8.2	6.9	1060	1060	1060													
196	[33,501]	AEDC	1960	Air	297	CON	5.59	2.68	3.6	18	as1	7.66	3.63	1.00	2.11	10.4	-	0	4.0	-	1.6	NR	6.6	5.9	1030	1030	1030													
197	[33,501]	AEDC	1960	Air	297	CON	5.59	2.68	3.6	18	as1	7.66	3.63	1.00	2.11	10.4	-	0	4.0	-	3.0	NR	6.0	6.0	992	992	992													
198	[33,501]	AEDC	1960	Air	297	CON	5.59	2.68	3.6	18	as1	7.66	3.63	1.00	2.11	10.4	-	0	4.0	-	6.0	NR	6.3	6.1	1060	1060	1060													
199	[33,501]	AEDC	1960	Air	297	CON	5.59	2.68	3.6	18	as1	7.66	3.63	1.00	2.11	10.4	-	0	4.0	-	9.0	NR	6.1	6.1	1060	1060	1060													
200	[33,501]	AEDC	1960	Air	297	CON	5.59	2.68	3.6	18	cs2	21.5	4.81	1.00	5.92	3.6	-	0	4.0	-	3.0	NR	16.5	16.5	260	260	260													
201	[33,501]	AEDC	1960	Air	297	CON	5.59	2.68	3.6	18	cs2	21.5	4.81	1.00	5.92	3.6	-	0</																						

Table 5.3 (Continued) - Cold-Flow Cylindrical and Second-Throat Diffuser Data

No.	Ref.	Entity	Year	Nozzle Configuration						Diffuser Configuration										Performance					
				Gas	T <sub>0</sub>	Type	D <sub>NT</sub>	Ref. P <sub>0</sub>	A <sub>NE</sub> /A <sub>NT</sub>	θ <sub>NE</sub>	Name	A <sub>DI</sub> /A <sub>NT</sub>	M <sub>DI</sub>	A <sub>DT</sub> /A <sub>DI</sub>	A <sub>DT</sub> /A <sub>NE</sub>	A <sub>DE</sub> /A <sub>DT</sub>	θ <sub>DI</sub>	θ <sub>DT</sub>	θ <sub>SUB</sub>	L <sub>DI</sub> /D <sub>DI</sub>	L <sub>DT</sub> /D <sub>DT</sub>	L <sub>D</sub> /D <sub>DT</sub>	P <sub>0</sub> /P <sub>BACK</sub>	(P <sub>CELL</sub> /P <sub>0</sub> ) × 10 <sup>5</sup>	
241	[33,50]	AEDC	1960	Air	289	TOP	1.12	2.68	100	0	as3	190	8.00	1.00	1.90	1.9	-	0	4.0	-	NR	NR	339.0	NR	7.46
242	[33,50]	AEDC	1960	Air	283	TOP	1.12	2.68	100	0	cs4	532	9.98	1.00	5.32	1.2	-	0	4.0	-	NR	NR	653.6	NR	1.89
243	[33,50]	AEDC	1960	Air	328	NR	6.05	2.68	11.0	19	cs2	18.3	4.62	1.00	1.67	3.6	-	0	4.0	-	NR	NR	13.0	NR	241
244	[33,50]	AEDC	1960	Air	297	CON	5.59	2.68	3.6	18	a1	7.50	3.61	1.00	2.07	-	-	0	-	-	9.1	9.1	6.8	6.8	1060
245	[33,50]	AEDC	1960	Air	291	CON	3.20	2.68	10.8	18	a1	22.8	4.89	1.00	2.10	-	-	0	-	-	9.1	9.1	18.5	18.5	195
246	[33,50]	AEDC	1960	Air	311	CON	2.11	2.68	25.0	18	a1	52.5	5.98	1.00	2.10	-	-	0	-	-	9.1	9.1	41.3	41.3	106
247	[33,50]	AEDC	1960	Air	297	TOP	2.29	2.68	23.7	0	a1	44.7	5.76	1.00	1.89	-	-	0	-	-	9.1	9.1	37.9	37.9	34.5
248	[51]	AEDC	1960	Air	300	CON	5.59	0.27	3.6	18	1a	7.49	3.61	0.65	1.35	1.5	6.0	0	0.0	0.0	0.4	9.1	4.8	4.8	2080
249	[51]	AEDC	1960	Air	313	CON	5.59	0.27	3.6	18	1a	7.49	3.61	0.65	1.35	1.5	6.0	0	0.0	0.3	0.4	9.1	5.3	5.3	2080
250	[51]	AEDC	1960	Air	332	CON	5.59	0.27	3.6	18	1a	7.49	3.61	0.65	1.35	1.5	6.0	0	0.0	0.5	0.4	9.1	8.7	5.9	1130
251	[51]	AEDC	1960	Air	316	CON	5.59	0.27	3.6	18	1a	7.49	3.61	0.65	1.35	1.5	6.0	0	0.0	0.7	0.4	9.1	5.6	5.6	1140
252	[51]	AEDC	1960	Air	316	CON	5.59	0.27	3.6	18	1a	7.49	3.61	0.65	1.35	1.5	6.0	0	0.0	1.0	0.4	9.1	5.6	5.6	1130
253	[51]	AEDC	1960	Air	318	CON	5.59	0.27	3.6	18	1a	7.49	3.61	0.65	1.35	1.5	6.0	0	0.0	1.3	0.4	9.1	5.8	5.8	1130
254	[51]	AEDC	1960	Air	321	CON	5.59	0.27	3.6	18	1a	7.49	3.61	0.65	1.35	1.5	6.0	0	0.0	1.7	0.4	9.1	5.8	5.8	1130
255	[51]	AEDC	1960	Air	323	CON	5.59	0.27	3.6	18	1a	7.49	3.61	0.65	1.35	1.5	6.0	0	0.0	2.0	0.4	9.1	5.8	5.6	1130
256	[51]	AEDC	1960	Air	328	CON	5.59	0.27	3.6	18	1a	7.49	3.61	0.65	1.35	1.5	6.0	0	0.0	2.2	0.4	9.1	6.0	6.0	1130
257	[51]	AEDC	1960	Air	329	CON	5.59	0.27	3.6	18	1a	7.49	3.61	0.65	1.35	1.5	6.0	0	0.0	2.2	0.4	9.1	6.0	6.0	1130
258	[51]	AEDC	1960	Air	331	CON	5.59	0.14	3.6	18	1a	7.49	3.61	0.65	1.35	1.5	6.0	0	0.0	0.0	0.4	9.1	4.9	4.9	1880
259	[51]	AEDC	1960	Air	329	CON	5.59	0.14	3.6	18	1a	7.49	3.61	0.65	1.35	1.5	6.0	0	0.0	0.3	0.4	9.1	5.4	5.4	1770
260	[51]	AEDC	1960	Air	314	CON	5.59	0.28	3.6	18	2a	7.49	3.61	0.80	1.65	1.3	12.0	0	0.0	0.3	0.3	9.1	5.9	5.3	2130
261	[51]	AEDC	1960	Air	315	CON	5.59	0.28	3.6	18	2a	7.49	3.61	0.80	1.65	1.3	12.0	0	0.0	0.4	0.3	9.1	6.0	6.0	1110
262	[51]	AEDC	1960	Air	321	CON	5.59	0.27	3.6	18	2a	7.49	3.61	0.80	1.65	1.3	12.0	0	0.0	0.7	0.3	9.1	6.0	6.0	1110
263	[51]	AEDC	1960	Air	319	CON	5.59	0.27	3.6	18	2a	7.49	3.61	0.80	1.65	1.3	12.0	0	0.0	1.8	0.3	9.1	5.9	5.9	1110
264	[51]	AEDC	1960	Air	317	CON	5.59	0.28	3.6	18	2a	7.49	3.61	0.80	1.65	1.3	12.0	0	0.0	1.0	0.3	9.1	6.0	6.0	1110
265	[51]	AEDC	1960	Air	319	CON	5.59	0.27	3.6	18	2a	7.49	3.61	0.80	1.65	1.3	12.0	0	0.0	1.2	0.3	9.1	6.1	6.1	1110
266	[51]	AEDC	1960	Air	318	CON	5.59	0.27	3.6	18	2a	7.49	3.61	0.80	1.65	1.3	12.0	0	0.0	1.3	0.3	9.1	6.1	6.1	1110
267	[51]	AEDC	1960	Air	317	CON	5.59	0.27	3.6	18	2a	7.49	3.61	0.80	1.65	1.3	12.0	0	0.0	2.0	0.3	9.1	6.4	6.3	1110
268	[51]	AEDC	1960	Air	313	CON	5.59	0.27	3.6	18	2a	7.49	3.61	0.80	1.65	1.3	12.0	0	0.0	3.0	0.3	9.1	6.8	6.3	1110
269	[51]	AEDC	1960	Air	322	CON	5.59	0.27	3.6	18	2a	7.49	3.61	0.80	1.65	1.3	12.0	0	0.0	4.0	0.3	9.1	6.9	6.6	1110
270	[51]	AEDC	1960	Air	322	CON	5.59	0.27	3.6	18	2a	7.49	3.61	0.80	1.65	1.3	12.0	0	0.0	6.0	0.3	9.1	6.8	6.8	1110
271	[51]	AEDC	1960	Air	322	CON	5.59	0.21	3.6	18	2a	7.49	3.61	0.80	1.65	1.3	12.0	0	0.0	7.2	0.3	9.1	6.9	6.8	1110
272	[51]	AEDC	1960	Air	321	CON	5.59	0.14	3.6	18	2a	7.49	3.61	0.80	1.65	1.3	12.0	0	0.0	0.3	0.3	9.1	5.7	5.7	2040
273	[51]	AEDC	1960	Air	321	CON	5.59	0.14	3.6	18	2a	7.49	3.61	0.80	1.65	1.3	12.0	0	0.0	0.4	0.3	9.1	6.3	6.3	1080
274	[51]	AEDC	1960	Air	321	CON	5.59	0.14	3.6	18	2a	7.49	3.61	0.80	1.65	1.3	12.0	0	0.0	0.7	0.3	9.1	6.1	6.1	1080
275	[51]	AEDC	1960	Air	321	CON	5.59	0.14	3.6	18	2a	7.49	3.61	0.80	1.65	1.3	12.0	0	0.0	0.8	0.3	9.1	6.1	6.1	1080
276	[51]	AEDC	1960	Air	321	CON	5.59	0.14	3.6	18	2a	7.49	3.61	0.80	1.65	1.3	12.0	0	0.0	0.8	0.3	9.1	6.1	6.1	1080
277	[51]	AEDC	1960	Air	321	CON	5.59	0.14	3.6	18	2a	7.49	3.61	0.80	1.65	1.3	12.0	0	0.0	1.0	0.3	9.1	6.2	6.1	1080
278	[51]	AEDC	1960	Air	321	CON	5.59	0.14	3.6	18	2a	7.49	3.61	0.80	1.65	1.3	12.0	0	0.0	2.0	0.3	9.1	6.5	6.5	1080
279	[51]	AEDC	1960	Air	321	CON	5.59	0.14	3.6	18	2a	7.49	3.61	0.80	1.65	1.3	12.0	0	0.0	4.0	0.3	9.1	7.0	6.8	1080
280	[51]	AEDC	1960	Air	321	CON	5.59	0.14	3.6	18	2a	7.49	3.61	0.80	1.65	1.3	12.0	0	0.0	6.0	0.3	9.1	7.0	6.9	1080
281	[51]	AEDC	1960	Air	321	CON	5.59	0.14	3.6	18	2a	7.49	3.61	0.80	1.65	1.3	12.0	0	0.0	7.2	0.3	9.1	7.0	7.0	1080
282	[51]	AEDC	1960	Air	310	CON	5.59	0.25	3.6	18	2b	7.49	3.61	0.57	1.17	1.8	12.0	0	0.0	0.2	0.3	9.1	4.7	4.7	2710
283	[51]	AEDC	1960	Air	318	CON	5.59	0.25	3.6	18	2b	7.49	3.61	0.57	1.17	1.8	12.0	0	0.0	0.3	0.3	9.1	4.8	4.8	2380
284	[51]	AEDC	1960	Air	321	CON	5.59	0.25	3.6	18	2b	7.49	3.61	0.57	1.17	1.8	12.0	0	0.0	0.4	0.3	9.1	4.9	4.9	1910
285	[51]	AEDC	1960	Air	321	CON	5.59	0.25	3.6	18	2b	7.49	3.61	0.57	1.17	1.8	12.0	0	0.0	0.5	0.3	9.1	5.0	5.0	1120
286	[51]	AEDC	1960	Air	326	CON	5.59	0.25	3.6	18	2b	7.49	3.61	0.57	1.17	1.8	12.0	0	0.0	0.7	0.3	9.1	5.2	5.2	1110
287	[51]	AEDC	1960	Air	327	CON	5.59	0.25	3.6	18	2b	7.49	3.61	0.57	1.17	1.8	12.0	0	0.0	0.8	0.3	9.1	5.3	5.2	1100
288	[51]	AEDC	1960	Air	326	CON	5.59	0.25	3.6	18	2b	7.49	3.61	0.57	1.17	1.8	12.0	0	0.0	0.8	0.3	9.1	5.2	5.2	1100
289	[51]	AEDC	1960	Air	309	CON	5.59	0.27	3.6</td																

Table 5.3 (Continued) - Cold-Flow Cylindrical and Second-Throat Diffuser Data

No.	Ref.	Entity	Year	Nozzle Configuration						Diffuser Configuration										Performance					
				Gas	T <sub>0</sub>	Type	D <sub>NT</sub>	Ref. P <sub>0</sub>	A <sub>NE</sub> /A <sub>NT</sub>	θ <sub>NE</sub>	Name	A <sub>DI</sub> /A <sub>NT</sub>	M <sub>DI</sub>	A <sub>DT</sub> /A <sub>DI</sub>	A <sub>DT</sub> /A <sub>NE</sub>	A <sub>DE</sub> /A <sub>DT</sub>	θ <sub>DI</sub>	θ <sub>DT</sub>	θ <sub>SUB</sub>	L <sub>DI</sub> /D <sub>DI</sub>	L <sub>DT</sub> /D <sub>DT</sub>	L <sub>D</sub> /D <sub>DT</sub>	P <sub>0</sub> /P <sub>BACK</sub>	(P <sub>CELL</sub> /P <sub>0</sub> ) × 10 <sup>5</sup>	
[K] [cm] [MPa] [deg]																							Start Unst.		
324	[51]	AEDC	1960	Air	327	CON	5.59	0.14	3.6	18	3c	7.49	3.61	0.40	0.82	2.5	12.0	0	0.0	0.8	0.5	9.1	3.9	3.9	13000
325	[51]	AEDC	1960	Air	327	CON	5.59	0.14	3.6	18	3c	7.49	3.61	0.40	0.82	2.5	12.0	0	0.0	1.0	0.5	9.1	3.9	3.8	16100
326	[51]	AEDC	1960	Air	327	CON	5.59	0.14	3.6	18	3c	7.49	3.61	0.40	0.82	2.5	12.0	0	0.0	2.0	0.5	9.1	3.9	3.8	22400
327	[51]	AEDC	1960	Air	327	CON	5.59	0.14	3.6	18	3a	7.49	3.61	0.40	0.82	2.5	12.0	0	0.0	4.0	0.5	9.1	3.9	6.1	23400
328	[51]	AEDC	1960	Air	322	CON	5.59	0.27	3.6	18	4a	7.49	3.61	0.65	1.35	1.5	18.0	0	0.0	0.8	0.4	9.1	6.1	6.0	3120
329	[51]	AEDC	1960	Air	318	CON	5.59	0.27	3.6	18	4a	7.49	3.61	0.65	1.35	1.5	18.0	0	0.0	0.8	0.4	9.1	8.0	8.6	1120
330	[51]	AEDC	1960	Air	329	CON	5.59	0.27	3.6	18	4a	7.49	3.61	0.65	1.35	1.5	18.0	0	0.0	1.0	0.4	9.1	5.6	5.5	1110
331	[51]	AEDC	1960	Air	329	CON	5.59	0.27	3.6	18	4a	7.49	3.61	0.65	1.35	1.5	18.0	0	0.0	1.2	0.4	9.1	5.5	5.5	1110
332	[51]	AEDC	1960	Air	329	CON	5.59	0.27	3.6	18	4a	7.49	3.61	0.65	1.35	1.5	18.0	0	0.0	1.3	0.4	9.1	5.5	5.5	1110
333	[51]	AEDC	1960	Air	329	CON	5.59	0.27	3.6	18	4a	7.49	3.61	0.65	1.35	1.5	18.0	0	0.0	1.3	0.4	9.1	5.5	5.5	1110
334	[51]	AEDC	1960	Air	329	CON	5.59	0.27	3.6	18	4a	7.49	3.61	0.65	1.35	1.5	18.0	0	0.0	1.7	0.4	9.1	6.6	5.6	1110
335	[51]	AEDC	1960	Air	329	CON	5.59	0.14	3.6	18	4a	7.49	3.61	0.65	1.35	1.5	18.0	0	0.0	0.8	0.4	9.1	6.3	5.6	3400
336	[51]	AEDC	1960	Air	330	CON	5.59	0.14	3.6	18	4a	7.49	3.61	0.65	1.35	1.5	18.0	0	0.0	0.8	0.4	9.1	6.3	5.9	1120
337	[51]	AEDC	1960	Air	329	CON	5.59	0.14	3.6	18	4a	7.49	3.61	0.65	1.35	1.5	18.0	0	0.0	0.9	0.4	9.1	5.7	5.7	1120
338	[51]	AEDC	1960	Air	329	CON	5.59	0.14	3.6	18	4a	7.49	3.61	0.65	1.35	1.5	18.0	0	0.0	1.0	0.4	9.1	5.6	5.6	1120
339	[51]	AEDC	1960	Air	329	CON	5.59	0.14	3.6	18	4a	7.49	3.61	0.65	1.35	1.5	18.0	0	0.0	1.1	0.4	9.1	5.6	5.6	1120
340	[51]	AEDC	1960	Air	330	CON	5.59	0.14	3.6	18	4a	7.49	3.61	0.65	1.35	1.5	18.0	0	0.0	1.3	0.4	9.1	5.6	5.6	1120
341	[51]	AEDC	1960	Air	329	CON	5.59	0.14	3.6	18	4a	7.49	3.61	0.65	1.35	1.5	18.0	0	0.0	1.3	0.4	9.1	5.7	5.6	1120
342	[51]	AEDC	1960	Air	329	CON	5.59	0.14	3.6	18	4a	7.49	3.61	0.65	1.35	1.5	18.0	0	0.0	1.5	0.4	9.1	6.7	5.8	1120
343	[51]	AEDC	1960	Air	311	CON	3.20	0.28	10.8	18	1a	22.8	4.89	0.65	1.37	1.5	6.0	0	0.0	0.5	0.4	9.1	22.2	17.2	232
344	[51]	AEDC	1960	Air	308	CON	3.20	0.28	10.8	18	1a	22.8	4.89	0.65	1.37	1.5	6.0	0	0.0	0.5	0.4	9.1	17.0	16.8	204
345	[51]	AEDC	1960	Air	303	CON	3.20	0.27	10.8	18	1a	22.8	4.89	0.65	1.37	1.5	6.0	0	0.0	0.8	0.4	9.1	16.8	16.8	199
346	[51]	AEDC	1960	Air	321	CON	3.20	0.27	10.8	18	1a	22.8	4.89	0.65	1.37	1.5	6.0	0	0.0	0.9	0.4	9.1	16.7	16.6	209
347	[51]	AEDC	1960	Air	321	CON	3.20	0.27	10.8	18	1a	22.8	4.89	0.65	1.37	1.5	6.0	0	0.0	1.0	0.4	9.1	16.3	16.3	209
348	[51]	AEDC	1960	Air	322	CON	3.20	0.27	10.8	18	1a	22.8	4.89	0.65	1.37	1.5	6.0	0	0.0	1.1	0.4	9.1	16.3	16.2	209
349	[51]	AEDC	1960	Air	321	CON	3.20	0.27	10.8	18	1a	22.8	4.89	0.65	1.37	1.5	6.0	0	0.0	1.2	0.4	9.1	16.6	16.5	209
350	[51]	AEDC	1960	Air	316	CON	3.20	0.27	10.8	18	1a	22.8	4.89	0.65	1.37	1.5	6.0	0	0.0	1.3	0.4	9.1	16.8	16.8	204
351	[51]	AEDC	1960	Air	316	CON	3.20	0.27	10.8	18	1a	22.8	4.89	0.65	1.37	1.5	6.0	0	0.0	1.5	0.4	9.1	16.9	16.9	204
352	[51]	AEDC	1960	Air	312	CON	3.20	0.27	10.8	18	1a	22.8	4.89	0.65	1.37	1.5	6.0	0	0.0	1.7	0.4	9.1	17.4	17.3	201
353	[51]	AEDC	1960	Air	369	CON	3.20	0.27	10.8	18	1a	22.8	4.89	0.65	1.37	1.5	6.0	0	0.0	2.0	0.4	9.1	19.8	17.6	201
354	[51]	AEDC	1960	Air	316	CON	3.20	0.27	10.8	18	1a	22.8	4.89	0.65	1.37	1.5	6.0	0	0.0	3.0	0.4	9.1	17.8	17.7	204
355	[51]	AEDC	1960	Air	317	CON	3.20	0.27	10.8	18	1a	22.8	4.89	0.65	1.37	1.5	6.0	0	0.0	4.0	0.4	9.1	18.6	18.5	206
356	[51]	AEDC	1960	Air	318	CON	3.20	0.27	10.8	18	1a	22.8	4.89	0.65	1.37	1.5	6.0	0	0.0	4.9	0.4	9.1	20.5	19.9	206
357	[51]	AEDC	1960	Air	316	CON	3.20	0.28	10.8	18	1a	22.8	4.89	0.65	1.37	1.5	6.0	0	0.0	6.0	0.4	9.1	17.0	16.9	239
358	[51]	AEDC	1960	Air	321	CON	3.20	0.28	10.8	18	1a	22.8	4.89	0.65	1.37	1.5	6.0	0	0.0	1.0	0.4	9.1	16.5	16.5	239
359	[51]	AEDC	1960	Air	323	CON	3.20	0.28	10.8	18	1a	22.8	4.89	0.65	1.37	1.5	6.0	0	0.0	4.0	0.4	9.1	18.5	18.2	242
360	[51]	AEDC	1960	Air	329	CON	3.20	0.27	10.8	18	1a	22.8	4.89	0.65	1.37	1.5	6.0	0	0.0	4.3	0.4	9.1	19.7	18.8	245
361	[51]	AEDC	1960	Air	329	CON	3.20	0.27	10.8	18	1a	22.8	4.89	0.65	1.37	1.5	6.0	0	0.0	4.3	0.4	9.1	20.9	18.9	245
362	[51]	AEDC	1960	Air	331	CON	3.20	0.27	10.8	18	1a	22.8	4.89	0.65	1.37	1.5	6.0	0	0.0	0.0	0.4	9.1	14.4	14.4	734
363	[51]	AEDC	1960	Air	329	CON	3.20	0.14	10.8	18	1a	22.8	4.89	0.65	1.37	1.5	6.0	0	0.0	0.3	0.4	9.1	16.3	15.6	637
364	[51]	AEDC	1960	Air	329	CON	3.20	0.14	10.8	18	1a	22.8	4.89	0.65	1.37	1.5	6.0	0	0.0	0.5	0.4	9.1	16.3	15.6	607
365	[51]	AEDC	1960	Air	329	CON	3.20	0.14	10.8	18	1a	22.8	4.89	0.65	1.37	1.5	6.0	0	0.0	0.6	0.4	9.1	15.8	15.8	588
366	[51]	AEDC	1960	Air	329	CON	3.20	0.14	10.8	18	1a	22.8	4.89	0.65	1.37	1.5	6.0	0	0.0	1.0	0.4	9.1	17.1	17.1	452
367	[51]	AEDC	1960	Air	311	CON	3.20	0.27	10.8	18	2a	22.8	4.89	0.80	1.68	1.3	12.0	0	0.0	0.3	0.3	9.1	15.5	15.2	447
368	[51]	AEDC	1960	Air	311	CON	3.20	0.27	10.8	18	2a	22.8	4.89	0.80	1.68	1.3	12.0	0	0.0	0.5	0.3	9.1	16.5	16.5	238
369	[51]	AEDC	1960	Air	312	CON	3.20	0.27	10.8	18	2a	22.8	4.89	0.80	1.68	1.3	12.0	0	0.0	0.5	0.3	9.1	16.9	16.9	201
370	[51]	AEDC	1960	Air	313	CON	3.20	0.27	10.8	18	2a	22.8	4.89	0.80	1.68	1.3	12.0	0	0.0	0					

Table 5.3 (Continued) - Cold-Flow Cylindrical and Second-Throat Diffuser Data

No.	Ref.	Entity	Year	Nozzle Configuration					Diffuser Configuration									Performance							
				Gas	T <sub>0</sub>	Type	D <sub>NT</sub>	Ref. P <sub>0</sub>	A <sub>NE</sub> /A <sub>NT</sub>	θ <sub>NE</sub>	Name	A <sub>DI</sub> /A <sub>NT</sub>	M <sub>DI</sub>	A <sub>DT</sub> /A <sub>DI</sub>	A <sub>DT</sub> /A <sub>NE</sub>	A <sub>DE</sub> /A <sub>DT</sub>	θ <sub>DI</sub>	θ <sub>DT</sub>	θ <sub>SUB</sub>	L <sub>DI</sub> /D <sub>DI</sub>	L <sub>DT</sub> /D <sub>DT</sub>	L <sub>D</sub> /D <sub>DT</sub>	P <sub>0</sub> /P <sub>BACK</sub>	(P <sub>CELL</sub> /P <sub>0</sub> ) × 10 <sup>5</sup>	
[K] [cm] [MPa] [deg]																				Start	Unst.				
407	[51]	AEDC	1960	Air	310	CON	3.20	0.27	10.8	18	3a	22.8	4.89	0.50	1.05	2.0	12.0	0	0.0	1.1	0.7	9.1	15.5	15.2	199
408	[51]	AEDC	1960	Air	307	CON	3.20	0.14	10.8	18	3a	22.8	4.89	0.50	1.05	2.0	12.0	0	0.0	0.8	0.7	9.1	15.9	15.8	509
409	[51]	AEDC	1960	Air	310	CON	3.20	0.14	10.8	18	3a	22.8	4.89	0.50	1.05	2.0	12.0	0	0.0	0.9	0.7	9.1	15.7	15.6	441
410	[51]	AEDC	1960	Air	311	CON	3.20	0.14	10.8	18	3a	22.8	4.89	0.50	1.05	2.0	12.0	0	0.0	1.0	0.7	9.1	15.9	15.8	431
411	[51]	AEDC	1960	Air	311	CON	3.20	0.14	10.8	18	3a	22.8	4.89	0.50	1.05	2.0	12.0	0	0.0	1.3	0.7	9.1	29.2	18.8	NR
412	[51]	AEDC	1960	Air	303	CON	3.20	0.28	10.8	18	3b	22.8	4.89	0.50	1.05	2.0	12.0	0	0.0	0.3	8.0	9.1	10.9	10.9	430
413	[51]	AEDC	1960	Air	306	CON	3.20	0.28	10.8	18	3b	22.8	4.89	0.50	1.05	2.0	12.0	0	0.0	0.5	8.0	9.1	12.2	12.2	199
414	[51]	AEDC	1960	Air	309	CON	3.20	0.28	10.8	18	3b	22.8	4.89	0.50	1.05	2.0	12.0	0	0.0	0.6	8.0	9.1	11.7	11.7	200
415	[51]	AEDC	1960	Air	309	CON	3.20	0.28	10.8	18	3b	22.8	4.89	0.50	1.05	2.0	12.0	0	0.0	0.8	8.0	9.1	11.5	11.5	206
416	[51]	AEDC	1960	Air	309	CON	3.20	0.28	10.8	18	3b	22.8	4.89	0.50	1.05	2.0	12.0	0	0.0	0.9	8.0	9.1	11.5	11.4	186
417	[51]	AEDC	1960	Air	309	CON	3.20	0.14	10.8	18	3b	22.8	4.89	0.50	1.05	2.0	12.0	0	0.0	0.6	8.0	9.1	11.2	11.2	583
418	[51]	AEDC	1960	Air	309	CON	3.20	0.27	10.8	18	3c	22.8	4.89	0.40	0.84	2.5	12.0	0	0.0	0.3	0.5	9.1	12.3	12.3	425
419	[51]	AEDC	1960	Air	322	CON	3.20	0.27	10.8	18	3c	22.8	4.89	0.40	0.84	2.5	12.0	0	0.0	0.9	0.5	9.1	12.9	12.8	1100
420	[51]	AEDC	1960	Air	322	CON	3.20	0.27	10.8	18	3c	22.8	4.89	0.40	0.84	2.5	12.0	0	0.0	1.0	0.5	9.1	12.5	12.5	1710
421	[51]	AEDC	1960	Air	324	CON	3.20	0.27	10.8	18	3c	22.8	4.89	0.40	0.84	2.5	12.0	0	0.0	1.3	0.5	9.1	12.3	12.3	2660
422	[51]	AEDC	1960	Air	326	CON	3.20	0.27	10.8	18	3c	22.8	4.89	0.40	0.84	2.5	12.0	0	0.0	2.0	0.5	9.1	12.1	12.1	4460
423	[51]	AEDC	1960	Air	329	CON	3.20	0.27	10.8	18	3c	22.8	4.89	0.40	0.84	2.5	12.0	0	0.0	4.0	0.5	9.1	12.1	12.1	5440
424	[51]	AEDC	1960	Air	329	CON	3.20	0.27	10.8	18	3c	22.8	4.89	0.40	0.84	2.5	12.0	0	0.0	6.0	0.5	9.1	12.1	12.1	6490
425	[51]	AEDC	1960	Air	328	CON	3.20	0.14	10.8	18	3c	22.8	4.89	0.40	0.84	2.5	12.0	0	0.0	0.2	0.5	9.1	12.2	12.2	9690
426	[51]	AEDC	1960	Air	328	CON	3.20	0.14	10.8	18	3c	22.8	4.89	0.40	0.84	2.5	12.0	0	0.0	0.3	0.5	9.1	13.0	13.0	718
427	[51]	AEDC	1960	Air	327	CON	3.20	0.14	10.8	18	3c	22.8	4.89	0.40	0.84	2.5	12.0	0	0.0	0.5	0.5	9.1	13.3	13.2	664
428	[51]	AEDC	1960	Air	327	CON	3.20	0.14	10.8	18	3c	22.8	4.89	0.40	0.84	2.5	12.0	0	0.0	0.5	0.5	9.1	13.2	13.2	1570
429	[51]	AEDC	1960	Air	327	CON	3.20	0.14	10.8	18	3c	22.8	4.89	0.40	0.84	2.5	12.0	0	0.0	1.0	0.5	9.1	13.9	13.9	1170
430	[51]	AEDC	1960	Air	327	CON	3.20	0.14	10.8	18	3c	22.8	4.89	0.40	0.84	2.5	12.0	0	0.0	1.3	0.5	9.1	13.6	13.6	1330
431	[51]	AEDC	1960	Air	327	CON	3.20	0.14	10.8	18	3c	22.8	4.89	0.40	0.84	2.5	12.0	0	0.0	2.0	0.5	9.1	13.2	13.2	2080
432	[51]	AEDC	1960	Air	329	CON	3.20	0.14	10.8	18	3c	22.8	4.89	0.40	0.84	2.5	12.0	0	0.0	6.0	0.5	9.1	13.3	13.3	6070
433	[51]	AEDC	1960	Air	306	CON	3.20	0.28	10.8	18	4a	22.8	4.89	0.65	1.37	1.5	18.0	0	0.0	0.5	0.4	9.1	15.4	15.4	522
434	[51]	AEDC	1960	Air	308	CON	3.20	0.28	10.8	18	4a	22.8	4.89	0.65	1.37	1.5	18.0	0	0.0	0.5	0.4	9.1	16.2	16.2	213
435	[51]	AEDC	1960	Air	304	CON	3.20	0.27	10.8	18	4a	22.8	4.89	0.65	1.37	1.5	18.0	0	0.0	0.6	0.4	9.1	17.0	16.9	207
436	[51]	AEDC	1960	Air	311	CON	3.20	0.28	10.8	18	4a	22.8	4.89	0.65	1.37	1.5	18.0	0	0.0	0.8	0.4	9.1	17.6	17.6	218
437	[51]	AEDC	1960	Air	309	CON	3.20	0.28	10.8	18	4a	22.8	4.89	0.65	1.37	1.5	18.0	0	0.0	1.0	0.4	9.1	17.8	17.8	218
438	[51]	AEDC	1960	Air	311	CON	3.20	0.27	10.8	18	4a	22.8	4.89	0.65	1.37	1.5	18.0	0	0.0	1.3	0.4	9.1	16.9	16.9	223
439	[51]	AEDC	1960	Air	313	CON	3.20	0.27	10.8	18	4a	22.8	4.89	0.65	1.37	1.5	18.0	0	0.0	1.6	0.4	9.1	16.6	16.6	221
440	[51]	AEDC	1960	Air	316	CON	3.20	0.27	10.8	18	4a	22.8	4.89	0.65	1.37	1.5	18.0	0	0.0	1.8	0.4	9.1	16.2	16.2	224
441	[51]	AEDC	1960	Air	316	CON	3.20	0.27	10.8	18	4a	22.8	4.89	0.65	1.37	1.5	18.0	0	0.0	1.9	0.4	9.1	16.3	16.3	224
442	[51]	AEDC	1960	Air	309	CON	3.20	0.28	10.8	18	4a	22.8	4.89	0.65	1.37	1.5	18.0	0	0.0	2.0	0.4	9.1	16.4	16.4	213
443	[51]	AEDC	1960	Air	316	CON	3.20	0.27	10.8	18	4a	22.8	4.89	0.65	1.37	1.5	18.0	0	0.0	2.1	0.4	9.1	17.1	16.6	224
444	[51]	AEDC	1960	Air	314	CON	3.20	0.27	10.8	18	4a	22.8	4.89	0.65	1.37	1.5	18.0	0	0.0	2.3	0.4	9.1	17.2	16.9	223
445	[51]	AEDC	1960	Air	318	CON	3.20	0.27	10.8	18	4a	22.8	4.89	0.65	1.37	1.5	18.0	0	0.0	3.0	0.4	9.1	17.0	19.3	225
446	[51]	AEDC	1960	Air	320	CON	3.20	0.28	10.8	18	4a	22.8	4.89	0.65	1.37	1.5	18.0	0	0.0	3.5	0.4	9.1	17.1	19.2	223
447	[51]	AEDC	1960	Air	319	CON	3.20	0.14	10.8	18	4a	22.8	4.89	0.65	1.37	1.5	18.0	0	0.0	0.8	0.4	9.1	17.9	17.9	529
448	[51]	AEDC	1960	Air	319	CON	3.20	0.14	10.8	18	4a	22.8	4.89	0.65	1.37	1.5	18.0	0	0.0	0.8	0.4	9.1	18.3	18.3	430
449	[51]	AEDC	1960	Air	318	CON	3.20	0.14	10.8	18	4a	22.8	4.89	0.65	1.37	1.5	18.0	0	0.0	1.0	0.4	9.1	18.9	18.9	430
450	[51]	AEDC	1960	Air	318	CON	3.20	0.14	10.8	18	4a	22.8	4.89	0.65	1.37	1.5	18.0	0	0.0	2.0	0.4	9.1	16.5	16.5	430
451	[51]	AEDC	1960	Air	319	CON	3.20	0.14	10.8	18	4a	22.8	4.89	0.65	1.37	1.5	18.0	0	0.0	2.1	0.4	9.1	16.7	16.4	430
452	[51]	AEDC	1960	Air	319	CON	3.20	0.14	10.8	18	4a	22.8	4.89	0.65	1.37	1.5	18.0	0	0.0	2.3	0.4	9.1	17.2	15.7	431
453	[51]	AEDC	1960	Air	319	CON	3.20	0.14	10.8	18	4a	22.8	4.89	0.65	1.37	1.									

Table 5.3 (Continued) - Cold-Flow Cylindrical and Second-Throat Diffuser Data

No.	Ref.	Entity	Year	Nozzle Configuration					Diffuser Configuration									Performance							
				Gas	T <sub>0</sub>	Type	D <sub>NT</sub>	Ref. P <sub>0</sub>	A <sub>NE</sub> /A <sub>NT</sub>	θ <sub>NE</sub>	Name	A <sub>DI</sub> /A <sub>NT</sub>	M <sub>DI</sub>	A <sub>DT</sub> /A <sub>DI</sub>	A <sub>DT</sub> /A <sub>NE</sub>	A <sub>DE</sub> /A <sub>DT</sub>	θ <sub>DI</sub>	θ <sub>DT</sub>	θ <sub>SUB</sub>	L <sub>DI</sub> /D <sub>DI</sub>	L <sub>DT</sub> /D <sub>DT</sub>	L <sub>D</sub> /D <sub>DT</sub>	P <sub>0</sub> /P <sub>BACK</sub>	(P <sub>CELL</sub> /P <sub>0</sub> ) × 10 <sup>5</sup>	
[K] [cm] [MPa] [deg]																				Start	Unst.				
490	[51]	AEDC	1960	Air	297	CON	2.11	0.27	25	18	2a	52.5	5.98	0.80	1.68	1.5	12.0	0	0.0	2.2	0.3	9.1	40.7	40.7	107
491	[51]	AEDC	1960	Air	297	CON	2.11	0.27	25	18	2a	52.5	5.98	0.80	1.68	1.5	12.0	0	0.0	2.3	0.3	9.1	42.0	41.8	107
492	[51]	AEDC	1960	Air	297	CON	2.11	0.27	25	18	2a	52.5	5.98	0.80	1.68	1.5	12.0	0	0.0	3.0	0.3	9.1	41.3	41.3	104
493	[51]	AEDC	1960	Air	297	CON	2.11	0.27	25	18	2a	52.5	5.98	0.80	1.68	1.5	12.0	0	0.0	4.0	0.3	9.1	41.5	41.5	104
494	[51]	AEDC	1960	Air	297	CON	2.11	0.27	25	18	2a	52.5	5.98	0.80	1.68	1.5	12.0	0	0.0	6.0	0.3	9.1	42.7	42.7	105
495	[51]	AEDC	1960	Air	296	CON	2.11	0.18	25	18	2a	52.5	5.98	0.80	1.68	1.5	12.0	0	0.0	1.0	0.3	9.1	42.7	40.8	151
496	[51]	AEDC	1960	Air	296	CON	2.11	0.18	25	18	2a	52.5	5.98	0.80	1.68	1.5	12.0	0	0.0	1.0	0.3	9.1	42.9	41.0	150
497	[51]	AEDC	1960	Air	296	CON	2.11	0.18	25	18	2a	52.5	5.98	0.80	1.68	1.5	12.0	0	0.0	2.0	0.3	9.1	40.3	40.3	150
498	[51]	AEDC	1960	Air	296	CON	2.11	0.18	25	18	2a	52.5	5.98	0.80	1.68	1.5	12.0	0	0.0	4.0	0.3	9.1	42.0	42.0	150
499	[51]	AEDC	1960	Air	318	CON	2.11	0.27	25	18	2b	52.5	5.98	0.57	1.19	1.8	12.0	0	0.0	0.3	0.3	9.1	27.6	27.6	288
500	[51]	AEDC	1960	Air	318	CON	2.11	0.27	25	18	2b	52.5	5.98	0.57	1.19	1.8	12.0	0	0.0	0.3	0.3	9.1	33.3	33.3	215
501	[51]	AEDC	1960	Air	318	CON	2.11	0.27	25	18	2b	52.5	5.98	0.57	1.19	1.8	12.0	0	0.0	0.7	0.3	9.1	35.7	35.7	171
502	[51]	AEDC	1960	Air	307	CON	2.11	0.27	25	18	2b	52.5	5.98	0.57	1.19	1.8	12.0	0	0.0	0.8	0.3	9.1	36.9	36.9	123
503	[51]	AEDC	1960	Air	308	CON	2.11	0.27	25	18	2b	52.5	5.98	0.57	1.19	1.8	12.0	0	0.0	2.0	0.3	9.1	35.6	34.7	123
504	[51]	AEDC	1960	Air	308	CON	2.11	0.27	25	18	2b	52.5	5.98	0.57	1.19	1.8	12.0	0	0.0	3.0	0.3	9.1	39.2	39.2	122
505	[51]	AEDC	1960	Air	308	CON	2.11	0.27	25	18	2b	52.5	5.98	0.57	1.19	1.8	12.0	0	0.0	1.0	0.3	9.1	50.8	50.8	127
506	[51]	AEDC	1960	Air	304	CON	2.11	0.32	25	18	2b	52.5	5.98	0.57	1.19	1.8	12.0	0	0.0	0.3	0.3	9.1	39.7	39.7	98.9
507	[51]	AEDC	1960	Air	318	CON	2.11	0.16	25	18	2b	52.5	5.98	0.57	1.19	1.8	12.0	0	0.0	0.3	0.3	9.1	29.9	24.6	418
508	[51]	AEDC	1960	Air	318	CON	2.11	0.16	25	18	2b	52.5	5.98	0.57	1.19	1.8	12.0	0	0.0	0.7	0.3	9.1	30.0	30.0	335
509	[51]	AEDC	1960	Air	318	CON	2.11	0.16	25	18	2b	52.5	5.98	0.57	1.19	1.8	12.0	0	0.0	1.0	0.3	9.1	31.1	31.1	577
510	[51]	AEDC	1960	Air	299	CON	2.11	0.16	25	18	2b	52.5	5.98	0.57	1.19	1.8	12.0	0	0.0	2.0	0.3	9.1	38.2	38.2	186
511	[51]	AEDC	1960	Air	299	CON	2.11	0.16	25	18	2b	52.5	5.98	0.57	1.19	1.8	12.0	0	0.0	2.0	0.3	9.1	35.2	34.1	158
512	[51]	AEDC	1960	Air	299	CON	2.11	0.16	25	18	2b	52.5	5.98	0.57	1.19	1.8	12.0	0	0.0	3.0	0.3	9.1	38.2	33.0	158
513	[51]	AEDC	1960	Air	305	CON	2.11	0.28	25	18	3a	52.5	5.98	0.50	1.05	2.0	12.0	0	0.0	0.7	0.7	9.1	36.0	35.7	155
514	[51]	AEDC	1960	Air	305	CON	2.11	0.28	25	18	3a	52.5	5.98	0.50	1.05	2.0	12.0	0	0.0	0.8	0.7	9.1	33.3	33.1	138
515	[51]	AEDC	1960	Air	305	CON	2.11	0.28	25	18	3a	52.5	5.98	0.50	1.05	2.0	12.0	0	0.0	0.8	0.7	9.1	33.6	33.3	138
516	[51]	AEDC	1960	Air	305	CON	2.11	0.21	25	18	3a	52.5	5.98	0.50	1.05	2.0	12.0	0	0.0	0.8	0.7	9.1	33.9	33.8	136
517	[51]	AEDC	1960	Air	306	CON	2.11	0.27	25	18	3a	52.5	5.98	0.50	1.05	2.0	12.0	0	0.0	0.9	0.7	9.1	35.0	34.6	130
518	[51]	AEDC	1960	Air	301	CON	2.11	0.28	25	18	3a	52.5	5.98	0.50	1.05	2.0	12.0	0	0.0	1.0	0.7	9.1	35.1	34.7	136
519	[51]	AEDC	1960	Air	302	CON	2.11	0.28	25	18	3a	52.5	5.98	0.50	1.05	2.0	12.0	0	0.0	1.1	0.7	9.1	35.1	34.7	136
520	[51]	AEDC	1960	Air	302	CON	2.11	0.27	25	18	3a	52.5	5.98	0.50	1.05	2.0	12.0	0	0.0	1.2	0.7	9.1	35.1	34.7	137
521	[51]	AEDC	1960	Air	302	CON	2.11	0.28	25	18	3a	52.5	5.98	0.50	1.05	2.0	12.0	0	0.0	1.3	0.7	9.1	34.8	34.5	136
522	[51]	AEDC	1960	Air	302	CON	2.11	0.27	25	18	3a	52.5	5.98	0.50	1.05	2.0	12.0	0	0.0	1.3	0.7	9.1	35.1	34.1	137
523	[51]	AEDC	1960	Air	302	CON	2.11	0.28	25	18	3a	52.5	5.98	0.50	1.05	2.0	12.0	0	0.0	1.4	0.7	9.1	36.9	34.1	136
524	[51]	AEDC	1960	Air	302	CON	2.11	0.27	25	18	3a	52.5	5.98	0.50	1.05	2.0	12.0	0	0.0	1.5	0.7	9.1	46.7	34.0	137
525	[51]	AEDC	1960	Air	304	CON	2.11	0.14	25	18	3a	52.5	5.98	0.50	1.05	2.0	12.0	0	0.0	1.2	0.7	9.1	33.1	32.9	191
526	[51]	AEDC	1960	Air	306	CON	2.11	0.14	25	18	3a	52.5	5.98	0.50	1.05	2.0	12.0	0	0.0	1.3	0.7	9.1	42.0	41.5	185
527	[51]	AEDC	1960	Air	304	CON	2.11	0.14	25	18	3a	52.5	5.98	0.50	1.05	2.0	12.0	0	0.0	2.0	0.7	9.1	37.3	33.5	185
528	[51]	AEDC	1960	Air	298	CON	2.11	0.28	25	18	3b	52.5	5.98	0.50	1.05	2.0	12.0	0	0.0	0.6	0.8	9.1	25.9	25.9	142
529	[51]	AEDC	1960	Air	299	CON	2.11	0.27	25	18	3b	52.5	5.98	0.50	1.05	2.0	12.0	0	0.0	0.7	0.8	9.1	27.0	26.7	107
530	[51]	AEDC	1960	Air	297	CON	2.11	0.28	25	18	3b	52.5	5.98	0.50	1.05	2.0	12.0	0	0.0	0.7	0.8	9.1	26.8	26.7	106
531	[51]	AEDC	1960	Air	299	CON	2.11	0.27	25	18	3b	52.5	5.98	0.50	1.05	2.0	12.0	0	0.0	1.0	0.8	9.1	25.4	25.3	102
532	[51]	AEDC	1960	Air	300	CON	2.11	0.27	25	18	3b	52.5	5.98	0.50	1.05	2.0	12.0	0	0.0	1.3	0.8	9.1	24.4	24.3	102
533	[51]	AEDC	1960	Air	299	CON	2.11	0.27	25	18	3b	52.5	5.98	0.50	1.05	2.0	12.0	0	0.0	1.3	0.8	9.1	24.4	24.3	102
534	[51]	AEDC	1960	Air	300	CON	2.11	0.14	25	18	3b	52.5	5.98	0.50	1.05	2.0	12.0	0	0.0	1.0	0.8	9.1	24.8	24.6	180
535	[51]	AEDC	1960	Air	299	CON	2.11	0.14	25	18	3b	52.5	5.98	0.50	1.05	2.0	12.0	0	0.0	1.0	0.8	9.1	24.7	24.7	156
536	[51]	AEDC	1960	Air	299	CON	2.11	0.14	25	18	3b	52.5	5.98	0.50	1.05	2.0	12.0	0	0.0	1.3	0.8	9.1	23.8	23.6	151
537	[51]	AEDC																							

Table 5.3 (Continued) - Cold-Flow Cylindrical and Second-Throat Diffuser Data

No.	Ref.	Entity	Year	Nozzle Configuration					Diffuser Configuration									Performance								
				Gas	T <sub>0</sub>	Type	D <sub>NT</sub>	Ref. P <sub>0</sub>	A <sub>NE</sub> A <sub>NT</sub>	θ <sub>NE</sub>	Name	A <sub>DI</sub> A <sub>NT</sub>	M <sub>DI</sub>	A <sub>DT</sub> A <sub>DI</sub>	A <sub>DT</sub> A <sub>NE</sub>	A <sub>DE</sub> A <sub>DT</sub>	θ <sub>DI</sub>	θ <sub>DT</sub>	θ <sub>SUB</sub>	L <sub>DI</sub> D <sub>DI</sub>	L <sub>DT</sub> D <sub>DT</sub>	L <sub>D</sub> D <sub>DT</sub>	P <sub>0</sub> P <sub>BACK</sub>	(P <sub>CELL</sub> P <sub>0</sub> ) × 10 <sup>5</sup>		
				[K]		[cm]	[MPa]		[deg]													Start	Unst.			
573	[51]	AEDC	1960	Air	297	CON	2.11	0.14	25	18	4a	52.5	5.98	0.65	1.37	1.5	18.0	0	0.0	5.2	0.4	9.1	43.3	43.3	153	
574	[51]	AEDC	1960	Air	299	TOP	2.29	0.28	23.7	0.0	3b	44.7	5.76	0.50	0.94	2.0	12.0	0	0.0	8.0	9.1	18.3	18.3	116		
575	[51]	AEDC	1960	Air	299	TOP	2.29	0.28	23.7	0.0	3b	44.7	5.76	0.50	0.94	2.0	12.0	0	0.0	0.5	8.0	9.1	19.3	19.3	56.2	
576	[51]	AEDC	1960	Air	300	TOP	2.29	0.28	23.7	0.0	3b	44.7	5.76	0.50	0.94	2.0	12.0	0	0.0	0.6	8.0	9.1	19.7	19.7	36.3	
577	[51]	AEDC	1960	Air	300	TOP	2.29	0.28	23.7	0.0	3b	44.7	5.76	0.50	0.94	2.0	12.0	0	0.0	0.7	8.0	9.1	19.6	19.6	36.3	
578	[51]	AEDC	1960	Air	300	TOP	2.29	0.28	23.7	0.0	3b	44.7	5.76	0.50	0.94	2.0	12.0	0	0.0	0.8	8.0	9.1	19.7	19.7	36.4	
579	[51]	AEDC	1960	Air	298	TOP	2.29	0.27	23.7	0.0	3b	44.7	5.76	0.50	0.94	2.0	12.0	0	0.0	1.0	8.0	9.1	19.9	19.9	36.4	
580	[51]	AEDC	1960	Air	300	TOP	2.29	0.28	23.7	0.0	3b	44.7	5.76	0.50	0.94	2.0	12.0	0	0.0	1.3	8.0	9.1	20.7	20.7	36.4	
581	[51]	AEDC	1960	Air	300	TOP	2.29	0.27	23.7	0.0	3b	44.7	5.76	0.50	0.94	2.0	12.0	0	0.0	1.7	8.0	9.1	22.5	22.5	36.4	
582	[51]	AEDC	1960	Air	299	TOP	2.29	0.27	23.7	0.0	3b	44.7	5.76	0.50	0.94	2.0	12.0	0	0.0	2.0	8.0	9.1	28.8	23.9	36.5	
583	[51]	AEDC	1960	Air	300	TOP	2.29	0.14	23.7	0.0	3b	44.7	5.76	0.50	0.94	2.0	12.0	0	0.0	0.3	8.0	9.1	18.9	18.9	102	
584	[51]	AEDC	1960	Air	300	TOP	2.29	0.14	23.7	0.0	3b	44.7	5.76	0.50	0.94	2.0	12.0	0	0.0	0.6	8.0	9.1	20.0	20.0	40.0	
585	[51]	AEDC	1960	Air	300	TOP	2.29	0.14	23.7	0.0	3b	44.7	5.76	0.50	0.94	2.0	12.0	0	0.0	0.8	8.0	9.1	20.0	20.0	40.0	
586	[51]	AEDC	1960	Air	300	TOP	2.29	0.14	23.7	0.0	3b	44.7	5.76	0.50	0.94	2.0	12.0	0	0.0	1.0	8.0	9.1	20.2	20.2	40.0	
587	[51]	AEDC	1960	Air	300	TOP	2.29	0.14	23.7	0.0	3b	44.7	5.76	0.50	0.94	2.0	12.0	0	0.0	1.2	8.0	9.1	20.4	20.4	40.0	
588	[51]	AEDC	1960	Air	300	TOP	2.29	0.14	23.7	0.0	3b	44.7	5.76	0.50	0.94	2.0	12.0	0	0.0	1.3	8.0	9.1	25.4	21.2	40.0	
589	[51]	AEDC	1960	Air	300	TOP	2.29	0.14	23.7	0.0	3b	44.7	5.76	0.50	0.94	2.0	12.0	0	0.0	2.0	8.0	9.1	31.5	24.0	40.9	
590	[6]	NASA JPL	1960	N2	NR	TOC	1.40	1.03	20.3	12.8	-	28.8	5.18	0.51	0.65	4.0	5.0	0	10.0	0.1	10.0	13.1	15.7	10.1	NR	
591	[52]	Thiokol	1960	N2	AMB	CON	0.64	0.31	5.86	8.2	-	30.5	5.25	1.00	5.20	NR	0.0	0	NR	-	5.8	NR	23.9	23.9	62.9	
592	[52]	Thiokol	1960	N2	AMB	CON	0.64	0.31	5.86	8.2	-	30.5	5.25	1.00	5.20	NR	0.0	0	NR	-	7.3	NR	28.6	28.6	52.4	
593	[52]	Thiokol	1960	N2	AMB	CON	0.64	0.31	5.86	8.2	-	30.5	5.25	1.00	5.20	NR	0.0	0	NR	-	8.7	NR	27.6	27.6	54.3	
594	[52]	Thiokol	1960	N2	AMB	CON	0.64	0.31	5.86	8.2	-	30.5	5.25	1.00	5.20	NR	0.0	0	NR	-	9.0	NR	28.4	28.4	52.7	
595	[52]	Thiokol	1960	N2	AMB	CON	0.64	0.31	5.86	8.2	-	30.5	5.25	1.00	5.20	NR	-7.0	0	NR	-	5.8	NR	23.0	23.0	95.7	
596	[52]	Thiokol	1960	N2	AMB	CON	0.64	0.31	5.86	8.2	-	30.5	5.25	1.00	5.20	NR	-7.0	0	NR	-	7.2	NR	20.7	20.7	106	
597	[52]	Thiokol	1960	N2	AMB	CON	0.64	0.31	5.86	8.2	-	30.5	5.25	1.00	5.20	NR	-7.0	0	NR	-	8.7	NR	20.6	20.6	107	
598	[52]	Thiokol	1960	N2	AMB	CON	0.64	0.31	5.86	8.2	-	30.5	5.25	1.00	5.20	NR	-7.0	0	NR	-	9.0	NR	21.3	21.3	103	
599	[52]	Thiokol	1960	N2	AMB	CON	0.64	0.31	5.86	8.2	-	30.5	5.25	1.00	5.20	NR	-7.0	0	NR	-	9.0	NR	19.7	19.7	111	
600	[52]	Thiokol	1960	N2	AMB	CON	0.64	0.31	5.86	8.2	-	20.3	4.74	1.00	3.46	NR	0.0	0	NR	-	5.3	NR	21.9	21.9	80.1	
601	[52]	Thiokol	1960	N2	AMB	CON	0.64	0.31	5.86	8.2	-	20.3	4.74	1.00	3.46	NR	0.0	0	NR	-	7.1	NR	19.1	19.1	91.8	
602	[52]	Thiokol	1960	N2	AMB	CON	0.64	0.31	5.86	8.2	-	20.3	4.74	1.00	3.46	NR	0.0	0	NR	-	8.8	NR	19.6	19.6	89.2	
603	[52]	Thiokol	1960	N2	AMB	CON	0.64	0.31	5.86	8.2	-	20.3	4.74	1.00	3.46	NR	-7.0	0	NR	-	10.9	NR	18.5	18.5	94.5	
604	[52]	Thiokol	1960	N2	AMB	CON	0.64	0.31	5.86	8.2	-	20.3	4.74	1.00	3.46	NR	-7.0	0	NR	-	5.2	NR	17.2	17.2	125	
605	[52]	Thiokol	1960	N2	AMB	CON	0.64	0.31	5.86	8.2	-	20.3	4.74	1.00	3.46	NR	-7.0	0	NR	-	7.0	NR	16.7	16.7	129	
606	[52]	Thiokol	1960	N2	AMB	CON	0.64	0.31	5.86	8.2	-	20.3	4.74	1.00	3.46	NR	-7.0	0	NR	-	8.9	NR	16.1	16.1	134	
607	[52]	Thiokol	1960	N2	AMB	CON	0.64	0.31	5.86	8.2	-	20.3	4.74	1.00	3.46	NR	-7.0	0	NR	-	11.0	NR	15.9	15.9	135	
608	[52]	Thiokol	1960	N2	AMB	CON	0.64	0.31	5.86	8.2	-	20.3	4.74	1.00	3.46	NR	-11.0	0	NR	-	5.3	NR	21.2	21.2	85.1	
609	[52]	Thiokol	1960	N2	AMB	CON	0.64	0.31	5.86	8.2	-	20.3	4.74	1.00	3.46	NR	-11.0	0	NR	-	5.3	NR	19.7	19.7	91.5	
610	[52]	Thiokol	1960	N2	AMB	CON	0.64	0.31	5.86	8.2	-	12.3	4.16	1.00	2.10	NR	0.0	0	NR	-	6.9	NR	12.2	12.2	197	
611	[52]	Thiokol	1960	N2	AMB	CON	0.64	0.31	5.86	8.2	-	12.3	4.16	1.00	2.10	NR	0.0	0	NR	-	9.1	NR	11.1	11.1	217	
612	[52]	Thiokol	1960	N2	AMB	CON	0.64	0.31	5.86	8.2	-	12.3	4.16	1.00	2.10	NR	0.0	0	NR	-	11.4	NR	12.1	12.1	198	
613	[52]	Thiokol	1960	N2	AMB	CON	0.64	0.31	5.86	8.2	-	12.3	4.16	1.00	2.10	NR	0.0	0	NR	-	14.0	NR	11.8	11.8	203	
614	[52]	Thiokol	1960	N2	AMB	CON	0.64	0.31	5.86	8.2	-	12.3	4.16	1.00	2.10	NR	-7.0	0	NR	-	9.1	NR	11.3	11.3	182	
615	[52]	Thiokol	1960	N2	AMB	CON	0.64	0.31	5.86	8.2	-	12.3	4.16	1.00	2.10	NR	-7.0	0	NR	-	11.4	NR	11.6	11.6	177	
616	[52]	Thiokol	1960	N2	AMB	CON	0.64	0.31	5.86	8.2	-	12.3	4.16	1.00	2.10	NR	-7.0	0	NR	-	14.0	NR	11.4	11.4	180	
617	[9]	P&W	1960	N2	AMB	TOP	1.27	NR	40	9	S1	41.5	5.66	0.64	0.66	9.1	5.6	0.5	5,10	0.0	6.7	NR	22.6	22.6	NR	
618	[9]	P&W	1960	N2	AMB	TOP	1.27	NR	40	9	S2	41.5	5.66	0.64	0.66	9.1	5.6	0.5	5,10	0.3	6.7	NR	22.4	22.4	NR	
619	[9]	P&W	1960	N2	AMB	TOP	1.27	NR	40	9	S3	41.5	5.66	0.64	0.66	9.1	5.6	0.5	5,10	0.0	10.1	NR	22.0	20.4	NR	
620	[9]	P&W	1960	N2	AMB	TOP	1.27	NR	40	9</																

Table 5.3 (Continued) - Cold-Flow Cylindrical and Second-Throat Diffuser Data

No.	Ref.	Entity	Year	Nozzle Configuration					Diffuser Configuration									Performance							
				Gas	T <sub>0</sub>	Type	D <sub>NT</sub>	Ref. P <sub>0</sub>	A <sub>NE</sub> A <sub>NT</sub>	θ <sub>NE</sub>	Name	A <sub>DI</sub> A <sub>NT</sub>	M <sub>DI</sub>	A <sub>DT</sub> A <sub>DI</sub>	A <sub>DT</sub> A <sub>NE</sub>	A <sub>DE</sub> A <sub>DT</sub>	θ <sub>DI</sub>	θ <sub>DT</sub>	θ <sub>SUB</sub>	L <sub>DI</sub> D <sub>DI</sub>	L <sub>DT</sub> D <sub>DT</sub>	L <sub>D</sub> D <sub>DT</sub>	P <sub>0</sub> P <sub>BACK</sub>	(P <sub>CELL</sub> P <sub>0</sub> ) × 10 <sup>5</sup>	
656	[5]	EAFB	1960	N2	270	TOP	0.94	7.00	11.0	6.0	-	15.4	4.41	1.00	1.40	-	0.0	0	-	-	8.2+	NR	13.0	13.0	69.2
657	[5]	EAFB	1960	N2	270	TOP	0.94	7.00	11.0	6.0	-	22.1	4.85	1.00	2.00	-	0.0	0	-	-	8.2+	NR	20.0	20.0	30.0
658	[5]	EAFB	1960	N2	270	TOP	0.94	7.00	11.0	6.0	-	33.1	5.36	1.00	3.00	-	0.0	0	-	-	8.2+	NR	34.0	34.0	19.1
659	[5]	EAFB	1960	N2	270	TOP	0.94	7.00	11.0	6.0	-	66.2	6.31	1.00	6.00	-	0.0	0	-	-	8.2+	NR	55.5	55.5	16.2
660	[5]	EAFB	1960	N2	270	TOP	0.61	7.00	26.0	6.0	-	26.8	5.09	1.00	1.03	-	0.0	0	-	-	8.2+	NR	20.4	20.4	152
661	[5]	EAFB	1960	N2	270	TOP	0.61	7.00	26.0	6.0	-	28.6	5.17	1.00	1.10	-	0.0	0	-	-	8.2+	NR	22.8	22.8	105
662	[5]	EAFB	1960	N2	270	TOP	0.61	7.00	26.0	6.0	-	31.2	5.28	1.00	1.20	-	0.0	0	-	-	8.2+	NR	25.6	25.6	64.5
663	[5]	EAFB	1960	N2	270	TOP	0.61	7.00	26.0	6.0	-	36.4	5.48	1.00	1.40	-	0.0	0	-	-	8.2+	NR	30.0	30.0	40.0
664	[5]	EAFB	1960	N2	270	TOP	0.61	7.00	26.0	6.0	-	41.6	5.66	1.00	1.60	-	0.0	0	-	-	8.2+	NR	35.6	35.6	28.1
665	[5]	EAFB	1960	N2	270	TOP	0.61	7.00	26.0	6.0	-	52.0	5.97	1.00	2.00	-	0.0	0	-	-	8.2+	NR	41.6	41.6	19.2
666	[5]	EAFB	1960	N2	270	TOP	0.61	7.00	26.0	6.0	-	72.8	6.45	1.00	2.80	-	0.0	0	-	-	8.2+	NR	56.4	56.4	13.3
667	[7]	NASA LeRC	1960	Air	294	CON	6.73	0.48	5.5	19.5	-	9.30	3.84	1.00	1.69	-	0	-	-	-	19.0	19.0	8.1	8.1	NR
668	[7]	NASA LeRC	1960	Air	294	CON	6.73	0.48	5.5	19.5	-	14.4	4.34	1.00	2.61	-	0	0	-	-	15.0	15.0	12.8	12.8	NR
669	[7]	NASA LeRC	1960	Air	294	CON	6.73	0.48	5.5	19.5	-	20.5	4.76	1.00	3.73	-	0	0	-	-	12.5	12.5	17.7	17.7	NR
670	[7]	NASA LeRC	1960	Air	294	CON	4.45	0.48	11.7	15	-	21.2	4.80	1.00	1.81	-	0	0	-	-	4.0	4.0	19.4	16.9	NR
671	[7]	NASA LeRC	1960	Air	294	CON	4.45	0.48	11.7	15	-	21.2	4.80	1.00	1.81	-	0	0	-	-	7.4	7.4	17.1	17.1	NR
672	[7]	NASA LeRC	1960	Air	294	CON	4.45	0.48	11.7	15	-	21.2	4.80	1.00	1.81	-	0	0	-	-	19.0	19.0	18.0	18.0	NR
673	[7]	NASA LeRC	1960	Air	294	CON	4.45	0.48	11.7	15	-	33.8	5.39	1.00	2.89	-	0	0	-	-	15.0	15.0	27.6	27.6	NR
674	[7]	NASA LeRC	1960	Air	294	CON	4.45	0.48	11.7	15	-	47.8	5.85	1.00	4.09	-	0	0	-	-	12.5	12.5	37.9	37.9	NR
675	[7]	NASA LeRC	1960	Air	294	CON	3.81	0.48	25	15	-	28.9	5.18	1.00	1.16	-	0	0	-	-	2.0	2.0	47.5	35.5	NR
676	[7]	NASA LeRC	1960	Air	294	CON	3.81	0.48	25	15	-	28.9	5.18	1.00	1.16	-	0	0	-	-	3.0	3.0	35.0	30.7	NR
677	[7]	NASA LeRC	1960	Air	294	CON	3.81	0.48	25	15	-	28.9	5.18	1.00	1.16	-	0	0	-	-	4.0	4.0	27.2	26.1	NR
678	[7]	NASA LeRC	1960	Air	294	CON	3.81	0.48	25	15	-	28.9	5.18	1.00	1.16	-	0	0	-	-	6.0	6.0	23.0	23.0	NR
679	[7]	NASA LeRC	1960	Air	294	CON	3.81	0.48	25	15	-	28.9	5.18	1.00	1.16	2.0	0	0	-	-	6.0	NR	21.9	21.9	NR
680	[7]	NASA LeRC	1960	Air	294	CON	3.81	0.48	25	15	-	28.9	5.18	1.00	1.16	-	0	0	-	-	12.0	12.0	23.3	23.3	210
681	[7]	NASA LeRC	1960	Air	294	CON	3.81	0.48	25	15	-	28.9	5.18	1.00	1.16	-	0	0	-	-	18.0	18.0	23.6	23.6	NR
682	[7]	NASA LeRC	1960	Air	294	CON	3.81	0.48	25	15	-	32.8	5.35	1.00	1.31	-	0	0	-	-	6.0	6.0	27.3	27.3	NR
683	[7]	NASA LeRC	1960	Air	294	CON	3.81	0.48	25	15	-	32.8	5.35	1.00	1.31	2.0	0	0	-	-	6.0	NR	25.4	25.4	NR
684	[7]	NASA LeRC	1960	Air	294	CON	3.81	0.48	25	15	-	46.1	5.80	1.00	1.84	-	0	0	-	-	14.0	14.0	36.4	36.4	NR
685	[7]	NASA LeRC	1960	Air	294	CON	3.81	0.48	25	15	-	50.8	5.94	1.00	2.03	2.0	0	0	-	-	6.0	6.0	39.6	39.6	NR
686	[7]	NASA LeRC	1960	Air	294	CON	3.81	0.48	25	15	-	50.8	5.94	1.00	2.03	2.0	0	0	-	-	6.0	NR	37.4	37.4	NR
687	[7]	NASA LeRC	1960	Air	294	CON	3.81	0.48	25	15	-	64.1	6.27	1.00	2.56	-	0	0	-	-	10.0	10.0	48.8	48.8	NR
688	[7]	NASA LeRC	1960	Air	294	CON	4.17	0.48	50	15	-	50.8	5.94	1.00	1.02	-	0	0	-	-	6.0	6.0	38.8	38.8	NR
689	[7]	NASA LeRC	1960	Air	294	CON	4.17	0.48	50	15	-	50.8	5.94	1.00	1.02	2.0	0	0	-	-	6.0	NR	35.8	35.8	NR
690	[7]	NASA LeRC	1960	Air	294	CON	4.17	0.48	50	15	-	53.5	6.01	1.00	1.07	-	0	0	-	-	4.0	4.0	46.5	42.0	NR
691	[7]	NASA LeRC	1960	Air	294	CON	4.17	0.48	50	15	-	53.5	6.01	1.00	1.07	-	0	0	-	-	6.0	6.0	40.3	40.3	NR
692	[7]	NASA LeRC	1960	Air	294	CON	4.17	0.48	50	15	-	53.5	6.01	1.00	1.07	-	0	0	-	-	8.0	8.0	39.9	39.9	NR
693	[7]	NASA LeRC	1960	Air	294	TIC	3.81	0.48	25	9.5	-	28.9	5.18	1.00	1.16	-	0	0	-	-	2.0	2.0	45.0	42.5	NR
694	[7]	NASA LeRC	1960	Air	294	TIC	3.81	0.48	25	9.5	-	28.9	5.18	1.00	1.16	-	0	0	-	-	4.0	4.0	31.0	30.3	NR
695	[7]	NASA LeRC	1960	Air	294	TIC	3.81	0.48	25	9.5	-	28.9	5.18	1.00	1.16	-	0	0	-	-	6.0	6.0	22.8	22.8	NR
696	[7]	NASA LeRC	1960	Air	294	TIC	3.81	0.48	25	9.5	-	28.9	5.18	1.00	1.16	-	0	0	-	-	10.0	10.0	22.5	22.5	NR
697	[7]	NASA LeRC	1960	Air	294	TIC	3.81	0.48	25	9.8	-	28.9	5.18	1.00	1.16	-	0	0	-	-	6.5	6.5	22.9	22.9	NR
698	[7]	NASA LeRC	1960	Air	294	TOP	3.81	0.48	25	9.8	-	50.9	5.94	1.00	2.04	-	0	0	-	-	6.5	6.5	41.8	41.8	NR
699	[7]	NASA LeRC	1960	Air	294	TOC	3.92	0.48	27	0.0	-	43.5	5.72	1.00	1.59	-	0	0	-	-	10.0	10.0	37.0	37.0	NR
700	[7]	NASA LeRC	1960	Air	700	TOC	8.85	0.48	63	0.0	-	69.3	6.38	1.00	1.10	-	0	0	-	-	8.0	8.0	55.0	55.0	NR
701	[7]	NASA LeRC	1960	Air	700	TOC	8.85	0.48	63	0.0	-	101	6.95	1.00	1.60	-	0	0	-	-	10.0	10.0	71.1	71.1	NR
702	[7]	NASA LeRC	1960	Air	294	CON	3.81	0.48	25	15	-	28.9	5.18	0.55	0.64	1.6	3.8	0	3.8	0.5	1.1	5.1	23.0	23.0	NR
703	[7]	NASA LeRC	1960	Air	294	CON	3.81	0.48	25	15	-	28.9	5.18	0.55	0.64	1.6	3.8	0	3.8	0.5	2.1	5.9	22.4	22.4	NR
704	[7]	NASA LeRC	1960	Air	294	CON	3.81	0.48	25	15	-	28.9	5.18	0.55	0.64	1.6	3.8	0	3.8	0.5	3.1	6.6	19.1	19.1	NR
705	[7]	NASA LeRC	1960	Air	294	CON	3.81	0.48	25	15	-	28.9	5.18	0.55	0.64	1.6	3.8	0	3.8	0.5	4.1	7.5	16.0	16.0	NR
706	[7]	NASA LeRC	1960	Air	294	CON	3.81	0.48	25	15	-	28.9	5.18	0.55	0.64	1.6	3.8	0	3.8	0.5	4.1	7.5	16.0	16.0</td	

Table 5.3 (Continued) - Cold-Flow Cylindrical and Second-Throat Diffuser Data

No.	Ref.	Entity	Year	Nozzle Configuration					Diffuser Configuration									Performance							
				Gas	T <sub>0</sub>	Type	D <sub>NT</sub>	Ref. P <sub>0</sub>	A <sub>NE</sub> /A <sub>NT</sub>	θ <sub>NE</sub>	Name	A <sub>DI</sub> /A <sub>NT</sub>	M <sub>DI</sub>	A <sub>DT</sub> /A <sub>DI</sub>	A <sub>DT</sub> /A <sub>NE</sub>	A <sub>DE</sub> /A <sub>DT</sub>	θ <sub>DI</sub>	θ <sub>DT</sub>	θ <sub>SUB</sub>	L <sub>DI</sub> /D <sub>DI</sub>	L <sub>DT</sub> /D <sub>DT</sub>	L <sub>D</sub> /D <sub>DT</sub>	P <sub>0</sub> /P <sub>BACK</sub>	(P <sub>CELL</sub> /P <sub>0</sub> ) × 10 <sup>5</sup>	
739	[53]	NASA LeRC	1960	N2	NR	CON	0.66	4.86	25	15	-	51.0	5.94	1.00	2.04	2.0	-	0	8.0	-	5.5	NR	42.4	42.4	NR
740	[53]	NASA LeRC	1960	N2	NR	CON	0.66	4.86	25	15	-	51.0	5.94	1.00	2.04	2.0	-	0	8.0	-	7.4	NR	38.1	38.1	NR
741	[53]	NASA LeRC	1960	N2	NR	CON	0.66	4.86	25	15	-	51.0	5.94	1.00	2.04	2.0	-	0	8.0	-	9.7	NR	36.5	36.5	NR
742	[53]	NASA LeRC	1960	N2	NR	CON	0.66	4.86	25	15	-	51.0	5.94	1.00	2.04	2.0	-	0	8.0	-	10.5	NR	37.5	37.5	NR
743	[53]	NASA LeRC	1960	N2	NR	CON	0.66	4.86	50	15	-	51.0	5.94	1.00	1.02	-	-	0	-	-	-	NR	38.0	38.0	NR
744	[53]	NASA LeRC	1960	N2	NR	CON	0.66	4.86	50	15	-	51.0	5.94	1.00	1.02	2.0	-	0	8.0	-	-	NR	35.5	35.5	NR
745	[53]	NASA LeRC	1960	N2	NR	80% TOP	0.66	4.86	25	4.0	-	28.0	5.11	1.00	1.12	-	-	0	-	-	4.0	NR	28.0	28.0	NR
746	[53]	NASA LeRC	1960	N2	NR	80% TOP	0.66	4.86	25	4.0	-	28.0	5.11	1.00	1.12	-	-	0	-	-	6.0	NR	24.5	24.5	NR
747	[53]	NASA LeRC	1960	N2	NR	80% TOP	0.66	4.86	25	4.0	-	28.0	5.11	1.00	1.12	-	-	0	-	-	9.3	NR	23.5	23.5	NR
748	[53]	NASA LeRC	1960	N2	NR	80% TOP	0.66	4.86	25	4.0	-	33.0	5.35	1.00	1.52	-	-	0	-	-	4.0	NR	32.5	32.5	NR
749	[53]	NASA LeRC	1960	N2	NR	80% TOP	0.66	4.86	25	4.0	-	33.0	5.35	1.00	1.32	-	-	0	-	-	6.0	NR	28.3	28.3	NR
750	[53]	NASA LeRC	1960	N2	NR	80% TOP	0.66	4.86	25	4.0	-	33.0	5.35	1.00	1.32	-	-	0	-	-	9.3	NR	27.8	27.8	NR
751	[53]	NASA LeRC	1960	N2	NR	80% TOP	0.66	4.86	25	4.0	-	33.0	5.35	1.00	1.32	-	-	0	-	-	16.0	NR	29.0	29.0	NR
752	[53]	NASA LeRC	1960	N2	NR	80% TOP	0.66	4.86	25	4.0	-	51.0	5.94	1.00	2.04	-	-	0	-	-	4.0	NR	47.1	47.1	NR
753	[53]	NASA LeRC	1960	N2	NR	80% TOP	0.66	4.86	25	4.0	-	51.0	5.94	1.00	2.04	-	-	0	-	-	6.0	NR	43.1	43.1	NR
754	[53]	NASA LeRC	1960	N2	NR	80% TOP	0.66	4.86	25	4.0	-	51.0	5.94	1.00	2.04	-	-	0	-	-	9.0	NR	42.7	42.7	NR
755	[53]	NASA LeRC	1960	N2	NR	CON	0.66	4.86	25	15	-	30.0	5.23	0.47	0.56	2.0	3.0	0	8.0	0.2	0.0	NR	24.3	24.3	NR
756	[53]	NASA LeRC	1960	N2	NR	CON	0.66	4.86	25	15	-	30.0	5.23	0.47	0.56	2.0	3.0	0	8.0	0.2	1.5	NR	18.5	18.5	NR
757	[53]	NASA LeRC	1960	N2	NR	CON	0.66	4.86	25	15	-	30.0	5.23	0.47	0.56	2.0	3.0	0	8.0	0.2	3.1	NR	15.9	15.9	NR
758	[53]	NASA LeRC	1960	N2	NR	CON	0.66	4.86	25	15	-	30.0	5.23	0.47	0.56	2.0	3.0	0	8.0	0.2	6.1	NR	15.6	12.2	NR
759	[53]	NASA LeRC	1960	N2	NR	CON	0.66	4.86	25	15	-	30.0	5.23	0.47	0.56	2.0	3.0	0	8.0	0.2	10.2	NR	19.5	11.3	NR
760	[53]	NASA LeRC	1960	N2	NR	CON	0.66	4.86	25	15	-	30.0	5.23	0.47	0.56	2.0	3.0	0	8.0	0.2	8.0	NR	16.0	12.3	120
761	[53]	NASA LeRC	1960	N2	NR	CON	0.66	4.86	25	15	-	30.0	5.23	0.47	0.56	2.0	3.0	0	8.0	0.2	2.8	NR	41.9	36.6	NR
762	[53]	NASA LeRC	1960	N2	NR	CON	0.66	4.86	25	15	-	30.0	5.23	0.47	0.56	2.0	6.0	0	8.0	0.2	NR	6.9	13.6	12.6	NR
763	[53]	NASA LeRC	1960	N2	NR	CON	0.66	4.86	25	15	-	30.0	5.23	0.47	0.56	2.0	6.0	0	8.0	0.2	NR	9.7	13.5	12.1	NR
764	[53]	NASA LeRC	1960	N2	NR	CON	0.66	4.86	25	15	-	30.0	5.23	0.47	0.56	2.0	15.0	0	8.0	0.2	NR	1.7	28.0	27.6	NR
765	[53]	NASA LeRC	1960	N2	NR	CON	0.66	4.86	25	15	-	30.0	5.23	0.47	0.56	2.0	15.0	0	8.0	0.2	NR	4.6	19.6	18.0	NR
766	[53]	NASA LeRC	1960	N2	NR	CON	0.66	4.86	25	15	-	30.0	5.23	0.47	0.56	2.0	15.0	0	8.0	0.2	NR	6.0	15.0	15.0	NR
767	[53]	NASA LeRC	1960	N2	NR	CON	0.66	4.86	25	15	-	30.0	5.23	0.47	0.56	2.0	15.0	0	8.0	0.2	NR	8.7	15.2	14.2	NR
768	[53]	NASA LeRC	1960	N2	NR	CON	0.66	4.86	25	15	-	30.0	5.23	0.54	0.65	2.0	3.0	0	8.0	0.2	0.0	NR	28.0	28.0	NR
769	[53]	NASA LeRC	1960	N2	NR	CON	0.66	4.86	25	15	-	30.0	5.23	0.54	0.65	2.0	3.0	0	8.0	0.2	1.5	NR	20.7	20.7	NR
770	[53]	NASA LeRC	1960	N2	NR	CON	0.66	4.86	25	15	-	30.0	5.23	0.54	0.65	2.0	3.0	0	8.0	0.2	2.9	NR	18.2	18.2	NR
771	[53]	NASA LeRC	1960	N2	NR	CON	0.66	4.86	25	15	-	30.0	5.23	0.54	0.65	2.0	3.0	0	8.0	0.2	5.8	NR	14.0	12.8	NR
772	[53]	NASA LeRC	1960	N2	NR	CON	0.66	4.86	25	15	-	30.0	5.23	0.54	0.65	2.0	3.0	0	8.0	0.2	9.7	NR	15.0	12.9	NR
773	[53]	NASA LeRC	1960	N2	NR	CON	0.66	4.86	25	15	-	30.0	5.23	0.54	0.65	2.0	6.0	0	8.0	0.2	NR	4.6	17.5	16.4	NR
774	[53]	NASA LeRC	1960	N2	NR	CON	0.66	4.86	25	15	-	30.0	5.23	0.54	0.65	2.0	6.0	0	8.0	0.2	NR	6.7	13.4	12.6	NR
775	[53]	NASA LeRC	1960	N2	NR	CON	0.66	4.86	25	15	-	30.0	5.23	0.54	0.65	2.0	6.0	0	8.0	0.2	NR	9.5	14.2	13.5	NR
776	[53]	NASA LeRC	1960	N2	NR	CON	0.66	4.86	25	15	-	30.0	5.23	0.54	0.65	2.0	15.0	0	8.0	0.2	NR	1.8	36.6	32.0	NR
777	[53]	NASA LeRC	1960	N2	NR	CON	0.66	4.86	25	15	-	30.0	5.23	0.54	0.65	2.0	15.0	0	8.0	0.2	NR	3.8	19.7	19.7	NR
778	[53]	NASA LeRC	1960	N2	NR	CON	0.66	4.86	25	15	-	30.0	5.23	0.54	0.65	2.0	15.0	0	8.0	0.2	NR	6.0	14.5	14.5	NR
779	[53]	NASA LeRC	1960	N2	NR	CON	0.66	4.86	25	15	-	30.0	5.23	0.54	0.65	2.0	15.0	0	8.0	0.2	NR	8.7	16.9	15.8	NR
780	[53]	NASA LeRC	1960	N2	NR	CON	0.66	4.86	25	15	-	30.0	5.23	0.60	0.72	2.0	3.0	0	8.0	0.2	0.0	NR	29.6	29.6	NR
781	[53]	NASA LeRC	1960	N2	NR	CON	0.66	4.86	25	15	-	30.0	5.23	0.60	0.72	2.0	3.0	0	8.0	0.2	1.4	NR	21.8	21.8	NR
782	[53]	NASA LeRC	1960	N2	NR	CON	0.66	4.86	25	15	-	30.0	5.23	0.60	0.72	2.0	3.0	0	8.0	0.2	2.7	NR	18.4	18.4	NR
783	[53]	NASA LeRC	1960	N2	NR	CON	0.66	4.86	25	15	-	30.0	5.23	0.60	0.72	2.0	3.0	0	8.0	0.2	5.5	NR	13.6	13.6	NR
784	[53]	NASA LeRC	1960	N2	NR	CON	0.66	4.86	25	15	-	30.0	5.23	0.60	0.72	2.0	3.0	0	8.0	0.2	9.1	NR	15.1	14.1	NR
785	[53]	NASA LeRC	1960	N2	NR	CON	0.66	4.86	25	15	-	30.0	5.23	0.60	0.72	2.0	15.0	0	8.0	0.2	NR	1.8	39.0	26.5	NR
786	[53]	NASA LeRC	1960	N2	NR	CON	0.66	4.86	25	15	-	30.0	5.23	0.60	0.72	2.0	15.0	0	8.0	0.2	NR	3.8	20.6	18.0	NR
787	[53]	NASA LeRC	1960	N2	NR	CON	0.66	4.86	25	15	-	30.0	5.23	0.60	0.72	2.0	15.0	0	8.0	0.2	NR	6.0	16.4	15.6	NR
788	[53]	NASA LeRC	1960	N2	NR	80% TOP	0.66	4.86	25	4.0	-	30.0	5.23	0.60	0.72	2.0	15.0	0	8.0	0.2	NR	8.7	16.6	16.0	NR
789	[53]	NASA LeRC	1960	N2	NR	80% TOP	0.66	4.86	25	4.0	-	30.0													

Table 5.3 (Continued) - Cold-Flow Cylindrical and Second-Throat Diffuser Data

No.	Ref.	Entity	Year	Nozzle Configuration					Diffuser Configuration										Performance						
				Gas	T <sub>0</sub>	Type	D <sub>NT</sub>	Ref. P <sub>0</sub>	A <sub>NE</sub> /A <sub>NT</sub>	θ <sub>NE</sub>	Name	A <sub>DI</sub> /A <sub>NT</sub>	M <sub>DI</sub>	A <sub>DT</sub> /A <sub>DI</sub>	A <sub>DT</sub> /A <sub>NE</sub>	A <sub>DE</sub> /A <sub>DT</sub>	θ <sub>DI</sub>	θ <sub>DT</sub>	θ <sub>SUB</sub>	L <sub>DI</sub> /D <sub>DI</sub>	L <sub>DT</sub> /D <sub>DT</sub>	L <sub>D</sub> /D <sub>DT</sub>	P <sub>0</sub> /P <sub>BACK</sub>	(P <sub>CELL</sub> /P <sub>0</sub> ) × 10 <sup>5</sup>	
[K] [cm] [MPa] [deg]																				Start	Unst.				
822	[54]	AEDC	1963	Air	300	CON	2.11	0.31	25	18	5a	52.5	5.98	0.44	0.92	2.3	12.0	0	0.0	1.0	0.6	9.1	88.5	85.5	29.1
823	[54]	AEDC	1963	Air	300	CON	2.11	0.31	25	18	5d	52.5	5.98	0.44	0.92	2.3	12.0	0	0.0	0.7	8.1	9.1	69.4	69.4	47.4
824	[54]	AEDC	1963	Air	300	CON	2.11	0.31	25	18	5d	52.5	5.98	0.44	0.92	2.3	12.0	0	0.0	0.8	8.1	9.1	73.5	73.5	29.3
825	[54]	AEDC	1963	Air	300	CON	2.11	0.31	25	18	5d	52.5	5.98	0.44	0.92	2.3	12.0	0	0.0	0.9	8.1	9.1	71.4	71.4	29.3
826	[54]	AEDC	1963	Air	300	CON	2.11	0.31	25	18	5d	52.5	5.98	0.44	0.92	2.3	12.0	0	0.0	1.0	8.1	9.1	70.4	70.4	29.3
827	[54]	AEDC	1963	Air	300	CON	2.11	0.31	25	18	5d	52.5	5.98	0.44	0.92	2.3	12.0	0	0.0	1.2	8.1	9.1	69.9	69.9	29.3
828	[54]	AEDC	1963	Air	300	CON	2.11	0.31	25	18	5d	52.5	5.98	0.44	0.92	2.3	12.0	0	0.0	1.3	8.1	9.1	68.0	68.0	30.1
829	[54]	AEDC	1963	Air	300	CON	2.11	0.31	25	18	5d	52.5	5.98	0.44	0.92	2.3	12.0	0	0.0	1.4	8.1	9.1	68.0	68.0	29.3
830	[54]	AEDC	1963	Air	300	CON	2.49	0.31	18.6	18	5d	37.7	5.53	0.44	0.89	2.3	12.0	0	0.0	0.7	8.1	9.1	54.9	54.6	51.7
831	[54]	AEDC	1963	Air	300	CON	2.49	0.31	18.6	18	5d	37.7	5.53	0.44	0.89	2.3	12.0	0	0.0	0.8	8.1	9.1	54.3	54.1	37.8
832	[54]	AEDC	1963	Air	300	CON	2.49	0.31	18.6	18	5d	37.7	5.53	0.44	0.89	2.3	12.0	0	0.0	0.9	8.1	9.1	52.6	52.6	37.8
833	[54]	AEDC	1963	Air	300	CON	2.49	0.31	18.6	18	5d	37.7	5.53	0.44	0.89	2.3	12.0	0	0.0	1.0	8.1	9.1	52.6	52.6	37.8
834	[54]	AEDC	1963	Air	300	CON	2.49	0.31	18.6	18	5d	37.7	5.53	0.44	0.89	2.3	12.0	0	0.0	1.2	8.1	9.1	51.8	51.8	40.8
835	[55]	AEDC	1963	Air	287	CON	1.20	2.13	18	18	1	73.1	6.46	1.00	4.06	-	-	0	-	-	5.7	5.7	59.4	59.4	47.4
836	[55]	AEDC	1963	Ar	251	CON	1.20	1.57	18	18	1	73.1	10.4	1.00	4.06	-	-	0	-	-	5.7	5.7	70.1	70.1	72.0
837	[55]	AEDC	1963	N2	256	CON	1.20	1.69	18	18	1	73.1	6.46	1.00	4.06	-	-	0	-	-	5.7	5.7	57.2	57.2	45.0
838	[55]	AEDC	1963	Air	261	CON	0.77	1.94	10.8	7.6	2	20.4	4.75	1.00	1.90	-	-	0	-	-	8.0	8.0	16.4	16.4	10.8
839	[55]	AEDC	1963	Ar	258	CON	0.77	1.45	10.8	7.6	2	20.4	6.61	1.00	1.90	-	-	0	-	-	8.0	8.0	15.5	15.5	15.9
840	[55]	AEDC	1963	He	281	CON	0.77	1.72	10.8	7.6	2	20.4	6.61	1.00	1.90	-	-	0	-	-	8.0	8.0	17.5	17.5	60.7
841	[55]	AEDC	1963	H2	278	CON	0.77	1.48	10.8	7.6	2	20.4	4.75	1.00	1.90	-	-	0	-	-	8.0	8.0	15.0	15.0	68.4
842	[55]	AEDC	1963	N2	271	CON	0.77	1.45	10.8	7.6	2	20.4	4.75	1.00	1.90	-	-	0	-	-	8.0	8.0	14.8	14.8	12.6
843	[56]	AEDC	1963	Air	284	CON	1.20	2.15	18	18	1	73.1	6.46	1.00	4.06	-	-	0	-	-	5.4	5.4	59.5	59.5	48.0
844	[56]	AEDC	1963	Air	289	CON	1.20	2.12	18	18	2	98.7	6.92	1.00	5.49	-	-	0	-	-	4.0	4.0	87.7	87.7	33.0
845	[56]	AEDC	1963	Air	288	CON	1.20	2.48	18	18	4	295	8.80	1.00	16.4	-	-	0	-	-	3.6	3.6	285.7	285.7	9.6
846	[56]	AEDC	1963	Air	286	CON	1.20	2.40	18	18	5	453	9.65	1.00	25.1	-	-	0	-	-	4.4	4.4	454.5	454.5	8.2
847	[56]	AEDC	1963	Air	289	CON	1.20	2.40	5.0	18	1	73.1	6.46	1.00	1.29	-	-	0	-	-	5.7	5.7	64.5	64.5	71.5
848	[56]	AEDC	1963	Air	292	CON	1.20	2.39	5.0	18	3	170	7.81	1.00	34.0	-	-	0	-	-	3.8	3.8	153.8	153.8	32.0
849	[56]	AEDC	1963	Air	293	CON	1.20	2.36	5.0	18	4	295	8.80	1.00	59.0	-	-	0	-	-	3.8	3.8	285.7	285.7	17.8
850	[56]	AEDC	1963	Air	283	CON	2.01	2.13	3.9	10	2	35.1	5.44	1.00	8.97	-	-	0	-	-	5.3	5.3	30.7	30.7	154
851	[56]	AEDC	1963	Air	288	CON	2.01	2.08	3.9	10	3	60.4	6.18	1.00	15.4	-	-	0	-	-	3.8	3.8	52.6	52.6	83.0
852	[56]	AEDC	1963	Air	283	CON	2.01	2.10	3.1	10	2	35.1	5.44	1.00	11.2	-	-	0	-	-	5.5	5.5	31.4	31.4	188
853	[56]	AEDC	1963	Air	285	CON	2.01	2.13	3.1	10	3	60.4	6.18	1.00	19.2	-	-	0	-	-	3.9	3.9	56.2	56.2	102
854	[56]	AEDC	1963	Air	282	CON	1.90	2.09	10.5	9.0	3	67.6	6.34	1.00	6.13	-	-	0	-	-	3.8	3.8	93.5	58.8	52.9
855	[56]	AEDC	1963	Air	281	CON	2.01	1.97	3.9	10	S3c	60.4	6.18	0.65	10.0	-	15.0	0	-	0.8	4.5	5.1	62.9	62.9	87.0
856	[56]	AEDC	1963	Air	281	CON	2.01	1.97	3.9	10	S5c	60.4	6.18	0.65	10.0	-	15.0	0	-	0.8	4.5	5.1	51.0	51.0	NR
857	[56]	AEDC	1963	Air	284	CON	1.90	2.12	10.5	9.0	S3b	67.6	6.34	0.57	3.65	-	15.0	0	-	0.8	4.6	5.1	43.7	43.7	42.6
858	[56]	AEDC	1963	Air	282	CON	1.90	2.12	10.5	9.0	S3b	67.6	6.34	0.57	3.65	-	15.0	0	-	0.8	4.6	5.4	159	159	44.6
859	[56]	AEDC	1963	Air	281	CON	1.90	2.12	10.5	9.0	S5b	67.6	6.34	0.57	3.65	-	15.0	0	-	1.0	4.6	5.5	42.0	42.0	27.5
860	[56]	AEDC	1963	Air	278	CON	1.90	2.07	10.5	9.0	S3c	67.6	6.34	0.65	4.17	-	15.0	0	-	0.8	4.5	5.1	185	185	27.5
861	[56]	AEDC	1963	Air	278	CON	1.90	2.05	10.5	9.0	S5c	67.6	6.34	0.65	4.17	-	15.0	0	-	0.8	4.5	5.1	37.6	37.6	27.5
862	[56]	AEDC	1963	Air	278	CON	1.90	2.05	10.5	9.0	S3c	67.6	6.34	0.65	4.17	-	15.0	0	-	0.0	4.5	4.9	45.0	45.0	27.5
863	[12]	AEDC	1965	Air	300	TOP	2.29	0.31	23.7	0.0	5d	128	7.53	0.44	2.37	2.3	12.0	0	0.0	0.8	8.1	9.1	59.9	59.9	15.5
864	[12]	AEDC	1965	Air	300	TOP	2.29	0.31	23.7	0.0	5d	128	7.53	0.44	2.37	2.3	12.0	0	0.0	0.9	8.1	9.1	59.9	59.9	15.1
865	[12]	AEDC	1965	Air	300	TOP	2.29	0.31	23.7	0.0	5d	128	7.53	0.44	2.37	2.3	12.0	0	0.0	0.9	8.1	9.1	61.7	59.9	15.1
866	[12]	AEDC	1965	Air	300	CON	3.20	0.31	10.8	18	6	22.7	4.88	0.58	1.21	1.7	6.0	0	0.0	0.6	0.2	9.1	38.0	33.6	204
867	[12]	AEDC	1965	Air	300	CON	3.20	0.31	10.8	18	6	22.7	4.88	0.58	1.21	1.7	6.0	0	0.0	0.7	0.2	9.1	36.4	36.4	188
868	[12]	AEDC	1965	Air	300	CON	2.11	0.32	25	18	6	52.3	5.98	0.58	1.21	1.7	6.0	0	0.0	0.6	0.2	9.1	84.0	94.2	88.8
869	[12]	AEDC	1965	Air	300	CON	2.11	0.31	25	18	6	52.3	5.98	0.58	1.21	1.7	6.0	0	0.0	0.8	0.2	9.1	93.5	97.6	89.1
870	[12]	AEDC	1965	Air																					

Table 5.3 (Continued) - Cold-Flow Cylindrical and Second-Throat Diffuser Data

No.	Ref.	Entity	Year	Nozzle Configuration				Diffuser Configuration										Performance							
				Gas	T <sub>0</sub>	Type	D <sub>NT</sub>	Ref. P <sub>0</sub>	A <sub>NE</sub> /A <sub>NT</sub>	θ <sub>NE</sub>	Name	A <sub>DI</sub> /A <sub>NT</sub>	M <sub>DI</sub>	A <sub>DT</sub> /A <sub>DI</sub>	A <sub>DE</sub> /A <sub>NE</sub>	A <sub>EE</sub> /A <sub>DT</sub>	θ <sub>DI</sub>	θ <sub>DT</sub>	θ <sub>SUB</sub>	L <sub>DI</sub> /D <sub>DI</sub>	L <sub>DT</sub> /D <sub>DT</sub>	L <sub>D</sub> /D <sub>DT</sub>	P <sub>o</sub> /P <sub>BACK</sub>	(P <sub>CELL</sub> /P <sub>o</sub> ) × 10 <sup>5</sup>	
905	[58]	ISRO	1998	N2	300	CON	0.91	4.50	20	20.5	-	33.0	5.35	1.00	1.65	-	-	0	-	-	7.1	7.1	28.5	28.5	87.7
906	[37]	ISRO	1998	N2	300	CON	1.74	4.00	9.0	20.5	1	11.1	4.04	1.00	1.23	-	-	0	-	-	8.0	8.0	9.5	9.5	NR
907	[37]	ISRO	1998	N2	300	CON	1.20	4.00	19	20.5	2	31.3	5.29	1.00	1.65	-	-	0	-	-	8.0	8.0	26.8	26.8	NR
908	[37]	ISRO	1998	N2	300	CON	1.14	4.00	21	20.5	3	34.6	5.42	1.00	1.65	-	-	0	-	-	8.0	8.0	29.2	29.2	NR
909	[37]	ISRO	1998	N2	300	CON	1.17	4.00	20	20.5	4	79.2	6.58	1.00	3.96	-	-	0	-	-	9.0	9.0	65.0	65.0	NR
910	[37]	ISRO	1998	N2	300	CON	1.14	4.00	20.8	20.5	5	82.8	6.65	1.00	3.98	-	-	0	-	-	9.0	9.0	68.5	68.5	NR
911	[37]	ISRO	1998	N2	300	CON	1.20	4.00	18.9	20.5	6	124	7.28	1.00	6.56	-	-	0	-	-	8.7	8.7	102	102	NR
912	[37]	ISRO	1998	N2	300	CON	1.17	4.00	20	20.5	7	131	7.37	1.00	6.53	-	-	0	-	-	8.7	8.7	108.5	108.5	NR
913	[37]	ISRO	1998	N2	300	CON	1.14	4.00	20.8	20.5	8	137	7.44	1.00	6.56	-	-	0	-	-	8.7	8.7	109.5	109.5	NR
914	[37]	ISRO	1998	N2	300	CON	1.20	4.00	18.9	20.5	9	211	8.21	1.00	11.3	-	-	0	-	-	8.9	8.9	185.0	185.0	NR
915	[37]	ISRO	1998	N2	300	CON	1.17	4.00	19.9	20.5	10	225	8.30	1.00	11.3	-	-	0	-	-	8.9	8.9	202.5	202.5	NR
916	[37]	ISRO	1998	N2	300	CON	1.14	4.00	20.8	20.5	11	235	8.38	1.00	11.3	-	-	0	-	-	8.9	8.9	215.0	215.0	NR
917	[59]	KAU	2007	N2	288	NR	NR	5.07	5.7	NR	-	28.4	5.16	1.00	5.00	NR	-	0	NR	-	5.0	6.6	22.5	22.5	289
918	[60]	KAU	2008	N2	AMB	CON	0.28	NR	35.0	15	-	56.3	6.08	1.00	1.61	-	-	0	NR	-	NR	12.4	39.9	NR	NR
919	[60]	KAU	2008	N2	AMB	CON	0.32	NR	26.8	15	-	43.1	5.71	1.00	1.61	-	-	0	NR	-	NR	12.4	31.7	NR	NR
920	[60]	KAU	2008	N2	AMB	CON	0.43	NR	14.6	15	-	23.4	4.92	1.00	1.61	-	-	0	NR	-	NR	12.4	19.0	NR	NR
921	[61]	YSU	2008	N2	AMB	CON	NR	3.55	25	15	A-1	30.0	5.23	0.63	1.20	NR	6.0	0	-	1.0	8.0	NR	18.1	NR	NR
922	[61]	YSU	2008	N2	AMB	CON	NR	3.55	25	15	A-2	30.0	5.23	0.63	1.20	NR	6.0	0	6.0	1.0	8.0	NR	15.1	NR	NR
923	[61]	YSU	2008	N2	AMB	CON	NR	3.55	25	15	B-1	40.0	5.61	0.63	1.60	NR	6.0	0	-	1.0	8.0	NR	22.2	NR	NR
924	[61]	YSU	2008	N2	AMB	CON	NR	3.55	25	15	B-2	40.0	5.61	0.63	1.60	NR	6.0	0	6.0	1.0	8.0	NR	20.2	NR	NR
925	[61]	YSU	2008	N2	AMB	CON	NR	3.55	25	15	C-1	50.0	5.91	0.63	2.00	NR	6.0	0	-	1.0	8.0	NR	27.6	NR	NR
926	[61]	YSU	2008	N2	AMB	CON	NR	3.55	25	15	C-2	50.0	5.91	0.63	2.00	NR	6.0	0	6.0	1.0	8.0	NR	24.8	NR	NR
927	[61]	YSU	2008	N2	AMB	CON	NR	3.55	25	15	D-1	60.0	6.17	0.63	2.40	NR	6.0	0	-	1.0	8.0	NR	33.5	NR	NR
928	[61]	YSU	2008	N2	AMB	CON	NR	3.55	25	15	D-2	60.0	6.17	0.63	2.40	NR	6.0	0	6.0	1.0	8.0	NR	30.3	NR	NR
929	[61]	YSU	2008	N2	AMB	CON	NR	3.55	49	15	E	60.0	6.17	0.63	2.40	NR	6.0	0	6.0	1.0	8.0	NR	30.3	NR	NR
930	[61]	YSU	2008	N2	AMB	TOP	NR	1.90	18.2	18	G-1	24.7	4.98	0.61	0.82	NR	6.0	0	6.0	1+	8+	NR	18.7	NR	NR
931	[61]	YSU	2008	N2	AMB	CON	NR	1.90	18.2	18	G-2	24.7	4.98	0.61	0.82	NR	6.0	0	6.0	1+	8+	NR	18.7	NR	NR
932	[61]	YSU	2008	N2	AMB	TIC	NR	4.83	69.5	NR	I-1	130	7.36	0.77	1.44	3.0	6.0	0	6.0	1.0	8.0	NR	47.6	NR	NR
933	[62-63]	CNU	2013	N2	AMB	CON	0.20	4.30	NR	NR	1	84.2	6.67	0.67	NR	9.7	5.0	0	6.0	1.0	8.0	15.7	43.6	NR	NR
934	[62-63]	CNU	2013	N2	AMB	CON	0.20	4.30	NR	NR	1	84.2	6.67	0.67	NR	9.7	5.0	0	6.0	0.0	8.0	10.7	42.0	NR	NR
935	[62-63]	CNU	2013	N2	AMB	CON	0.20	4.30	NR	NR	2	84.2	6.67	0.67	NR	9.7	5.0	0	6.0	0.5	8.0	15.7	41.8	NR	NR
936	[62-63]	CNU	2013	N2	AMB	CON	0.20	4.30	NR	NR	3	84.2	6.67	0.67	NR	9.7	5.0	0	6.0	0.0	8.0	15.7	41.5	NR	NR
937	[62-63]	CNU	2013	N2	AMB	CON	0.20	4.30	NR	NR	4	84.2	6.67	0.67	NR	9.7	5.0	0	6.0	1.0	8.0	15.7	50.0	NR	NR
938	[62-63]	CNU	2013	N2	AMB	CON	0.20	4.30	NR	NR	5	84.2	6.67	0.67	NR	9.7	5.0	0	6.0	1.0	8.0	15.7	48.5	NR	NR
939	[62-63]	CNU	2013	N2	AMB	CON	0.20	4.30	NR	NR	6	84.2	6.67	0.67	NR	9.7	5.0	0	6.0	1.0	8.0	15.7	45.5	NR	NR
940	[62-63]	CNU	2013	N2	AMB	CON	0.20	4.30	NR	NR	7	84.2	6.67	0.67	NR	9.7	5.0	0	6.0	1.0	7.0	15.7	43.1	NR	NR
941	[62-63]	CNU	2013	N2	AMB	CON	0.20	4.30	NR	NR	8	84.2	6.67	0.67	NR	9.7	5.0	0	6.0	1.0	9.0	15.7	42.0	NR	NR
942	[62-63]	CNU	2013	N2	AMB	CON	0.20	4.30	NR	NR	9	84.2	6.67	0.67	NR	9.7	5.0	0	6.0	1.0	12.0	15.7	41.8	NR	NR
943	[62-63]	CNU	2013	N2	AMB	CON	0.20	4.30	NR	NR	10	84.2	6.67	0.67	NR	9.7	5.0	0	6.0	1.0	8.0	10.7	46.6	NR	NR
944	[62-63]	CNU	2013	N2	AMB	CON	0.20	4.30	NR	NR	11	84.2	6.67	0.67	NR	9.7	5.0	0	6.0	1.0	8.0	20.8	41.5	NR	NR
945	[62-63]	CNU	2013	N2	AMB	CON	0.20	4.30	NR	NR	A	70.7	6.41	0.76	NR	9.7	5.0	0	6.0	1.1	8.0	NR	46.5	NR	NR
946	[62-63]	CNU	2013	N2	AMB	CON	0.20	4.30	NR	NR	B	104	7.00	0.52	NR	9.7	5.0	0	6.0	0.9	8.0	NR	51.4	NR	NR
947	[62-63]	CNU	2013	N2	AMB	CON	0.20	4.30	NR	NR	C	125	7.29	0.43	NR	9.7	5.0	0	6.0	0.8	8.0	NR	58.8	NR	NR
948	[62-63]	CNU	2013	N2	AMB	CON	0.20	4.30	NR	NR	D	84.2	6.67	0.64	NR	9.7	5.0	0	6.0	1.0	8.0	NR	46.6	NR	NR
949	[62-63]	CNU	2013	N2	AMB	CON	0.20	4.30	NR	NR	E	84.2	6.67	1.00	NR	9.7	5.0	0	6.0	1.0	6.4	NR	65.5	NR	NR
950	[62-63]	CNU	2013	N2	AMB	CON	0.20	4.30	NR	NR	F	84.2	6.67	0.80	NR	9.7	5.0	0	6.0	1.0	7.1	NR	56.8	NR	NR
951	[62-63]	CNU	2013	N2	AMB	CON	0.20	4.30	NR	NR	G	84.2	6.67	0.57	NR	9.7	5.0	0	6.0	1.0	13.5	NR	48.9	NR	NR
952	[40]	ISRO	2015	N2	NR	NR	4.00	70	NR	SVC	89.0	6.76	0.50	0.64	4.0	6.0	0	5.0	1.0	8.0	8.0	17.1	34.5	31.6	17.1
953	[64]	STRI	2019	Air	300	NR	0.72	NR	53	NR	-	70.0	6.40	0.54	1.32	4.0	6.0	0	6.0	0.8	8.0	NR	30.3	28.0	NR
954	[64]	STRI	2019	Air	300	NR	0.86	NR	37	NR	-	45.6	5.79	0.59	1.23	4.0	6.0	0	6.0	0.8	8.0	NR	27.0	19.2	NR
955	[64]	STRI	2019	Air	300	NR	0.86	NR	37	NR	-	45.6	5.79	0.56	1.23	4.0	6.0	0	6.0	0.8	8.0	NR	27.3	19.0	NR
956	[64]	STRI	2019	Air	300	NR	0.78	NR	45	NR	-	57.9	6.12	0.55	1.29	4.0	6.0	0	6.0	0.8	8.0	NR	33.5	23.7	NR
957	[L2]	NASA SSC	2020	N2	301	TOP	0.313	18.94	69.4	5.4	ND4-E	90.4	5.84	0.57	0.74	-	6.0	0	-	0.44	2.75	4.87	64.7	57.4	73.0
958	[L2]	NASA SSC	2020	N2	301	TOP	0.475	9.89	36.5	6.0	ND4-E	47.5	5.81	0.57	0.74	-	6.0	0	-	0.44	2.75	4.87	55.4	27.0	129
959	[L2]	NASA SSC	2021	N2	299	FAIR	0.318	4.39	15	0.0	CYL-E	36.2	5.48	1.00	2.41	-	-	0	-	-	11.6	11.6	31.0	31.0	171
960	[65]	PU	2021	N2	AMB	TOP	0.305	2.76	25	15.0	#1	47.8	5.85	0.57	1.09	NR	6.0	0	7.0	1.0	8.0	NR	21.5	20.0	NR
961	[65]	PU	2021	N2	AMB	TOP, θ <sub>n</sub> = 29°	0.305	2.76	25	7.															

Table 6 - Centerbody Diffuser Data

No.	Ref.	Entity	Year	Nozzle Configuration					Shell Configuration					Centerbody Configuration							Performance							
				Prop.	Type	D <sub>NT</sub>	Ref. P <sub>0</sub>	A <sub>NE</sub> A <sub>NT</sub>	θ <sub>NE</sub>	Name	A <sub>DI</sub> A <sub>NT</sub>	M <sub>DI</sub>	A <sub>DE</sub> A <sub>DI</sub>	θ <sub>DI</sub>	θ <sub>SUB</sub>	Δ	R <sub>TIP</sub> R <sub>DI</sub>	L <sub>BODY</sub> D <sub>DI</sub>	D <sub>BODY</sub> D <sub>DI</sub>	R <sub>TAIL</sub> R <sub>DI</sub>	θ <sub>TIP</sub>	θ <sub>BODY</sub>	θ <sub>TAIL</sub>	P <sub>o</sub> P <sub>BACK</sub>	(P <sub>CELL</sub> P <sub>0</sub> ) × 10 <sup>5</sup>			
[cm] [MPa] [deg]																							Start Unst.					
O:F																												
972	[13-16]	DLR	2005	LOX/LH2	6.0	TOP	3.00	6.00	100	NR	-	105.0	4.87	0.67	2.0	12.0	6.0	NR	NR	NR	NR	0.0	-6.0	49.3	47.3	80.0		
973	[42]	NASA SSC	2020	GOX/GH2	6.2	TOP	0.32	5.00	76.9	19	CB-2-E	107.6	4.72	0.75	1.4	-	0.0	0.32	0.12	3.7	0.68	0.50	25.0	0.0	-22.5	45.1	44.8	133
974	[TR]	NASA SSC	2021	LOX/GH2	6.0	TOP	2.31	4.39	76.7	19	CB-1	106.9	4.81	0.75	1.4	-	0.0	0.32	0.12	3.7	0.68	0.50	25.0	0.0	-22.5	40.8	40.8	95.7
975	[TR]	NASA SSC	2021	LOX/GH2	6.2	TOP	2.31	4.39	76.7	19	CB-2	106.9	4.75	0.75	1.4	-	0.0	0.32	0.12	3.7	0.68	0.50	25.0	0.0	-22.5	41.2	40.5	106
TO [K]																								Start Unst.				
976	[42]	NASA SSC	2020	C2H6	535	TOP	0.32	5.00	76.9	19	CB-2-E	107.6	4.73	0.75	1.4	-	0.0	0.32	0.12	3.7	0.68	0.50	25.0	0.0	-22.5	41.0	40.1	119
Hot-Fire Data																								Start Unst.				
977	[9]	P&W	1960	N2	AMB	TOP	1.27	NR	40.0	9.0	PlA	41.5	5.66	0.66	5.3	-	6, 10	0.0	NR	NR	0.80	NR	15.0	-1.0	-10.0	21.6	19.9	NR
978	[9]	P&W	1960	N2	AMB	TOP	1.27	NR	40.0	9.0	PlB	41.5	5.66	0.66	5.3	-	6, 10	0.26	NR	NR	0.80	NR	15.0	-1.0	-10.0	21.2	19.9	NR
979	[9]	P&W	1960	N2	AMB	TOP	1.27	NR	40.0	9.0	PlC	41.5	5.66	0.66	5.3	-	6, 10	0.41	NR	NR	0.80	NR	15.0	-1.0	-10.0	20.1	20.1	NR
980	[9]	P&W	1960	N2	AMB	TOP	1.27	NR	40.0	9.0	PlD	41.5	5.66	0.66	5.3	-	6, 10	0.57	NR	NR	0.80	NR	15.0	-1.0	-10.0	19.0	19.0	NR
981	[9]	P&W	1960	N2	AMB	TOP	1.27	NR	40.0	9.0	P2B	41.5	5.66	0.55	5.3	-	6, 10	-0.27	NR	NR	0.73	NR	15.0	-1.0	-10.0	20.5	19.0	NR
982	[9]	P&W	1960	N2	AMB	TOP	1.27	NR	40.0	9.0	P2C	41.5	5.66	0.55	5.3	-	6, 10	-0.43	NR	NR	0.73	NR	15.0	-1.0	-10.0	19.1	18.1	NR
983	[9]	P&W	1960	N2	AMB	TOP	1.27	NR	40.0	9.0	P2D	41.5	5.66	0.55	5.3	-	6, 10	-0.59	NR	NR	0.73	NR	15.0	-1.0	-10.0	17.8	17.4	NR
984	[9]	P&W	1960	N2	AMB	TOP	1.27	NR	40.0	9.0	P3A	41.5	5.66	0.59	5.3	-	6, 10	0.0	NR	NR	0.76	NR	15.0	-1.0	-10.0	21.4	20.2	NR
985	[9]	P&W	1960	N2	AMB	TOP	1.27	NR	40.0	9.0	P3B	41.5	5.66	0.59	5.3	-	6, 10	-0.26	NR	NR	0.76	NR	15.0	-1.0	-10.0	20.3	19.4	NR
986	[9]	P&W	1960	N2	AMB	TOP	1.27	NR	40.0	9.0	P3C	41.5	5.66	0.59	5.3	-	6, 10	-0.41	NR	NR	0.76	NR	15.0	-1.0	-10.0	19.0	19.0	NR
987	[9]	P&W	1960	N2	AMB	TOP	1.27	NR	40.0	9.0	P3D	41.5	5.66	0.59	5.3	-	6, 10	-0.57	NR	NR	0.76	NR	15.0	-1.0	-10.0	17.8	17.8	NR
988	[10]	AEDC	1963	Air	300	CON	3.20	0.31	10.8	18.0	5d-CB	65.2	6.29	2.63	2.3	12.0	0	-1.37	NR	NR	0.18	NR	12.0	0.0	0.0	43.9	43.9	55.0
989	[10]	AEDC	1963	Air	300	CON	2.11	0.31	25.0	18.0	5d	150	7.59	2.63	2.3	12.0	0	-1.35	NR	NR	0.18	NR	12.0	0.0	0.0	90.9	90.9	30.0
990	[10]	AEDC	1963	Air	300	CON	3.20	0.31	10.8	18.0	6	22.7	4.88	1.21	1.7	6.0	0	-0.40	NR	NR	0.17	NR	6.0	0.0	0.0	26.7	26.2	19.0
991	[10]	AEDC	1963	Air	300	CON	3.20	0.31	10.8	18.0	6	22.7	4.88	1.21	1.7	6.0	0	-0.68	NR	NR	0.17	NR	6.0	0.0	0.0	25.6	24.8	18.9
992	[10]	AEDC	1963	Air	300	CON	3.20	0.31	10.8	18.0	6	22.7	4.88	1.21	1.7	6.0	0	-1.00	NR	NR	0.17	NR	6.0	0.0	0.0	36.8	36.5	18.4
993	[10]	AEDC	1963	Air	300	CON	2.11	0.32	25.0	18.0	6-CB	52.3	5.98	1.21	1.7	6.0	0	-0.20	NR	NR	0.17	NR	6.0	0.0	0.0	58.1	57.1	90.0
994	[10]	AEDC	1963	Air	300	CON	2.11	0.31	25.0	18.0	6-CB	52.3	5.98	1.21	1.7	6.0	0	-0.77	NR	NR	0.17	NR	6.0	0.0	0.0	60.6	60.6	90.0
995	[10]	AEDC	1963	Air	300	CON	2.11	0.31	25.0	18.0	6-CB	52.3	5.98	1.21	1.7	6.0	0	-1.00	NR	NR	0.17	NR	6.0	0.0	0.0	80.6	80.0	90.0
996	[11]	Aerojet	1965	Air	750	NR	3.20	4.25	40.0	NR	1	61.5	6.08	0.95	-	-	-	-0.50	0.08	1.5	0.62	0.16	16.0	0.0	-16.0	33.0	NR	455
997	[11]	Aerojet	1965	Air	750	NR	3.20	4.25	40.0	NR	2	61.5	6.08	0.95	-	-	-	-0.30	0.08	1.5	0.62	0.16	23.0	0.0	-16.0	33.0	NR	455
998	[11]	Aerojet	1965	Air	750	NR	3.20	4.25	40.0	NR	3	61.5	6.08	0.95	-	-	-	-0.30	0.08	1.5	0.62	0.16	30.0	0.0	-16.0	33.0	NR	455
999	[11]	Aerojet	1965	Air	750	NR	3.20	4.25	40.0	NR	4	61.5	6.08	0.95	-	-	-	-0.30	0.18	1.5	0.62	0.16	16.0	0.0	-16.0	33.0	NR	455
1000	[11]	Aerojet	1965	Air	750	NR	3.20	4.25	40.0	NR	5	61.5	6.08	0.95	-	-	-	-0.30	0.18	1.5	0.62	0.16	23.0	0.0	-16.0	33.0	NR	455
1001	[11]	Aerojet	1965	Air	750	NR	3.20	4.25	40.0	NR	6	61.5	6.08	0.95	-	-	-	-0.30	0.18	1.5	0.62	0.16	30.0	0.0	-16.0	34.0	NR	441
1002	[11]	Aerojet	1965	Air	750	NR	3.20	4.25	40.0	NR	7	61.5	6.08	0.95	-	-	-	-0.30	0.32	1.5	0.62	0.16	16.0	0.0	-16.0	33.0	NR	455
1003	[11]	Aerojet	1965	Air	750	NR	3.20	4.25	40.0	NR	8	61.5	6.08	0.95	-	-	-	-0.50	0.32	1.5	0.62	0.16	23.0	0.0	-16.0	33.0	NR	455
1004	[11]	Aerojet	1965	Air	750	NR	3.20	4.25	40.0	NR	9	61.5	6.08	0.95	-	-	-	-0.30	0.32	1.5	0.62	0.16	30.0	0.0	-16.0	33.0	NR	455
1005	[20]	CNU	2016	N2	AMB	CON	0.20	4.30	45.0	NR	A	84.2	6.67	1.20	9.8	-	6.0	0.0	-	3.2	0.80	-	5.0	0.0	-6.0	47.7	NR	NR
1006	[20]	CNU	2016	N2	AMB	CON	0.20	4.30	45.0	NR	B	84.2	6.67	1.20	9.8	-	6.0	0.0	-	3.2	0.80	-	10.0	0.0	-6.0	46.5	NR	NR
1007	[20]	CNU	2016	N2	AMB	CON	0.20	4.30	45.0	NR	C	84.2	6.67	1.20	9.8	-	6.0	0.0	-	3.2	0.80	-	15.0	0.0	-6.0	43.2	NR	NR
1008	[20]	CNU	2016	N2	AMB	CON	0.20	4.30	45.0	NR	D	84.2	6.67	1.20	9.8	-	6.0	0.0	-	3.2	0.80	-	20.0	0.0	-6.0	47.7	NR	NR
1009	[20]	CNU	2016	N2	AMB	CON	0.20	4.30	45.0	NR	E	84.2	6.67	1.20	9.8	-	6.0	0.0	-	3.2	0.80	-	30.0	0.0	-6.0	52.7	NR	NR
1010	[20]	CNU	2016	N2	AMB	CON	0.20	4.30	45.0	NR	F	84.2	6.67	1.20	9.8	-	6.0	-0.28	-	3.2	0.80	-	15.0	0.0	-6.0	46.6	NR	NR
1011	[20]	CNU	2016	N2	AMB	CON	0.20	4.30	45.0	NR	G	84.2	6.67	1.20	9.8	-	6.0	-0.50	-	3.2	0.80	-	15.0	0.0	-6.0	49.1	NR	NR
1012	[																											

Table 7 - Spike Diffuser Data

No.	Ref.	Entity	Year	Nozzle Configuration					Shell Configuration					Spike Configuration					Performance								
				Prop.	Type	D <sub>NT</sub>	Ref. P <sub>0</sub>	A <sub>NE</sub> A <sub>NT</sub>	θ <sub>NE</sub>	Name	A <sub>DI</sub> A <sub>NT</sub>	M <sub>DI</sub>	L <sub>DI</sub> D <sub>DI</sub>	θ <sub>DI</sub>	θ <sub>SHL</sub>	Δ	D <sub>TTP</sub> D <sub>DI</sub>	L <sub>SPK</sub> / D <sub>DI</sub>	1	2	3	1	2	3	P <sub>0</sub> P <sub>BACK</sub>	(P <sub>CELL</sub> P <sub>0</sub> ) × 10 <sup>5</sup>	
				[cm]	[MPa]						<[deg]>					<[deg]>					Start Unst.						
O:F																											
1015	[42]	NASA SSC	2020	GOX/GH2	6.1	TOP	0.318	4.14	76.9	19	SPK-3X-E	107.6	4.74	0.38	-5.7	21.1	0.37	0.13	1.73	-	-	24	-	-	41.0	39.5	254
1016	[TR]	NASA SSC	2021	LOX/GH2	6.1	TOP	2.312	3.55	76.7	19	SPK-1X	106.9	4.76	0.38	-5.7	21.1	0.47	0.00	1.82	-	-	24	-	-	34.6	32.3	104
1017	[TR]	NASA SSC	2021	LOX/GH2	6.1	TOP	2.312	3.55	76.7	19	SPK-2X	106.9	4.76	0.38	-5.7	21.1	0.42	0.09	1.77	-	-	24	-	-	34.9	32.7	101
1018	[TR]	NASA SSC	2021	LOX/GH2	6.1	TOP	2.312	3.55	76.7	19	SPK-3X	106.9	4.76	0.38	-5.7	21.1	0.38	0.18	1.75	-	-	24	-	-	35.2	33.1	102
1019	[TR]	NASA SSC	2021	LOX/GH2	5.8	TOP	2.312	3.55	76.7	19	SPK-3X	106.9	4.85	0.38	-5.7	21.1	0.37	0.18	1.75	-	-	24	-	-	35.7	33.7	110
1020	[TR]	NASA SSC	2021	LOX/GH2	6.0	TOP	2.312	3.55	76.7	19	SPK-4X	106.9	4.79	0.38	-5.7	21.1	0.56	0.22	1.73	-	-	24	-	-	35.3	34.0	113
1021	[TR]	NASA SSC	2021	LOX/GH2	6.1	TOP	2.312	3.55	76.7	19	SPK-4X	106.9	4.76	0.38	-5.7	21.1	0.35	0.22	1.73	-	-	24	-	-	36.3	34.7	107
1022	[TR]	NASA SSC	2021	LOX/GH2	5.6	TOP	2.312	3.55	76.7	19	SPK-4X	106.9	4.91	0.38	-5.7	21.1	0.35	0.22	1.73	-	-	24	-	-	37.8	35.9	116
1023	[TR]	NASA SSC	2021	LOX/GH2	6.0	TOP	2.312	3.55	76.7	19	SPK-3Y	106.9	4.79	0.38	-5.7	21.1	0.38	0.18	1.73	-	-	24	-	-	36.2	34.7	98.2
1024	[TR]	NASA SSC	2021	LOX/GH2	6.1	TOP	2.312	3.55	76.7	19	SPK-4Y	106.9	4.76	0.38	-5.7	21.1	0.36	0.22	1.71	-	-	24	-	-	35.0	34.9	89.9
TO [K]																											
1025	[42]	NASA SSC	2020	C2H6	535	TOP	0.318	3.55	76.9	19	SPK-3X-E	107.6	4.7	0.38	-5.7	21.1	0.37	0.13	1.72	-	-	24	-	-	35.2	32.7	123
1026	[42]	NASA SSC	2020	C2H6	635	TOP	0.376	10.34	100	14.8	SPK-SRP-E	111.5	4.49	0.27	-5.7	21.1	0.54	0.13	1.93	-	-	24	-	-	29.1	27.2	220
1027	[42]	NASA SSC	2020	C2H6	635	TOP	0.318	10.34	140	11.2	SPK-SRP-E	156.3	4.72	0.27	-5.7	21.1	0.54	0.13	1.93	-	-	24	-	-	40.1	40.1	170
1028	[42]	NASA SSC	2020	C2H6	635	TOP	0.282	10.34	177	7.5	SPK-SRP-E	198.2	4.89	0.27	-5.7	21.1	0.54	0.13	1.93	-	-	24	-	-	56.5	47.4	75.2
Cold-Flow Data																											
1029	[21]	NASA LeRC	1962	N2	NR	CON	0.66	3.04	25.0	15.0	-	35.4	5.45	1.40	0.0	10.8	NR	0.0	-	-	12	-	-	15.8	10.2	NR	
1030	[21]	NASA LeRC	1962	N2	NR	CON	0.66	3.04	25.0	15.0	-	35.4	5.45	1.97	0.0	12.0	NR	0.0	-	-	12	-	-	18.8	9.9	NR	
1031	[21]	NASA LeRC	1962	N2	NR	CON	0.66	3.04	25.0	15.0	-	35.4	5.45	0.74	0.0	10.8	NR	0.0	-	-	15	-	-	14.6	9.4	NR	
1032	[21]	NASA LeRC	1962	N2	NR	CON	0.66	3.04	25.0	15.0	-	35.4	5.45	1.00	0.0	12.0	NR	0.0	-	-	15	-	-	17.0	10.2	NR	
1033	[21]	NASA LeRC	1962	N2	NR	CON	0.66	3.04	25.0	15.0	-	35.4	5.45	1.20	0.0	13.3	NR	0.0	-	-	15	-	-	15.2	9.2	NR	
1034	[21]	NASA LeRC	1962	N2	NR	CON	0.66	3.04	25.0	15.0	-	35.4	5.45	1.20	0.0	15.0	NR	0.0	-	-	15	-	-	18.0	10.2	NR	
1035	[21]	NASA LeRC	1962	N2	NR	CON	0.66	3.04	25.0	15.0	-	35.4	5.45	1.20	0.0	21.5	NR	0.0	-	-	15	-	-	25.1	17.0	NR	
1036	[21]	NASA LeRC	1962	N2	NR	CON	0.66	3.04	25.0	15.0	-	35.4	5.45	0.28	0.0	21.5	NR	0.0	-	-	24	-	-	11.4	9.7	NR	
1037	[21]	NASA LeRC	1962	N2	NR	CON	0.66	3.04	25.0	15.0	-	35.4	5.45	0.74	0.0	24.0	NR	0.0	-	-	24	-	-	18.4	15.2	NR	
1038	[21]	NASA LeRC	1962	N2	NR	CON	0.66	3.04	25.0	15.0	-	35.4	5.45	0.74	0.0	27.4	NR	0.0	-	-	30	-	-	17.2	11.4	NR	
1039	[21]	NASA LeRC	1962	N2	NR	CON	0.66	3.04	25.0	15.0	-	35.4	5.45	0.74	0.0	30.0	NR	0.0	-	-	30	-	-	19.4	14.2	NR	
1040	[21]	NASA LeRC	1962	N2	NR	CON	0.66	3.04	25.0	15.0	-	35.4	5.45	1.17	0.0	13.3	NR	0.16	-	-	15	-	-	18.7	10.9	NR	
1041	[21]	NASA LeRC	1962	N2	NR	CON	0.66	3.04	25.0	15.0	-	35.4	5.45	1.71	0.0	13.3	NR	0.32	-	-	15	-	-	23.5	12.4	NR	
1042	[21]	NASA LeRC	1962	N2	NR	CON	0.66	3.04	25.0	15.0	-	35.4	5.45	1.66	0.0	13.3	NR	0.48	-	-	15	-	-	28.4	16.1	NR	
1043	[21]	NASA LeRC	1962	N2	NR	CON	0.66	3.04	25.0	15.0	-	35.4	5.45	1.20	0.0	27.4	NR	0.0	155	-	-	15	30	-	17.6	12.4	NR
1044	[21]	NASA LeRC	1962	N2	NR	CON	0.66	3.04	25.0	15.0	-	35.4	5.45	0.94	0.0	30.0	NR	0.0	1.17	-	-	15	30	-	22.1	19.2	NR
1045	[21]	NASA LeRC	1962	N2	NR	CON	0.66	3.04	25.0	15.0	-	35.4	5.45	1.20	0.0	30.0	NR	0.0	1.36	-	-	15	30	-	21.2	16.8	NR
1046	[21]	NASA LeRC	1962	N2	NR	CON	0.66	3.04	25.0	15.0	-	35.4	5.45	1.17	0.0	30.0	NR	0.0	1.55	-	-	15	30	-	23.2	11.6	NR
1047	[21]	NASA LeRC	1962	N2	NR	CON	0.66	3.04	25.0	15.0	-	35.4	5.45	1.20	0.0	30.0	NR	0.0	1.75	-	-	15	30	-	28.4	10.4	NR
1048	[22]	AEDC	1973	Air	NR	CON	7.72	NR	1.6	18.0	-	4.0	2.94	1.65	0.0	8.0	0.65	0.16	1.96	-	-	12	-	-	3.7	NR	3460
1049	[22]	AEDC	1973	Air	NR	CON	6.43	NR	1.7	18.0	-	5.8	3.33	1.65	0.0	8.0	0.52	0.16	1.96	-	-	12	-	-	5.4	NR	1672
1050	[22]	AEDC	1973	Air	NR	CON	7.72	NR	1.6	18.0	-	4.0	2.94	1.59	0.0	12.5	0.46	0.0	1.14	0.66	-	18	15	-	3.5	NR	7520
1051	[22]	AEDC	1973	Air	NR	CON	7.72	NR	1.6	18.0	-	4.0	2.94	1.59	0.0	12.5	0.54	0.0	1.14	0.66	-	18	15	-	4.0	NR	6050
1052	[22]	AEDC	1973	Air	NR	CON	7.72	NR	1.6	18.0	-	4.0	2.94	1.59	0.0	12.5	0.63	0.0	1.14	0.66	-	18	15	-	4.3	NR	3550
1053	[22]	AEDC	1973	Air	NR	CON	7.72	NR	1.6	18.0	-	4.0	2.94	1.59	0.0	12.5	0.71	0.0	1.14	0.66	-	18	15	-	4.1	NR	3410
1054	[22]	AEDC	1973	Air	NR	CON	7.72	NR	1.6	18.0	-	4.0	2.94	1.59	0.0	12.5	0.60	0.0	0.67	0.70	0.66	12	25	11.1	4.8	NR	3460
1055	[22]	AEDC	1973	Air	NR	CON	6.43	NR	1.7	18.0	-	5.8	3.33	1.59	0.0	12.5	0.48	0.0	0.67	0.70	0.66	12	25	11.1	3.2	NR	5460
1056	[23]	AEDC	1974	Air	NR	CON	5.21	NR	3.0	13.3	-	8.8	3.78	1.31	0.0	8.0	0.41	0.16	1.96	-	-	12	-	-	7.5	NR	860
1057	[23]	AEDC	1974	Air	NR	CON	3.71	NR	2.9	12.0	-</td																